Examining the Role of Autophagy in Skeletal Muscle Cell Death and Differentiation

by

Michael Elliott McMillan

A thesis

presented to the University of Waterloo

in fulfilment of the

thesis requirement for the degree of

Doctor of Philosophy

in

Kinesiology

Waterloo, Ontario, Canada, 2014

Author's Declaration

This thesis consists of material all of which I authored or co-authored; please see Statement of Contributions included in the thesis. This is a true copy of the thesis, including all final revisions, as accepted by all examiners.

I understand that my thesis may be made electronically available to the public.

Elliott M. McMillan

Statement of Contributions

Chapter II was conceived and designed by Elliott M. McMillan and Dr. Joe Quadrilatero. All sample collections and data analyses were performed by Elliott M. McMillan. Editing of this chapter was performed by Elliott M. McMillan and Dr. Joe Quadrilatero. Chapter II of this thesis is largely presented as published in:

 Autophagy is required and protects against apoptosis during myoblast differentiation. *Biochemical Journal* Immediate Publication, doi: 10.1042/BJ20140312

Chapter III was conceived and designed by Elliott M. McMillan and Dr. Joe Quadrilatero. Darin Bloemberg, in the lab of Dr. Joe Quadrilatero assisted with production of stable shRNA expressing cell lines, collection of subcellular enriched fractions and analysis of co-localization data. Elliott M. McMillan performed all sample collection and data analysis not listed above. Editing of the thesis chapter was performed by Dr. Joe Quadrilatero, Darin Bloemberg and Elliott M. McMillan

Chapter IV was conceived and designed by Elliott M. McMillan and Dr. Joe Quadrilatero. Andrew Mitchell, in the lab of Dr. Joe Quadrilatero assisted with sample preparation, collection and analysis of flow cytometry data. Elliott M. McMillan performed all sample collection and data analysis not listed above. Editing of this thesis chapter was performed by Dr. Joe Quadrilatero, Andrew Mitchell and Elliott M. McMillan.

All aspects of this thesis not listed above were authored by myself, Elliott M. McMillan

Abstract

Autophagy is catabolic process which sequesters large portions of cytoplasm as well as selected organelles and proteins for degradation. Recently, autophagy has been a topic of much debate owing to conflicting evidence regarding its role in cell death signaling. Interestingly, both apoptotic signaling and altered autophagy have been observed in states associated with muscular atrophy and dysfunction. However, the cross-talk between these two cell death-related processes is not well understood in skeletal muscle. Interestingly, myogenesis and the ability of muscle to regenerate, requires myoblast differentiation, a process which requires highly regulated cell death signaling. The interplay between autophagy and apoptosis and the integrated role between these two supposed cell death systems during myoblast differentiation is unknown. The purpose of this thesis was to examine the relationship between autophagy and apoptotic signaling during myoblast differentiation as well as during myotube apoptotic stress and recovery. Chapter II reveals that autophagy is induced during myoblast differentiation, but more importantly, is required for muscle cell differentiation and protection against cell death. Chapter III determined that the induction of autophagy is required for the regulation of apoptosis during muscle cell differentiation through the prevention of mitochondrial-mediated apoptotic signaling. Chapter IV established that autophagy is required for the protection and recovery of muscle cell viability and mitochondrial function during moderate levels of apoptotic stress. Together this thesis supports autophagy as a regulator of apoptotic processes in skeletal muscle. Furthermore, this thesis highlights a role for autophagy in skeletal muscle differentiation and recovery from apoptotic stress.

Acknowledgements

I would first like to thank my wife, Jen Stark, for being my true north. You have provided me with the direction, dedication and determination I needed to grind through this thesis. You have been my motivation for the present and my inspiration for the future.

I would also like to thank Dr. Joe Quadrilatero. You gave me the opportunity and freedom to explore my passions and the challenges I needed to shape me into a young scientist. Thank you. Dear fellow students of the Muscle Biology and Cell Death Lab. I could not have done this without your love and support. It is has been an honour to have worked alongside such intelligent independent minds. Dearest Darin and Mitch, the two of you have made my time in this lab so memorable for so many reasons. Your friendship, ridiculousness and brilliance have been instrumental in my education and sanity. Without the both of you, I would not have been able to complete this thesis or salvage my sanity. Mitch, you will make a great spyentist, and stay at home dad. Darin, mmmhmmm. Troy, well you know what I want to say but thank you for your critical ear and friendship. Moe, it was the best of times, it was the worst of times but we are coming out very strong. Good luck my brothers and sisters.

Thank you to my friends and colleagues in the Tupling lab. Dan, you are a great friend and a great scientist. Thank you for your friendship, humour and critical ear. Eric, thank you for your elderly wisdom. To Val, Chris and Ian thank you for your support, advice, wisdom and friendship. Dr. Tupling, thank you for sharing with me your enthusiasm for science and always being a positive influence in my development.

Thank you to my family, Dodi, Brian, Daniel and Collin as well as Bill, Cindy and Tim for your love and support. I cannot wait to come home!

Table of Contents

List of Figures

List of Abbreviations

ΔΨ, trans-membrane potential

3MA, 3-methyladenine;

AIF, apoptosis inducing factor

AKT, protein kinase B;

AMPK, AMP-activated protein kinase;

ANT, adenine nucleotide translocase

APAF1, apoptotic protease activating factor 1

ARC, apoptosis repressor with caspase recruitment domain

ATG, autophagy-related;

ATG12, autophagy-related 12;

ATG4B, autophagy-related 4B;

ATG5, autophagy-related 5;

ATG7, autophagy-related 7;

BCL2, B-cell CLL/lymphoma 2;

BCLXL, B-cell CLL/lymphoma XL;

BECN1, beclin 1;

bHLH, basic helix loop helix,

BNIP3, BCL2/adenovirus E1B 19 kDa interacting protein 3;

CARD, caspase recruitment domain

CASP, caspase

CASP3, caspase-3;

CPN, calpain

CQ, chloroquine;

CTS, cathepsin

DAPK, death associated protein kinase

DISC, death inducing signaling complex

ENDOG, endonuclease G

FOXO3A, forkhead box O3A;

GABARAP, gamma-aminobutyric acid receptor associated protein

GFP-LC3B, green fluorescent protein-LC3B;

IMM, inner mitochondrial membrane

MAC, mitochondrial apoptosis channel

MAP1LC3B (LC3B), microtubule-associated protein 1 light chain 3 beta;
MAPK8/JNK1, mitogen-activated protein kinase 8/c-Jun N-terminal kinase 1;
MOMP, mitochondrial outer membrane permeabilization
mPTP, mitochondrial permeability transition pore
MTOR, mechanistic target of rapamycin;
MYF-5, myogenic regulatory factor 5
MYH, myosin heavy chain
MYOD, myogenic determination factor
MYOG, myogenin
OMM, outer mitochondrial membrane
PAX, paired box gene
PE, phosphatidylethanolamine
PGC1, peroxisome proliferator c co-transcription factor 1
PIK3C3/VPS34, class III phosphatidylinositol 3-kinase;
PI(3)P, phosphatidylinositol – 3 phosphate
PL, phosphatidylserine
ROS, reactive oxygen species
SCR, scramble shRNA.
shAtg7, short hairpin RNA against ATG7;
SMAC, second mitochondria derived activator of caspases
SQSTM1/p62, sequestosome 1;
TLR4, toll like receptor 4
TNF, tumour necrosis factor
TNFR, tumour necrosis factor receptor
TRAF6, TNFR associated factor 6
ULK1, unc-51 like kinase 1;
UPS, ubiquitin proteasome system
VDAC, voltage dependent anion channel
XIAP, x-linked inhibitor of apoptosis

CHAPTER I: Introduction, Literature Review and Statement of the Problem

Introduction

Apoptosis and autophagy are two catabolic phenomena essential for skeletal muscle development and maintenance[1-3]. However, apoptotic signaling can also result in the cleavage of a number of cytoskeletal structures and the destruction of organelles which collectively impair muscle function and induce deleterious remodeling[4-7]. Similarly, autophagy is a degradative process which sequesters damaged or long lived proteins/organelles within a double membrane bound vesicle and delivers the sequestered cargo to the lysosome for degradation[8,9]. This process can contribute to muscle atrophy[8,9]. Both apoptosis and autophagy have been classified as cell death types I and II, respectively, due to their involvement and association with the destruction and removal of stressed or dying cells[10,11]. Despite major differences in the appearance of these two supposedly independent forms of cell death, recent evidence supports a remarkable level of cross-talk between the two systems[12]. Furthermore, their roles as independent processes have been documented in both beneficial as well as deleterious capacities[2,6,13,14]. Little is known regarding the integration of autophagy and apoptosis in developing and/or mature skeletal muscle, and whether they both contribute to the same end goal of cell death, or if they are both activated during similar conditions but with opposing commitments. The purpose of this literature review is to first discuss the regulation of skeletal muscle developmental and regenerative processes and how they are influenced by cell stress and apoptotic signaling. Second, it will outline the machinery and regulation of apoptosis and autophagy with a special emphasis on skeletal muscle where possible. Finally, this review will discuss the controversy regarding the role of autophagy in cell death processes and skeletal muscle biology/physiology.

Skeletal Muscle Differentiation and Myotube Formation Requires Cell Stress and Apoptotic Signaling

The determination of embryonic progenitor cells and satellite cells into a committed myogenic cell type, and the fusion of these myoblasts to produce mature myotubes requires the hierarchical induction and transcriptional activity of a specific set of basic helix loop helix (bHLH) transcription factors collectively known as myogenic regulatory factors (MRFs)[15]. The expression of myogenic determination protein (MYOD) and myogenic factor-5 (MYF-5), two bHLH transcription factors, results in the formation of a committed myogenic cell known as the myoblast[16]. In the absence of MYOD skeletal muscle develops with minimal abnormalities; however, a prolonged and 4-fold compensatory increase in MYF-5 expression drives the formation of myoblasts and the production of mature skeletal muscle[17]. In contrast, MYF-5$^{-/-}$ mice die at birth due to breathing difficulties and rib defects, yet skeletal muscle is formed and MYOD expression is not impaired[18]. However, MYOD$^{-/-}$:MYF-5$^{-/-}$ double knockout mice are immobile and die soon after birth with no detectable levels of muscle specific gene expression or myoblasts[19]. These results highlight a partial redundancy between these primary MRFs and during embryonic development but also demonstrate that their expression is essential for the determination of skeletal myoblast. Satellite cells are non-committed myogenic precursor cells which have a remarkable ability to promote regeneration of damaged skeletal muscle by re-entering the cell cycle, committing to a skeletal myocyte lineage, differentiating, and fusing with the damaged fiber or producing a new myotube[16]. Following a similar genetic program as found in myogenesis, satellite cells begin to express primary MRFs following muscle injury. Interestingly, MYOD$^{-/-}$ mice have a reduced capacity to regenerate skeletal muscle in a number of injury models and have a lack of differentiated myoblasts[20]. Furthermore, in adult skeletal

muscle following injury there is an increased number of undifferentiated satellite cells in MYOD null mice[20]. Collectively, these data suggests that primary MRFs such as MYOD and MYF-5 are essential for the determination and production of myoblast cells prior to the formation of myotubes during development and in mature skeletal muscle.

MRFs contain a conserved DNA binding domain that binds to E-Box motif and promotes transcription of several myogenic specific genes required for the formation of mature skeletal myotubes[21]. For example, the expression of secondary MRFs such as myogenin and MRF4 are impaired in MYOD:MYF-5 double knockout mice supporting the hierarchical expression of MRFs during myogenesis and myoblast differentiation[17-19]. Similarly, ablation of myogenin results in embryos with an increase in myoblast content, normal levels of MYOD and MYF-5, but a total lack of myofibers and death at birth[22]. Both myogenin as well as MRF4 are responsible for the activation of the terminal differentiation program, myoblast fusion, and expression of muscle specific proteins such as creatine kinase and myosin heavy chain[21,22]. Myogenin levels transiently increase as muscle cells become terminally differentiated and as myogenin expression attenuates, there is an increase in MRF4 protein for several days to ensure terminal differentiation[21,23-25]. In addition to myogenin and MRF4, primary MRFs such as MYOD promote the expression of myogenic enhancing factors (MEFs) which are transcription factors that also play vital roles in controlling muscle-specific proteins[16,21]. Furthermore, MEF-2 sites are found within the promoter regions of muscle specific genes such as myogenin suggesting an amplification loop to ensure proper and terminal differentiation of myoblasts[26].

Myoblast differentiation is associated with a number of stress-related events which are typically associated with cell death. First, significant remodeling and reprograming of organelles and organelle networks not only occurs with myoblast differentiation, but is essential for the

development of healthy myotube formation. For example, myoblasts contain endoplasmic reticulum (ER) which undergos a transition to sarcoplasmic reticulum during myotube formation[27]. ER remodeling can result in promotion of ER-stress signaling, toxic levels of cytosolic calcium, and the prolonged activation of MAPKs resulting in increased apoptotic protease activity[28]. However, myoblast fusion requires the induction of ER-stress and cells which fuse to form myotubes following regulated ER-stress pathways are less sensitive to apoptosis as a mature muscle[29,30]. In addition, increased mitochondrial reactive oxygen species (ROS) generation and mitochondrial fission occur during early stages of myoblast differentiation[31,32]. These events are commonly associated with increases in apoptotic signaling and cell death[33]. However, inhibition of mitochondrial ROS or fission during myoblast differentiation impairs myotube formation and terminal differentiation. This suggests that these potentially apoptotic precursors are required for myoblast differentiation and survival[32,34]. Furthermore, remodeling of the cell membrane is essential for the fusion of myoblasts and the formation of a syncytial cell type. A process integral to this hallmark morphological transition from a myoblast to a myotube is the exposures of phosphatidylserine (PL) residues[35]. Typically PL exposure occurs with apoptotic cell death and signals the removal of apoptotic bodies via macrophages[36]. However, in muscle differentiation PL exposure is required in the development of the tissue and not its destruction[35,36].

In addition to significant remodeling, myogenic differentiation requires the activation of a number of signaling pathways to enhance the activity of MRFs. Interestingly, many of these pathways are best characterized as responses to, or factors contributing to, cell stress/death[2,30,31,34,37]. For example, the activation of the MAPK family protein p38 is associated with cell stress and can promote the induction of cell death[37,38]. However, activation of p38 is

required for myoblast differentiation as it enhances the transcriptional activity of both MYOD and MEF2a/c[37,39]. Furthermore, the activation of apoptotic signaling pathways is required for the promotion of myoblast differentiation[2,29]. The induction of CASP3 classically results in cell death. However, tightly regulated induction of CASP3 is required for myoblast differentiation and myoblast fusion through cleavage mediated activation of mammalian sterile twenty-like kinase (MST); a factor which enhances the activity of MRFs[2]. How CASP3 is regulated during myoblast differentiation is not well understood. However, research suggests that the induction of ER-stress induced caspase-12 is involved in CASP3activation during differentiation, further supporting the promotion of a required "cell death" signaling during myoblast differentiation.

A number of alterations occur throughout the determination as well as the differentiation process to protect against cell death. For example, the expression of MRFs and the promotion of myogenesis in both embryonic development and during muscle regeneration required the expression of paired box (PAX) transcription factors such as, PAX3 and PAX7 respectively[16,21]. The expression of PAX3 during embryogenesis mitigates the number of apoptotic cells within the somite and neural tube but also increases the expression of both MYOD and anti-apoptotic BCL2 proteins in myogenic precursor cells[40,41]. Furthermore, anti-apoptotic protein X-linked inhibitor of apoptosis (XIAP) is attenuated during differentiation whereas apoptosis repressor with caspase recruitment domain (ARC) is upregulated upon differentiation[42]. Upon myoblast differentiation, autocrine upregulation of IGF-II requires MTOR-mediated transcriptional events and results in an increase of protein kinase B (AKT)1/2 activity[43,44]. AKT activity promotes myoblast differentiation through the negative regulation of FoxO transcription factors as well as promotion of MRF activity[45,46]. Furthermore, the activation of AKT also enhances the resistance to cell death and prevents anoikis during myoblast differentiation through the post-translational

regulation of BCL2 proteins such as Bad[47,48]. In addition, myoblast differentiation requires the transition from a predominantly glycolytic cell type to a myotube generating ATP predominantly through aerobic metabolism[49-51]. An important signaling factor in this transition is AMP-activated protein kinase (AMPK)[52]. Accordingly, AMPK subunits are upregulated during differentiation and are suggested to promote the reprogramming of primary substrate utilization[53]. However, the increase in AMPK is also required to provide resistance to cell death induction in newly formed myotubes[53]. Similarly, the induction of c-Jun N-terminal kinase (JNK) in response to diverse types of cell stress can contribute to cell death[54-56]. However, the transient induction of JNK during myoblast differentiation has been shown to enable myoblast survival during differentiation[57]. Taken together, myoblast differentiation is a highly regulated process and requires potentially lethal signaling cascades to ensure hierarchical regulation of MRFs, in addition to significant organelle and structural remodeling. A thorough understanding on the regulation of cell death processes during myoblast differentiation may enhance our ability to promote muscle formation during embryogenesis as well as following myotrauma or apoptotic events.

Apoptosis Machinery and Regulation

Apoptosis is classically defined by morphological changes to the cell including chromatin condensation, cell shrinkage, and membrane blebbing[36]. In these terms, mature skeletal muscle apoptosis is anything but classical. For example, apoptosis in skeletal muscle is commonly known as myonuclear apoptosis, a process which is proposed to result in the destruction of individual myonuclei along with the associated myonuclear domain[58]. As a result, the loss of the myonuclear domain attenuates fiber size while maintaining a consistent myonuclear number to cytoplasmic volume[58,60]. Over the past decade evidence has challenged this concept suggesting

that “apoptosis” in skeletal muscle does not occur[61,62]. Although the morphological hallmarks of apoptosis may differ in skeletal muscle, apoptotic signaling does occur within the myofiber[59]. With over 400 cellular substrates, caspases, such as CASP3, are the primary proteolytic enzyme involved in apoptotic signaling[4]. Caspases can cleave architectural proteins and induce cellular remodeling, cleave enzymes and proteins within the nucleus to inhibit DNA repair processes, as well as alter membrane proteins and contractile proteins in order to induce membrane blebbing and targeting for infiltrating immune cells[36,63]. Considering the lethality of active caspases, the induction of such cell death effector enzymes are tightly controlled by several highly conserved signaling cascades[36]. Moreover the activation of caspases in skeletal muscle has significant consequences related to muscle remodeling and function[6,59].

The induction of apoptosis in skeletal muscle typically occurs through two primary pathways; the extrinsic death-receptor pathway as well as the intrinsic or mitochondrial mediated pathway[36,59]. Briefly, the death-receptor pathway is an extracellular signaling pathway initiated through the binding of cell death ligands to a transmembrane death receptor resulting in the formation of a death inducing signaling complex (DISCs) and the activation of apical CASP 8/10[64]. Activation of CASP8/10 promotes the cleavage-mediated activation of death effector caspases such as CASP3[64]. In a number of cell types, cell death signaling from extrinsic pathways may not be sufficient to induce apoptosis and therefore CASP8 or 10 enzyme activation must truncate pro-apoptotic BCL2 proteins such as BID in order to promote the activation of intracellular death pathways mediated by the mitochondria[36,65]. Mitochondria are the central component of the intrinsic pathways of apoptosis and are especially important in skeletal muscle apoptotic signaling[66]. Mitochondria participate in apoptosis through the release of apoptotic proteins such as CYTO C, second derived activator of caspases (SMAC), apoptosis

inducing factor (AIF), and endonuclease G (Endo G)[67]. Within the mitochondria these factors do not participate in apoptotic signaling and require mitochondrial outer membrane permeabilization (MOMP) and remodeling of the inner mitochondrial membrane (IMM) prior to their release[67]. The induction of MOMP largely depends on presence and function of the BCL2 family of proteins[68]. The BCL2 family is divided into two groups; the anti-apoptotic proteins such as BCL2 and BCLXL, and the pro-apoptotic proteins which include BAX and BAK as well as the BH-3 only proteins such as BAD, PUMA, BNIP3 and BID which activate BAX and BAK[68]. MOMP can result from BAX/BAK induced mitochondrial apoptosis channel (MAC) formation[68]. BAX activation by upstream BH-3 proteins promotes the translocation of BAX to the mitochondria. Here, BAX undergoes a conformational change required to support oligomerization with additional mitochondrial bound BAX molecules[69]. On the other hand, BAK is constitutively localized to the outer mitochondrial membrane (OMM) even though it is in an inactive form. Activation of BAK exposes a BH-3 domain and a BCL2 binding groove which promotes the formation of BAK dimers required for MOMP[70]. In cell free systems, BAX/BAK can permeate lipid membranes by forming both proteinaceous channels composed of multiple BAX/BAK oligomers or and/or lipidic pores free of BAX/BAK proteins[69,71]. In skeletal muscle the opening of the mitochondrial permeability transition pore (mPTP) has been extensively studied and implicated in cell death signaling[66]. The mPTP is active at a low conductance to maintain an appropriate membrane potential $\Delta\Psi$ in order to facilitate cytosolic Ca^{2+} buffering and the production of ATP[72]. The mPTP spans the OMM to the mitochondrial matrix and is composed of the voltage-dependent anion channel (VDAC), the adenine nucleotide translocase (ANT), and cyclophilin D (Cyp D)[73]. mPTP opening occurs due to: i) increased uptake via the mitochondrial Ca^{2+} uniporter, ii) high levels of ROS produced from the mitochondrial electron

transport chain and other cellular compartments and iii) stimulation of VDAC and/or ANT by BAX/BAK[66,74,75]. mPTP opening causes a massive influx of high molecular weight solutes directly into the matrix, leading to swelling of the IMM and to physical rupture of the OMM [66,76].

A number of factors can protect the cell from MOMP through interactions with pro-apoptotic BCL2 proteins. First, upstream BH-3 proteins are required for the activation of BAX/BAK[68]. BH-3 proteins are activated via transcriptional upregulation following intracellular stress events such as ER-stress and DNA damage[68,77]. The activity of BH-3 proteins can also depend upon phosphorylation status mediated by PI3K/AKT activity and MAPKs[55,78-80]. Furthermore, proteolytic cleavage mediated by CASP8 can also activate BH-3 proteins[81]. The mechanisms which BCL2 proteins interact with each other in order to induce, or protect from MOMP is unclear. Although the activation of BAX/BAK by BH-3 proteins is an important step in potentiating apoptosis, an increase in BAX/BAK expression relative to the level of anti-apoptotic BCL2 proteins can also promote apoptosis[68]. For example, hindlimb suspension causes a significant increase in BAX and a reduction in BCL2, which is associated with an increase in CYTO C release and DNA fragmentation[82]. The anti-apoptotic protein ARC can inhibit MOMP through direct inhibitory interactions with cytosolic BAX which blocks BAX translocation to the mitochondria[83]. Heat shock protein 70 (Hsp70) can also inhibit MOMP by inhibiting the c-Jun N-terminal kinase (JNK)-mediated phosphorylation of BID as well as inhibiting BAX activation, AIF nuclear translocation as well as directly impairing the activation of CASP3[84-88]. Together, anti-apoptotic BCL2 proteins, ARC, and Hsp70 can mitigate apoptosis by inhibiting the upstream events leading to MOMP.

The release of apoptotic factors from the mitochondria followed by the activation of caspases represents a biochemically defining moment in apoptosis and typically marks the point

of no-return in cell death[89]. Differential kinetics and temporal regulation of the release of apoptotic factors from the mitochondria suggest that different stimuli induce different pores which mediate the release of selective proteins. For example, the formation of BAX/BAK pores promotes the initial release of CYTO C and SMAC over the release of AIF and ENDOG [90]. Interestingly, the release of CYTO C and SMAC occurs simultaneously suggesting the release from a common source[90]. The full release of CYTO C and SMAC promote the activation of CASP9 followed by CASP3 and ultimately apoptosis[36]. For the activation of caspase-independent cell death, the release of AIF and ENDOG must occur[91,92]. The release of AIF can occur following BAX activation and induction of mPTP opening[91,93]. It is important to note that pro-apoptotic proteins such as AIF and CYO C while residing within the mitochondria during basal states are essential for normal mitochondrial function. Therefore, not only does the release of these apoptotic proteins induce cell death signaling, but it also impairs mitochondrial function and can induce secondary damage through increased ROS generation and metabolic stress[94].

A significant stage in mitochondrial-mediated apoptosis occurs with the activation of the apoptosome and CASP9 activation[95,96]. The apoptosome is an assembly of apoptotic protease activating factor (APAF1), CYTO C, dATP/ATP, and proCASP9[96,97]. In the cytosol, CYTO C binds to APAF1, which is followed by the hydrolysis of dATP or ATP when available in high concentrations[96,97]. The hydrolysis of dATP or ATP extends the conformation of APAF1, which unblocks the caspase recruitment domain (CARD) and the recruitment of proCASP9 via its N-terminal CARD domain[98,99]. The high concentration of proCASP9 at the apoptosome promotes proximity induced dimerization and activation of CASP9[98,99]. However, the release of smac is required to inhibit XIAP which constitutively suppresses caspase dimer formation through direct interactions with proCASP9 as well as CASP3[100]. Additionally, Smac must also bind to and

remove XIAP from directly blocking the catalytic site on active and inactive CASP3/7[101]. Furthermore, heat shock protein 70 (HSP70) can also bind to AIF following the release from the mitochondria and inhibit its translocation to the nucleus where it can promote caspase-independent DNA fragmentation and apoptosis[84]. Considering the major impact apoptosis has on cell physiology, viability, and ultimately tissue formation and function, a number of regulatory mechanisms have evolved to regulate apoptotic activity. However, apoptosis is only one form of cell death. Autophagy or "type II cell death" is a paradigm that has been proposed, and its regulation is also fundamental to the muscle cell viability and function.

Autophagic Machinery and Regulation

Macroautophagy is a process in which a double membrane structure, known as the phagophore, is produced and begins to sequester a portion of the cytoplasm[8,9]. The phagophore elongates and engulfs the cytosolic constituents forming a double membrane structure known as the autophagosome which contains the autophagic cargo to be degraded[8,9]. The mature autophagosome binds with the lysosome then the inner membrane and autophagic cargo become degraded via lysosomal hydrolases and cathepsins[8,9]. The degraded cargo is then recycled back into the cytosol to be reused for metabolic and biogenesis purposes[8,9]. Although multiple forms of autophagy are documented, the focus of the proposed research will be on macroautophagy, herein referred to as autophagy. Evidence suggests that autophagy in skeletal muscle is peculiar when compared to other tissues. For example, skeletal muscle has a particularly high level of basal and starvation-induced autophagy compared to other tissues[102]. In addition, the induction of autophagy in skeletal muscle can be both rapid and enduring suggesting both rapid post-translational and prolonged transcriptional regulation[102-104]. Furthermore, the induction of autophagy and the rate of autophagosome formation and flux differ significantly across muscle

types[105]. Importantly, the induction as well as inhibition of autophagy in skeletal muscle induces deleterious alteration to muscle function, viability, and size[1,13,104,106].

The induction of autophagy requires the activity of a multi-protein complex composed of BECN1, VPS34, VPS15, and AMBRA1which will herein be referred to as the BECN1 complex. Assembly of the BECN1 complex promotes the activation of VPS34 and the production of phosphatidylinositole–3 phosphate (PI(3)P)[8]. The formation of PI(3)P results in the recruitment of lipid adaptor proteins, double FYVE-containing protein 1 (DFCP1) and WD repeat domain phosphoinositide-interacting protein (WIPI) required for the localization of downstream autophagic membrane proteins [107,108]. PI(3)P production is critical for autophagosome formation in skeletal muscle. For example, the phosphoinositide 3-phosphatase, JUMPY, can reduce PI(3)P production and negatively regulate autophagy during nutrient starvation in C2C12 myoblasts[109,110]. In addition, inhibition of autophagy can be accomplished by administration of 3 methyladenine (3MA) to inhibit PI(3)P production[111,112].

A number of proteins can regulate the production of PI(3)P production by interacting with the BECN1 complex. Interestingly, BECN1 was originally discovered as a member of the BCL2 family due to the possession of a BH-3 domain[113,114]. Therefore, it was hypothesized that anti-apoptotic proteins such as BCL2 and BCLXL may be able to regulate autophagy in response to various stress stimuli. When BCL2 is bound to BECN1, Vps34 activity is suppressed and autophagy is reduced[113]. The affinity of BCL2 and BCLXL for BECN1 is relatively low[115]. As such, competitive binding of BCL2/BCLXL by other BH-3 only proteins such as BAD, BIK, NOXA, PUMA, BIM-EL, and BNIP3 which have a greater affinity to the anti-apoptotic BCL2 proteins, disrupts the interaction between BCL2 and BECN1[116,117]. For example, knockdown of Bad impairs starvation-induced autophagy and knockdown of BCL2 can result in an increase in

autophagy[116,118]. Together, these data suggest that the content of BCL2-related proteins may influence autophagy induction. Changes to autophagy in skeletal muscle are also associated with altered BECN1 and/or BCL2 family proteins[13,103,119-124]. For example, increases in autophagic markers are associated with a reduction in BCL2 protein content in the white gastrocnemius of the hypertensive rats (McMillan et al. 2014, unpublished data). Autophagy induction mediated through the BECN1 complex also involves post-translational modification of either BECN1 and/or BCL2/BCLXL[125]. Phosphorylation of BCL2 by JNK1 during starvation and exercise is essential for autophagy induction[103,126]. In support of these findings, increased markers of autophagy induction are associated with an increase in BCL2 phosphorylation in skeletal muscle (McMillan et al. 2014, unpublished data). Dissociation of BCL2/BCLXL from the BECN1 complex also occurs with direct modification to the BECN1 protein[125,127,128]. For example, the death associated protein kinase (DAPK) phosphorylates BECN1 resulting in its disassociation from BCLXL and/or BCL2[127,128]. Furthermore, toll like receptor – 4 (TLR-4) stimulation resulted in the recruitment of BECN1 to the tumor necrosis factor receptor (TNFR1) associated factor 6 (TRAF6) and subsequent ubiquitination. The ubiquitination of BECN1 ultimately increases Vsp34 kinase activity and autophagy[129,130].

In addition to the BECN1 complex, the ULK1/2 kinase complex is also involved in the induction stages of autophagy[8,9]. Under basal states where nutrients are abundant, the ULK1/2 complex, composed of ATG13, ATG10, and FIP200, is inhibited though interactions with TORC1 of the mTORC1 complex[131]. Under nutrient poor conditions low mTOR activity results in the disassociation of mTOR from the ULK1/2 complex and the autophosphorylation of ULK1/2 as well as ULK1/2-mediated phosphorylation of ATG13 and FIPP200 which stabilizes the protein complex and promotes autophagy[132,133]. Once the ULK1/2 complex has been

activated, ULK1-mediated phosphorylation of FIP200 promotes the localization of the complex to the site of autophagy induction[133,134]. However, the downstream targets of the mammalian ULK1/2 kinase complex have not been fully elucidated. One study has shown that the ULK1/2 complex can phosphorylate AMBRA1 of the BECN1 complex to enhance autophagy induction[135].

Once BECN1 and the ULK1/2 complexes have created products for the initial membrane, this pre-autophagosomal membrane is elongated by two ubiquitin-like conjugation systems; ATG12-ATG5 and LC3B-PE. First, the assembly of a protein complex composed primarily of ATG12-ATG5-ATG16 develops E3 ligase-like activity required for the lipidation of the autophagosome[136,137]. The first conjugation step in this reaction is the activation ATG12 via E1-like enzyme ATG7[138]. This is followed by the conjugation of ATG12 to ATG5 through the E2-like activity of ATG10[139]. The ATG12-ATG5 conjugate is then bound to ATG16[137]. This newly produced E3-like enzyme complex translocates to the developing autophagosomal membrane. There, it assists in the localization of the second conjugation system as well as localizing integral autophagosomal membrane proteins such as LC3B-II to both the inner and outer autophagosomal membrane[8,137,111,112]. The production of LC3B-II involves the second conjugation system which is required to bind LC3B-I to phosphatidylethanolamine (PE) producing LC3B-II. First, LC3B is cleaved by ATG4 producing LC3-I which can now bind to PE[140]. Following activation by the E3-like enzyme ATG7, LC3B-I is conjugated to PE by the E2-like activity of ATG3 producing a lipidated LC3BI also referred to as LC3B-II[141]. Alterations to the production of these ubiquitin-like conjugation systems can dramatically affect skeletal muscle autophagy. For example, knockdown of ATG7 results in impaired autophagy and inhibition of LC3B-II production in both basal and challenged states[1]. Furthermore, knockdown of ATG5 results in attenuated

autophagosomes in a model of Pompe's disease[142]. Moreover, a reduction in ATG12-ATG5 conjugation is associated with reduced autophagy in exercised mice treated with doxorubicin[123]. Together, both conjugation systems permit the elongation and maturation of the double membrane autophagosome and the complete sequestration of targeted autophagic cargo.

Autophagy was originally thought of as a bulk degradation system, sequestering large portions of the cytosol in a non-specific manner. However, research shows that autophagy is far more sophisticated and specific. Autophagy adaptor proteins are responsible for selecting targets and either directing them to the autophagosome or tethering autophagic substrates to proteins of the autophagosomal membrane[143]. In this way, cargo may be delivered to the autophagosomal membrane. In addition, given the number of sources for phagophore development, it is also possible that the development of the membrane may be localized to the site of cargo recognition. Regardless, several post-translational modifications of organelle membrane proteins and aged/damaged proteins are important in selective autophagy[144-148]. For example, damaged proteins and organelles can be targeted for ubiquitination. This post translational modification allows the substrate to be located and bound by an autophagy specific adaptor protein such as sequestrasome (SQSTM1/p62) and/or NBR[147,149,150]. As these adaptor proteins bind to one side of the ubiquitinated protein/organelle the other binds to autophagosomal-specific proteins such as LC3B or GABARAP[147]. Both the adaptor protein and selected cargo become engulfed by the autophagosome and degraded[150]. As such, adaptor protein content measured by western blotting, flow cytometry, or immunohistochemistry are commonly used to determine autophagic flux as a reduction in adaptor protein can reflect an increase in the degradation of autophagic material[111,112].

In the late stages of autophagy, the mature autophagosome fuses with the lysosome, and the lysosome degrades the autophagic cargo[151]. Binding of LC3 on the outer membrane of the autophagosome and to dynein along microtubules has been suggested to mobilize the autophagosome towards cellular pools rich in lysosomes[152,153]. Fusion of the autophagosome with the lysosome produces a morphologically distinct structure called the autophagolysosome[9]. In this structure the outer membrane of the autophagosome is bound to the lysosome and the inner membrane and autophagic cargo is exposed to the lumen of the lysosomal. This allows cathepsins and other proteolytic hydrolases to degrade the autophagic cargo and inner membrane while the outer autophagosomal membrane is recovered via ATG4[8]. The release of degradative products can be used for energy metabolism, organelle biogenesis as well as negatively regulating autophagy through activation of mTOR and mitigation of metabolic stress[154,155].

The Involvement of Autophagy in Cell Death

The induction of cell stress caused by nutrient or growth factor deprivation, ER/SR-stress, hypoxia, oxidative stress, DNA damage as well as mitochondrial damage can induce an autophagic response[11,12,104,148,156-159]. Considering these cell stresses can produce an apoptotic or even necrotic response, cell stress at high levels is also often accompanied by the induction of autophagy and cell death mechanisms. The association of autophagy in dying cells has led to a paradigm of autophagic cell death[11]. Autophagic cell death is defined by morphological features such as the accumulation of autophagosomes within a dying cell that is not associated with chromatin condensation or phagocytosis of blebbing cell bodies[11]. However, the term "autophagic cell death" has led to the interpretation of cell death being executed by autophagic processes which may be a misinterpretation in certain situations[11]. The direct induction of cell death by autophagy is rarely observed in many contexts. One mechanism in which autophagy has

been suggested to induce cell death is through the degradation of critical regulators of the anti-apoptotic/stress response. For example, upon prolonged exposure to ROS the induction of autophagy was shown to potentiate cell death by degrading the antioxidant catalase[160]. Under certain circumstances autophagy can in fact directly contribute to cell death. Overexpression of ATG1 in drosophila fat and salivary glands results in the massive induction of autophagy and cell death[161]. Interestingly, cell death was inhibited by a loss of ATG8 which also suppressed autophagy, suggesting that in this case autophagy contributed to cell death[161]. Furthermore, cell death was also mediated by apoptotic processes since CASP3 or p53 inhibition mitigated cell death in fat cells[161]. In this model of autophagic cell death, the over-activation of autophagy promoted cell death through the utilization of apoptotic machinery. Signs of autophagic cell death are also found in apoptotic resistant cell types suggesting autophagic cell death can be independent of apoptosis. For example, apoptosis resistant $BAX^{-/-}$:$BAK^{-/-}$ fibroblasts use autophagic machinery to induce cell death when treated with apoptotic inducers such as etoposide[162]. These results suggest that autophagy may indeed directly induce cell death when apoptosis is compromised. It is noteworthy that these effects may be tissue specific as well as dependent upon the trigger of cell death[12]. For example, hematopoietic cells of the same genetic background ($BAX^{-/-}$:$BAK^{-/-}$) undergo a prolonged activation of autophagy as a result of growth factor withdrawal or nutrient suppression. Instead of cell death, the induction of autophagy in this condition is related to cell survival since knockdown of autophagy proteins result in increased cell death[163]. Moreover, apoptotic death can occur in response to starvation, growth factor withdrawal, hypoxia, heat shock, DNA damage, and ER-stress. Interestingly, autophagy has been shown to occur during these conditions as well. However, in these situations autophagy has been shown to protect the cell or at least prolong cell viability[156,163-167].

The role of autophagy in cell death is further complicated by the dual role of autophagy related proteins. For example, caspase activation can cleave BECN1 which not only inhibits the activation of autophagy, but produces a truncated version of BECN1 that contributes to MOMP[168,169,170,171]. Normal autophagy induction relies on the recycling of ATGs from the autophagolysosome to rapidly produce more autophagosomes following lysosomal fusion. Interestingly, CASP3-mediated cleavage of ATG4 inhibits autophagy and promotes apoptosis. Research has also demonstrated that the cleaved product of ATG4 changes its localization and directly induces apoptosis via mitochondrial-mediated pathways[172]. Furthermore, Pyo et al. found that the interactions between ATG5 and FADD can produce a truncated form of ATG5 which promotes MOMP[173]. Data by Yousefi et al. support these findings by showing an apoptotic role of ATG5 following cleavage by calpains. The 24 kDa ATG5 fragment translocates to the mitochondria and participates in MOMP through interactions with anti-apoptotic protein BCLXL[174]. In certain contexts and cell types the induction of autophagy can mitigate cell stress and attenuate apoptotic signaling through the removal of damaged proteins and organelles. However, the close induction kinetics and dual role of certain autophagy proteins also questions whether or not autophagy is strictly a protective adaptation to cell stress or a process which is attempting to promote apoptotic events.

The dual role of autophagy in skeletal muscle physiology and pathophysiology

The ambivalent role of autophagy in cell protection or cell death is extended to skeletal muscle research where autophagy as a promoter of muscle health or disease is controversial. The induction of autophagy in skeletal muscle and many other tissues has been described as a double edge sword. For example, the induction of autophagy can provide the cell with metabolic substrates in times of starvation and prevent cell death[166]. In contrast, such stress can lead to

muscle atrophy and dysfunction; an effect that is attenuated by the inhibition of autophagy[104]. As these examples demonstrate, the role of autophagy in skeletal muscle health and disease is controversial and suggest that autophagy can either be beneficial or deleterious.

Impairments to autophagy result in detrimental effects to skeletal muscle of mice during perinatal periods of life. For example, muscle-specific deletions of histone deacetylases 1 and 2 abolish autophagy induction and results in characteristics of a neonatal myopathy and perinatal lethality. Interestingly, both muscle defects and survival are rescued by high fat feeding during the weaning phase[175]. These data suggests that the lack of autophagy results in metabolic stress which can lead to the destruction of skeletal muscle during early stages of life. Furthermore, basal levels of autophagy in mature skeletal muscle are also essential for muscle homeostasis. For example, deletion of ATG7 in mature skeletal muscle inhibits basal and induced autophagy which promotes the development of myopathic phenotypes including impaired contractile force and muscle atrophy[1]. Regulation of autophagy via mTOR requires the upstream formation of the TSC1/2 complex. Similarly, TSC1-deficient mice develop a late onset myopathy characterized by degenerative myofibers, centrally located nuclei, and reduced muscle weight and constitutively active mTOR by 9 months of age. Mice lacking TSC1 have elevated basal mTORC1 activity as well as impaired basal and starvation induced autophagy. This produces a myopathic phenotype since inhibition of mTORC1 allows basal and starvation induced autophagy to occur and also restores muscle integrity[3]. The accumulation of damaged organelles and proteotoxicity accompanies several myopathies including Duchene muscular dystrophy and collagen VI-1a muscular dystrophy as well as sarcopenia[14,176,177]. In these models of muscle disease, the basal levels of autophagy are significantly attenuated which is proposed to promote a number of myopathic features. Accordingly, the forced induction of autophagy via a low protein

diet or genetic upregulation of autophagy proteins or signaling factors can ameliorate muscle inflammation, fibrosis, apoptosis, and myofiber damage as well as improve contractile strength in both sarcopenia and myopathic animals[14,176-178]. Collectively, these results show that deletion of autophagy in healthy mature skeletal muscle results in the buildup of toxic protein aggregates and impaired organelles which contribute to the development of myopathy. In myopathic conditions the reduction in basal autophagy also contributes to muscle impairments[179]. However, in both healthy and diseased skeletal muscle, upregulation of autophagic flux can effectively remove toxic protein aggregates, clear damaged organelles, and re-establish muscle viability and function[180,181].

In contrast, autophagy can also induce a number of deleterious changes to skeletal muscle function and size. Cachexic muscle wasting is associated with an increase in p38 kinase activity which promotes the upregulation of the catabolic processes including autophagy and apoptosis[13]. Collectively, the induction of these catabolic systems results in muscle dysfunction, diminished mass, and a rapid decline in protein synthesis[181]. Furthermore, when cultured myotubes are exposed to an apoptosis-inducing agent, myotubes undergo atrophy. Interestingly, myotube diameter can be recovered when myotubes are pre-treated with 3MA prior to the addition of apoptotic stimuli to culture media[106]. Similarly, overexpression of PGC1α in aged animal's results in lower autophagy as well as attenuated apoptosis, improved mitochondrial and contractile function, and increased muscle mass[182]. Muscle atrophy in a number of models including starvation and denervation can be abrogated through the inhibition of FOXO3A transcription factor[183]. Importantly, Massaerio et al. found that in addition to the upregulation of ubiquitin proteasome system (UPS) factors, FOXO3A signaling also induces autophagy related genes which directly contribute to muscle atrophy[1,183]. For example, the inhibition of BNIP3, a

transcriptional target of FOXO3A and a potent inducer of autophagy, mitigates autophagy and recovers muscle mass during several atrophic conditions[1]. These results demonstrate that the increase in autophagy occurs during muscle atrophy and has a direct role in promoting the loss of muscle mass and functional impairments.

Autophagy also contributes to the pathogenesis of a variety of myopathies. For example, Pompe's disease is caused by a mutation in the acid alpha-glucosidase gene resulting in an inability to breakdown glycogen via the lysosomal pathway. Autophagic vesicles containing glycogen accumulate and increase muscle dysfunction as well as impair enzyme replacement therapies[184]. By ablating autophagy through crossing Pompe's disease mice with ATG5-deficient mice, Raben et al. were able to mitigate muscle vacuolization and improve the effectiveness of enzyme replacement therapy[142]. Spinal and Bulbar myopathies as well as sporadic inclusion body myositis are characterized by increased autophagy with impaired flux resulting in vacuolated fibers, misaligned sarcomeres, and the accumulation of autophagic substrates[120]. It is possible that the inability to degrade autophagic cargo may result in a reduction of metabolic substrates and further promotion of cell stress through both metabolic and structural impairments. This in turn may stimulate an increase in apoptotic signaling where more catabolic events could result in a further requirement and perpetual induction of autophagy.

Statement of the problem

The induction of autophagy in skeletal muscle is currently described as the cliché double edged sword. In one situation promoting autophagy may improve the clearance of damaged organelles and proteins thus, reducing cytotoxity and promoting required turnover and biogenesis of cellular constituents. In contrast, the induction of autophagy can also promote muscle wasting as well as vacuolated fibers and misaligned contractile filaments, thus contributing to muscle

impairments. Also, indirect evidence exists which supports an association between autophagy and apoptosis in skeletal muscle. However, the relationship between autophagy and apoptosis in skeletal muscle has not been directly investigated and the conclusion that autophagy is a cell death process in skeletal muscle may be inaccurate.

Since cell death signaling is increased upon muscle damage/disease as well as during the myoblast differentiation process. A better understanding of the role of autophagy in apoptotic signaling during physiological processes such as myoblast differentiation could be useful in developing strategies to improve muscle development and regeneration. Furthermore, exploring the role of autophagy during pathological cell stress causing apoptotic signaling and atrophy will improve our understanding of the role of autophagy in the skeletal muscle cell stress response. Importantly, examining the cross-talk between autophagy and apoptosis will provide us with insight and basic knowledge of processes that regulate life and death of skeletal muscle. This thesis sought to test the hypothesis that autophagy contributes to cell protection against apoptotic signaling during physiological and pathological stresses occurring in response to myoblast differentiation and cisplatin-induced injury, respectively.

<u>The main objectives of this thesis are as follows:</u>

1. Determine if autophagy occurs during myoblast differentiation and if autophagy is required for differentiation.

2. Characterize the induction of autophagy in myoblast differentiation.

3. Elucidate signaling mechanisms involved in autophagy induction during myoblast differentiation.

4. Determine if autophagy protects the differentiating myoblast from apoptotic cell death.

5. Elucidate the direct role of autophagy in regulating apoptotic signaling during myoblast differentiation.

6. Characterize both apoptosis and autophagy in response to cisplatin-induced cell stress in differentiated myotubes.

7. Determine the role of autophagy in apoptotic signaling in response to submaximal levels of cell stress caused by cisplatin.

8. Determine if autophagy is altered during recovery from submaximal levels of cell stress in myotubes.

9. Examine the interplay between autophagy and apoptosis during recovery from submaximal levels of apoptotic stress in myotubes.

<u>The main hypotheses (and outcomes) of this thesis were:</u>

1. Autophagy will be increased during myoblast differentiation and required for the differentiation of myoblasts. Moreover, autophagy will be regulated by stress signaling.

(Our data support this hypothesis. Autophagy was increased during myoblast differentiation and was induced by JNK activity. Inhibition of autophagy impaired differentiation and increased cell death)

2. Autophagy is induced to regulate physiological levels of CASP activity

(Our data support this hypothesis. The induction of autophagy during myoblast differentiation is required to control CASP3 activity through the regulation of mitochondrial-mediated apoptotic signaling.)

3. In response to pathological apoptotic stress induced by cisplatin both autophagy and apoptosis will increase.

(Our data support this hypothesis. Autophagy was increased in conditions with elevated apoptotic signaling)

4. The induction of autophagy is required to protect from apoptotic signaling in response to submaximal levels of stress.

(Our data support this hypothesis. Inhibition of autophagy at submaximal levels of stress increased apoptotic signaling and promoted further determents to mitochondrial function)

5. Autophagy will be required to attenuate apoptotic signaling as the myotubes recovery from submaximal levels of apoptotic signaling.

(Our data support this hypothesis. An increase in autophagic flux was observed during recovery of myotubes which was required to improve mitochondrial viability and attenuate apoptotic signaling)

CHAPTER II – Autophagy is required and protects against apoptosis during myoblast differentiation

OVERVIEW

Several degradative systems assist in formation of multinucleated, terminally differentiated myotubes. However, the role of autophagy in this process has not been examined. GFP-LC3B puncta, LC3B-II protein, and LysoTracker fluorescence increased during C2C12 differentiation. Importantly, accumulation of LC3B-II protein occurred in chloroquine (CQ) treated cells throughout differentiation. Furthermore, BECN1, ATG7, and ATG12-5 protein increased, while SQSTM1/p62 protein was rapidly reduced during differentiation. A transient decrease in BECN1:BCL2 association was observed from D0.5 to D2 of differentiation. Chemical inhibition of JNK during differentiation reduced LC3B-II protein and GFP-LC3B puncta, and maintained BECN1:BCL2 association. Inhibition of autophagy by 3MA or shRNA against ATG7 (shAtg7) resulted in lower myosin heavy chain expression, as well as impaired myoblast fusion and differentiation. Interestingly, 3MA treatment during differentiation increased transient CASP3 activation, DNA fragmentation, and the percentage of apoptotic nuclei. Similarly, shAtg7 cells had increased DNA fragmentation during differentiation compared to controls. Collectively, these data demonstrate that autophagy increases and is required during myoblast differentiation. Moreover, autophagy protects differentiating myoblast from apoptotic cell death.

INTRODUCTION

Cellular differentiation is associated with rapid biochemical and morphological alterations as well as the removal of pre-existing structures and proteins. A rapid way to alter cell morphology, signaling pathways, genetic programs, and function is through the degradation of pre-existing structural and signaling proteins as well as organelles[131]. Previous work has shown that degradative processes are essential in the differentiation of myoblasts and in the formation of mature myotubes[185-187]. Although several degradative systems such as the ubiquitin proteasome system, calpains, and caspases are involved in myoblast differentiation, skeletal muscle formation requires organelle remodeling as well as significant morphological changes which may not be fully supported by these processes. In this case, myoblast differentiation may require the induction of autophagy; a bulk degradative process involved in the sequestration and targeted destruction of protein aggregates and superfluous/damaged organelles[8].

Alterations to autophagy have been observed during the differentiation of several cell types including osteogenic, mesenchymal, neuroblastoma, and glioma-initiating cells[188-190]. Interestingly, autophagy seems to be involved in the differentiation of cell types which require significant morphological and biochemical remodeling as well as cells which become terminally differentiated[131]. For example, erythroid cells undergo enucleation and removal of organelles during terminal differentiation[191]. Given these findings it seems likely that autophagy may play a role during myoblast differentiation; a process that involves significant remodeling

The induction of myoblast differentiation requires the activation of several signaling kinases which are also associated with the regulation of autophagy in skeletal muscle. For example, myoblast differentiation and myotube formation require AKT and MTOR signaling, two signaling kinases which inhibit autophagy in mature skeletal muscle[44,46,192]. In contrast,

differentiating myoblasts have altered AMPK activity. AMPK can induce autophagy through the activation of ULK1/2 as well as through the promotion of FOXO3A transcriptional activity[53,193]. In addition, myoblast differentiation is also associated with alterations to apoptotic proteins which could either induce or inhibit autophagy[125,194]. An understanding of processes involved in myoblast differentiation as well as how these processes are regulated is vital to optimize muscle development and regeneration. Therefore, the purpose of this work was to characterize alterations to autophagy during myoblast differentiation, and to investigate its regulation and potential role in myoblast differentiation and myotube formation.

METHODS

Cell culture and treatments

Mouse C2C12 skeletal myoblasts (ATCC) were plated between passes 2-5 in polystyrene cell culture dishes (BD Biosciences) or on gelatin (Sigma) coated coverslips in growth media (GM) consisting of low-glucose Dulbecco's Modified Eagles Medium (DMEM; Hyclone, Thermo Scientific) containing 10% fetal bovine serum (FBS; Hyclone, Thermo Scientific) with 1% penicillin/streptomycin (Hyclone, Thermo Scientific) and incubated at 37ºC in 5% CO_2. At 24 hr intervals, culture dishes were aspirated of GM, washed with warmed phosphate buffered saline (PBS; Hyclone, Thermo Scientific), and fresh GM replaced. At 80-90% confluence, differentiation was induced by replacing GM with differentiation media (DM) consisting of DMEM supplemented with 2% horse serum (Hyclone, Thermo Scientific) and 1% penicillin/streptomycin. Cells were collected as subconfluent myoblasts prior to DM addition (D0) as well as at 12 hrs (D0.5), 24 hrs (D1), 36 hrs (D1.5), 48 hrs (D2), 72 hrs (D3) and 120 hrs

(D5) following the addition of DM. Cells were removed from culture dishes by trypsinization (0.25% trypsin with 0.2g/L EDTA; Thermo Scientific), collected by centrifugation (800 x g for 5 min), resuspended/washed in PBS, and frozen at -80ºC until further analysis.

To measure autophagic flux over a full 24 hour period of differentiation[195,196], chloroquine salt (CQ) (Sigma-Aldrich) was added to warm media at a working concentration of 10µM for 24 hrs prior to collection of cells. To inhibit JNK activity 10µM SP600125 (LC Laboratories) was added to cell cultures in warm media and replaced every 24 hrs. Autophagy was inhibited by incubating cells with 5mM 3-methyladenine [3MA (Sigma-Aldrich)] and replaced every 24 hrs. In pilot experiments, 5mM 3MA was the lowest dose which attenuated LC3B-II production and did not have any effects on other PI3K targets such as AKT throughout the differentiation period (Appendix 1).

Transient expression of GFP-LC3B and stable knockdown of ATG7

C2C12 myoblasts grown on gelatin coated coverslips were transiently transfected with GFP-LC3B plasmid DNA generously provided by Dr. Terje Johansen (Institute of Medical Biology; University of Tromsø) to qualitatively examine the presence of autophagic puncta. Plasmid DNA was transfected into myoblasts once cultures reached 50-60% confluence using Lipofectamine 2000 (Life Technologies) according to manufactures instructions. Briefly, Lipofectamine 2000 (6µl) and plasmid DNA (3µg) were separately diluted in Opti-MEM (Gibco) and incubated at room temperature for 5 min. The diluted Lipofectamine and DNA solutions were complexed for 5 min at room temperature. Cells were washed twice with Opti-MEM. A total of 100µl of Lipo/DNA complexes (6µl/3µg) was added to 400µl of Opti-MEM for a final transfection volume of 500µl/well and incubated for 12 hrs at 37ºC with 5% CO_2. Transfection media was then aspirated and cells were washed 2x with warm PBS and incubated

overnight in GM. Once GFP-LC3B transfected cells reached 80-90% confluence they were treated with reagents discussed above and induced to differentiate. Glass coverslips of cells transfected with GFP-LC3B were removed from culture dishes, washed 2x in warm PBS and mounted on glass slides using Prolong Gold Antifade Reagent (Life Technologies).

The ATG7 (TR30017) and scramble (TR30013) HuSH-29 shRNA plasmids (Origene) were transfected into C2C12 cells using Lipofectamine 2000 (Life Technologies) according to the manufactures instructions. Stable clones were obtained using puromycin (Enzo Life Sciences), passaged, and characterized for ATG7 and LC3B protein content.

Fluorescence microscopy

For immunofluorescence analysis of myosin heavy chain expression cells were grown on glass coverslips in culture dishes and removed at indicated time points. Coverslips were washed 2 x 5 min with PBS. Cells were then fixed with 4% formaldehyde-PBS for 10 min at room temperature, and washed 2 x 5 min with PBS. Next, cells were permeabilized with 0.5% Triton X100 for 10 min, and washed 2 x 5 min in PBS. Cells were then blocked with 10% goat serum (Sigma-Aldrich) (in PBS) for 30 min, incubated with a primary antibody against myosin heavy chain (Developmental Studies Hybridoma Bank; MF20) diluted in blocking solution for 1 hr, and washed 2 x 5 min with PBS. An anti-mouse PE-conjugated secondary antibody (Santa Cruz) was diluted in blocking solution and incubated with cells for 1 hr, cells were then washed 2 x 5 min in PBS, counterstained with DAPI nuclear stain (Life Technologies) for 5 min, washed 2 x 5 min in PBS, and mounted with Prolong Gold Antifade Reagent (Life Technologies). The fusion index was calculated as the percentage of nuclei present in multinucleated (two or more nuclei) cells relative to total nuclei. The differentiation index was calculated as the percentage of cells expressing myosin heavy chain relative to total cell number.

To visualize lysosomal content, live cells were incubated with LysoTracker Red (LTR; 50nM) (Life Technologies) for 30 min. Cells were then washed 3 x 5 min in PBS and fixed with 4% formaldehyde-PBS, and counterstained with Hoescht NucBlue (Life Technologies) for 5 min at room temperature to visualize nuclei.

To image healthy and apoptotic nuclei, Hoechst NucBlue staining was conducted as follows. Cells were washed 3 x 5 in PBS and incubated in Hoechst NucBlue for 5 min at room temperature. Nuclei presenting with bright and fragmented nuclei were considered apoptotic while cells with round un-fragmented nuclei without signs of chromatin condensations were considered healthy. Cells were washed and mounted on glass slides using Prolong Gold Antifade Reagent (Life Technologies). Slides were visualized with an Axio Observer Z1 structured-illumination fluorescent microscope equipped with standard Red/Green/Blue filters, an AxioCam HRm camera, and AxioVision software (Carl Zeiss).

Immunoprecipitation

Immunoprecipitation of BECN1:BCL2 was performed using ImmunoCruz IP/WB Optima B system (Santa Cruz Biotechnology) according to the manufactures protocol. Briefly, 500µl of PBS, 50µl of suspended (25% v/v) IP matrix, and 5µg of BECN1 primary antibody (Santa Cruz) were combined and gently resuspended. Matrix:antibody complexes were formed overnight during rotation at 4ºC. Frozen pelleted cells were resuspended and lysed in 200µl of immunoprecipitation lysis buffer [(50 mM Tris; pH 7.9, 150 mM NaCl, 1 mM EDTA, 1% Triton X100), protease inhibitor cocktail (Roche Applied Sciences) and phosphatase inhibitor cocktail (Thermo Scientific)] on ice for 30 min while shaking. Protein assays were conducted using the BCA method. Matrix:antibody complexes were then centrifuged at 28000g for 1 min at 4ºC and washed twice in PBS. 500µg of cell lysates were added to the pelleted matrix:antibody complex

and gently resuspended. Matrix and lysates were complexed by overnight rotation at 4ºC. Matrix complexes were then centrifuged at 28000g for 1 min to pellet the matrix and the supernatant aspirated and discarded. The pellet was washed 3 x in PBS. After the last wash the pelleted matrix received 50µl of sample buffer containing sodium dodecyl sulfate (SDS) and boiled for 3 min at 95ºC. The IP pellet was then centrifuged at 28000g for 30 seconds and equal volumes of supernatant were loaded on a 12% SDS-PAGE gel and transferred onto PVDF membranes as described below.

Immunoblotting

Immunoblotting was conducted as previously described by our lab[197,198]. Briefly, cells were lysed in ice cold lysis buffer (20 mM HEPES, 10 mM NaCl, 1.5 mM MgCl, 1 mM DTT, 20% glycerol and 0.1% Triton X100; pH 7.4) with protease (Roche Applied Sciences) and phosphatase (Thermo Scientific) inhibitor cocktails. Equal amounts of cell lysates were loaded and separated on 7.5-15% SDS-PAGE gels, transferred onto PVDF membranes (Bio-Rad Laboratories), and blocked for 1 hr at room temperature or overnight at 4°C with 5% milk-Tris-buffered saline-Tween 20 (milk-TBST). Membranes were incubated either overnight at 4°C or for 1 hr at room temperature with primary antibodies against: AKT, pAKT (Thr^{308}), ULK1, pULK1 (Ser^{467}), FOXO3A, pFOXO3A ($Ser^{318/321}$), AMPKα, pAMPKα (Thr^{172}), BECN1, ATG7, ATG12-5, ATG4B, LC3B, pJNK1 (Thr^{183}/Try^{185}) (Cell Signaling Technology); BCL2, BCLXL, JNK1 (Santa Cruz Biotechnology); myogenin, myosin heavy chain (Developmental Studies Hybridoma Bank), SQSTM1/p62 (Progen Biotechnik), BNIP3, PIK3C3/VPS34, and Actin (Sigma-Aldrich). Membranes were then washed with TBST, incubated with the appropriate horseradish peroxidase (HRP)-conjugated secondary antibodies (Santa Cruz Biotechnology) for 1 hr at room temperature, washed with TBST, and bands visualized using enhanced

chemiluminescence western blotting detection reagents (BioVision) and the ChemiGenius 2 Bio-Imaging System (Syngene). The approximate molecular weight for each protein was estimated using Precision Plus Protein WesternC Standards and Precision Protein Strep-Tactin HRP Conjugate (Bio-Rad Laboratories). Equal loading and quality of transfer was confirmed by staining membranes with Ponceau S (BioShop). All immunoblotting was performed and quantified in duplicate.

Proteolytic enzyme activity assay and DNA fragmentation

Enzymatic activity of CASP3 was determined in cells using the substrate Ac-DEVD-AMC (Enzo Life Sciences). Cells were isolated as mentioned above (without protease inhibitor cocktail) and incubated in duplicate in black 96-well plates (Costar) with fluorogenic substrate at room temperature. Fluorescence was measured using a SPECTRAmax Gemini XS microplate spectrofluorometer (Molecular Devices) with excitation and emission wavelengths of 360 nm and 440 nm, respectively. CASP3 activity was normalized to total protein content and expressed as fluorescence intensity in arbitrary units (AU) per milligram protein.

DNA fragmentation, a hallmark of apoptotic cell death, was determined using the Cell Death Detection ELISA^{PLUS} Kit (Roche Diagnostics). Briefly, cells were collected as described above and homogenized in the supplied lysis buffer and centrifuged at 200 g for 10 min at room temperature. 20µl of supernatant was incubated with 80µl of anti-histone-biotin/anti-DNA-POD reagent in a streptavidin-coated microplate for 2 hours at room temperature with gentle shaking. Each well was then aspirated and washed several times followed by the addition of 100µl of ABTS substrate solution. Absorbance was measured at 405nm and 490nm with a SPECTRAmax Plus spectrophotometer (Molecular Devices). Absorbance was normalized to total protein content and expressed as AU per mg protein.

Statistical analysis

A One-Way repeated measure ANOVA was used to assess the effect of differentiation. If a main effect of differentiation was observed, Tukey's post hoc test was used to determined differences from D0 within each group independently. To examine differences between groups on specific time points (within the same day) a Students T-Test was used. $p<0.05$ was considered statistically significant.

RESULTS

Markers of autophagy are altered during myoblast differentiation

The induction of myoblast differentiation resulted in the appearance of GFP-LC3B puncta, indicating an increase in autophagosome formation (Fig. 1A). To quantify this observation we examined LC3B-I and LC3B-II protein content. Compared to D0, LC3B-II was elevated ($p<0.05$) on D1 and thereafter throughout differentiation, supporting the observed increase in GFP-LC3B puncta. In addition, non-lipidated LC3B-I protein content was greater on D2 ($p<0.05$) and D3 ($p<0.01$) relative to D0 (Fig. 1B). SQSTM1/p62 is an autophagic adaptor protein which can be degraded during increased autophagy[143] and thus has been used to determine autophagic activity[112]. In support of increasing LC3B-II protein and GFP-LC3B puncta, SQSTM1 protein was dramatically reduced in differentiating cells ($p<0.001$) (Fig. 1C).

The formation of the autophagosome requires the upregulation of several autophagy related proteins as well as the assembly of protein kinase complexes[8]. To determine if these autophagy related proteins are altered during differentiation we first measured the protein content of BECN1 and PIK3C3/VPS34, two proteins integral to the production of phosphatidylinositol

3-phosphate and the expansion of the autophagosomal membrane[8]. Although PIK3C3 was not significantly elevated during differentiation, BECN1 protein ($p<0.05$) increased throughout differentiation (Fig. 1D). The induction of autophagy is also associated with the activation of the ULK1 kinase complex[8]. Interestingly, an early increase ($p<0.001$) in ULK1 protein was observed (D0.5 vs D0); however, ULK1 protein levels returned to baseline on D1 and D2, and declined further on D3 ($p<0.05$) and D5 ($p<0.01$) (Fig. 1E). However, phosphorylation of ULK1 (Ser^{467}) and the resulting pULK1/ULK1 ratio did not differ significantly from D0 throughout differentiation.

The lipidation of LC3B requires activation through proteolytic modifications made by ATG4B[8]. LC3B-I is then activated by E2-like enzymes such as ATG7 and conjugated to phosphatidylethanolamine via the E3-like activity of the ATG12-5-16 conjugation complex[8]. During differentiation of C2C12 myoblasts, ATG4B protein levels were lower ($p<0.01$) on D5 vs D0 (Fig. 1F). In contrast, ATG7 and ATG12-5 protein were significantly elevated ($p<0.05$) throughout differentiation (Fig. 1F). Collectively, these findings suggested that upstream and downstream autophagy-related proteins are significantly altered during myoblast differentiation.

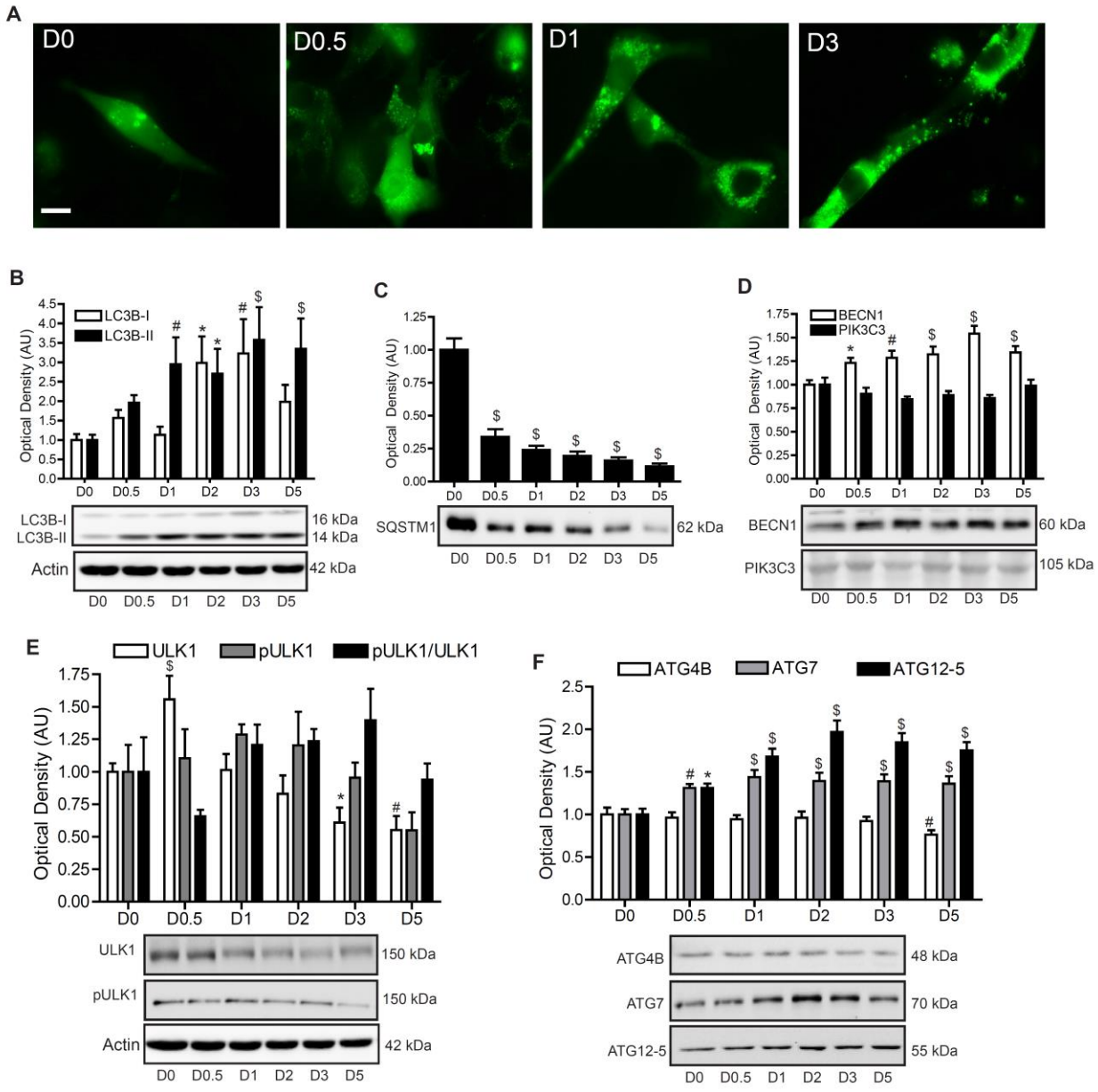

Fig. II - 1: Markers of autophagy are altered during myoblast differentiation

(A) Representative images of GFP-LC3B puncta in differentiating C2C12 myoblasts. Representative immunoblots and quantitative analysis of (**B**) LC3B-I and LC3B-II protein, (**C**) SQSTM1/p62 protein, (**D**) BECN1 and PIK3C3/VPS34 protein, (**E**) ULK and pULK1 (Ser^{467}) protein, and (**F**) ATG4B, ATG7, and ATG12-5 protein in differentiating myoblasts. Also shown are representative Actin loading control blots. Scale bar=10µm. A one-way ANOVA was used to examine the effect of differentiation. $^{*}p<0.05$, $^{\#}p<0.01$, $^{\$}p<0.001$ compared to D0; (*n*=3-6).

Increased lysosomal content and autophagic flux during myoblast differentiation

To determine if the changes to autophagic proteins were indicative of increased autophagic flux, we first investigated lysosomal content. We observed an increase ($p<0.05$) in LysoTracker fluorescence during differentiation (D0.5, D1, D3 vs. D0) (Fig. 2A & 2B). Interestingly, the LC3B-II/I ratio was not statistical different from D0 despite a 90% increase on D0.5 and a 50% increase on D1 (Fig. 2C). To ensure that the observed increase in LC3B-II protein and decline in SQSTM1 protein were due to increased autophagic flux, we treated cells for 24 hours with 10μM of CQ. Compared to non-treated cells, greater GFP-LC3B puncta along with an accumulation of LC3B-II protein ($p<0.001$) were observed in D0 myoblasts and differentiating cells (Fig. 2D & 2E). The accumulation of LC3B-II protein in D0 CQ treated cells suggests basal levels of autophagy are occurring in proliferating myoblast. However, the accumulation of LC3B-II in D0 myoblasts was significantly less ($p<0.001$) compared to differentiating cells (D1, D2, D3); providing evidence that autophagic flux is increased further during myoblast differentiation.

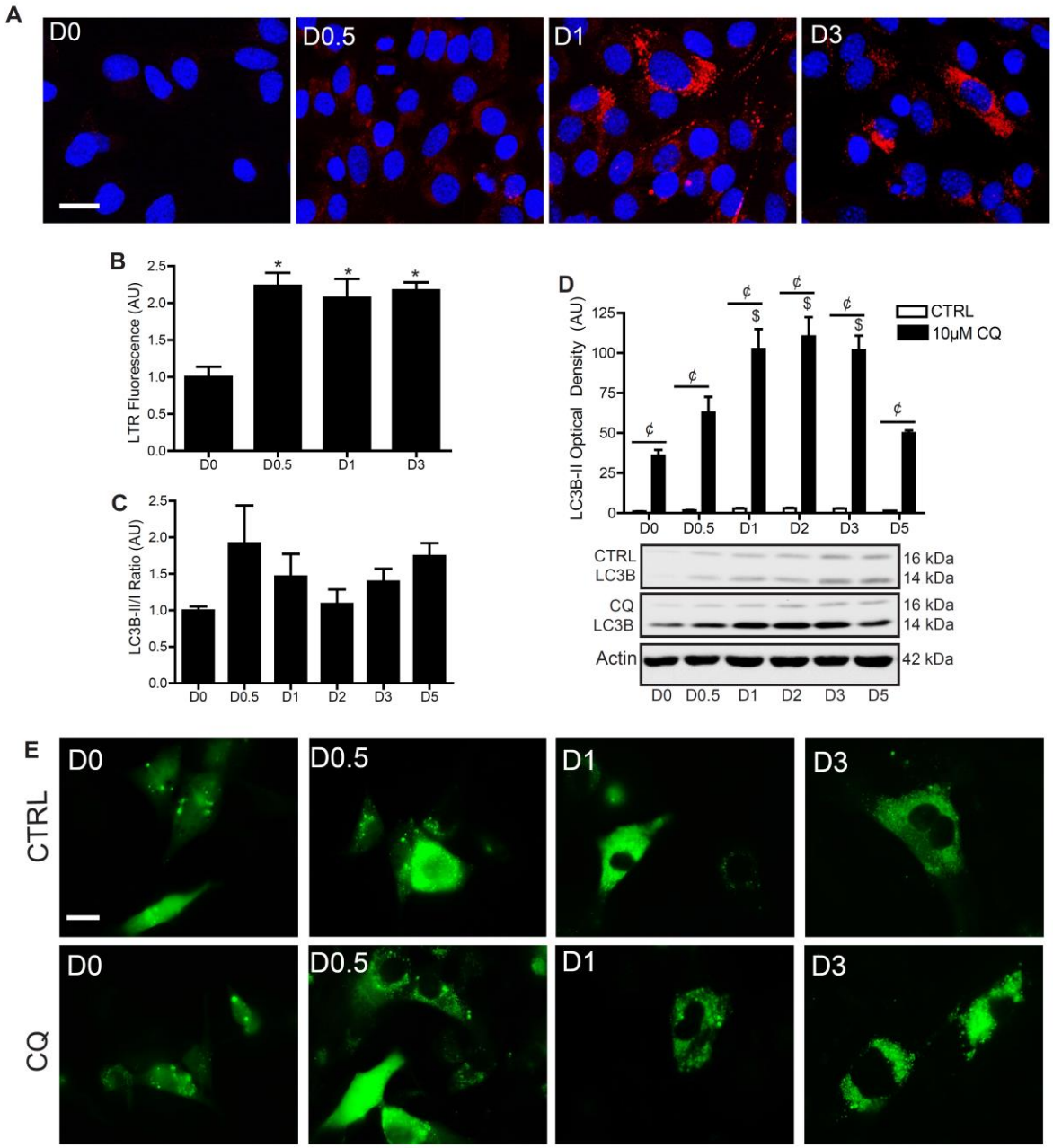

Fig. II - 2: Increase in lysosomal content and autophagic flux during myoblast differentiation

(**A**) Representative images of lysosomal content and, (**B**) quantitative analysis of LysoTracker Red fluorescence during myoblast differentiation. (**C**) Quantitative analysis of the LC3B-II/I protein ratio during myoblast differentiation. (**D**) Representative immunoblots of LC3B-I and LC3B-II as well as quantitative analysis of LC3B-II protein accumulation over 24 hours from CTRL and CQ treated C2C12 cells. LC3B CTRL and CQ experiments were conducted and blotted simultaneously. However, for representative purposes membranes are shown as separate CTRL and CQ images. Also shown is a representative Actin loading control blot. (**E**)

Representative images of GFP-LC3B puncta from CTRL and CQ treated differentiating myoblasts. Scale bar=10μm. A one-way ANOVA was used to examine the effect of differentiation. A Students T-Test was used to determine differences between CTRL and CQ groups within the same time point. $^{*}p<0.05$, $^{\$}p<0.001$ compared to D0. $^{¢}p<0.001$ between treatment at same time point; (*n*=3).

Induction of autophagy during myoblast differentiation requires JNK activity

Myoblast differentiation and autophagy regulation share several signaling pathways. For example, AMPK has previously been shown to be involved in skeletal muscle development as well as autophagy regulation[53,193]. We observed no change in AMPKα protein throughout differentiation (Fig. 3A). In contrast, pAMPKα (Thr^{172}) levels increased upon induction of differentiation, becoming statistically significant ($p<0.05$) by D2. Similarly, the ratio of pAMPKα/AMPKα was elevated during differentiation, becoming statistically significant on D5 ($p<0.05$). These results suggest that the activation of AMPKα increases during myoblast differentiation. However, considering the lack of change in pULK1 (Ser^{467}), an AMPK target, AMPKα may not be involved in the induction of autophagy during myoblast differentiation. Thus, AMPK may be supporting other roles such as the transition from a predominantly glycolytic metabolism to a more oxidative phenotype[31,51,52,199].

AKT and FOXO3A have important roles in both myoblast differentiation and autophagy regulation[46,104]. AKT protein significantly increased ($p<0.05$) on D3 of differentiation (Fig. 3B). Relative to D0, phosphorylated AKT (Thr^{308}) increased several-fold during differentiation, becoming significantly greater ($p<0.001$) on D3. Similarly, the ratio of pAKT/AKT gradually increased with differentiation reaching significance on D3 ($p<0.01$) and D5 ($p<0.05$) compared to D0 myoblasts (Fig. 3B). A downstream target of AKT and transcription factor involved in the expression of several autophagy related genes in skeletal muscle is FOXO3A[46,104]. Interestingly,

FOXO3A protein and the pFOXO3A/FOXO3A ratio were not statistically altered during differentiation. However, similar to AKT phosphorylation, pFOXO3A ($Ser^{318/321}$) levels increased ($p<0.01$) throughout differentiation (Fig. 3C).

Since we observed an increase in BECN1 protein we investigated the expression of several BCL2 family members which have been shown to interact with BECN1 to regulate autophagy induction. BCL2 protein increased during differentiation, becoming significantly greater than D0 on D2 ($p<0.001$), D3 ($p<0.01$) and D5 ($p<0.05$) (Fig. 3D). Similarly, BCLXL protein gradually increased but only reached significance ($p<0.01$) on D5 (Fig. 3D). BNIP3 is a member of the BCL2 protein family and can exert both autophagic and apoptotic functions [12,143]. Although BNIP3 protein gradually increased during differentiation, it only reached significance on D5 ($p<0.05$) (Fig. 3D). Together, this suggests a role for BCL2 in myoblast differentiation and possibly in the regulation of autophagy.

Previous research has shown an important role for JNK in differentiation and regulation of autophagy through interactions with BCL2[200]. Interestingly, JNK1 protein did not change during myoblast differentiation. However, we observed a transient but non-significant increase pJNK1 (Thr^{183}/Try^{185}) levels on D0.5 (85%) and D1 (112%) before declining. Similarly, a transient yet non-significant increase in the pJNK1/JNK1 ratio was observed on D0.5 (119%) and D1 (72%) (Fig. 3E). Although the rise in pJNK1/JNK1 ratio did not reach statistical significance relative to D0, immunoprecipitation assays demonstrated a reduction in the association between BECN1 and BCL2 on D0.5 ($p<0.05$), D1 ($p<0.01$) and D2 ($p<0.05$) (Fig. 3F). This dissociation is required for the induction of autophagy which can be mediated by JNK. Interestingly, treatment of differentiating cells with the JNK inhibitor SP600125 maintained the association between BECN1 and BCL2 during the early days of differentiation (D0.5, D1, D2).

Furthermore, compared to CTRL (untreated) cells at the same time point, JNK inhibition resulted in a significantly higher association between BECN1 and BCL2 on D0.5 ($p<0.05$) and D2 ($p<0.05$) (Fig. 3F). Importantly, cells treated with SP600125 did not show increased LC3B-II protein content or appearance of GFP-LC3B puncta during differentiation. Furthermore, compared to CTRL cells at the same time point, cells treated with the JNK inhibitor had lower LC3B-II protein on D0.5, D1, and D2 ($p<0.05$) (Fig. 3G and 3H). Collectively, these data suggests that JNK plays a key role in regulating the association between BECN1 and BCL2, as well as the production of LC3B-II and the promotion of autophagy shortly after the induction of myoblast differentiation.

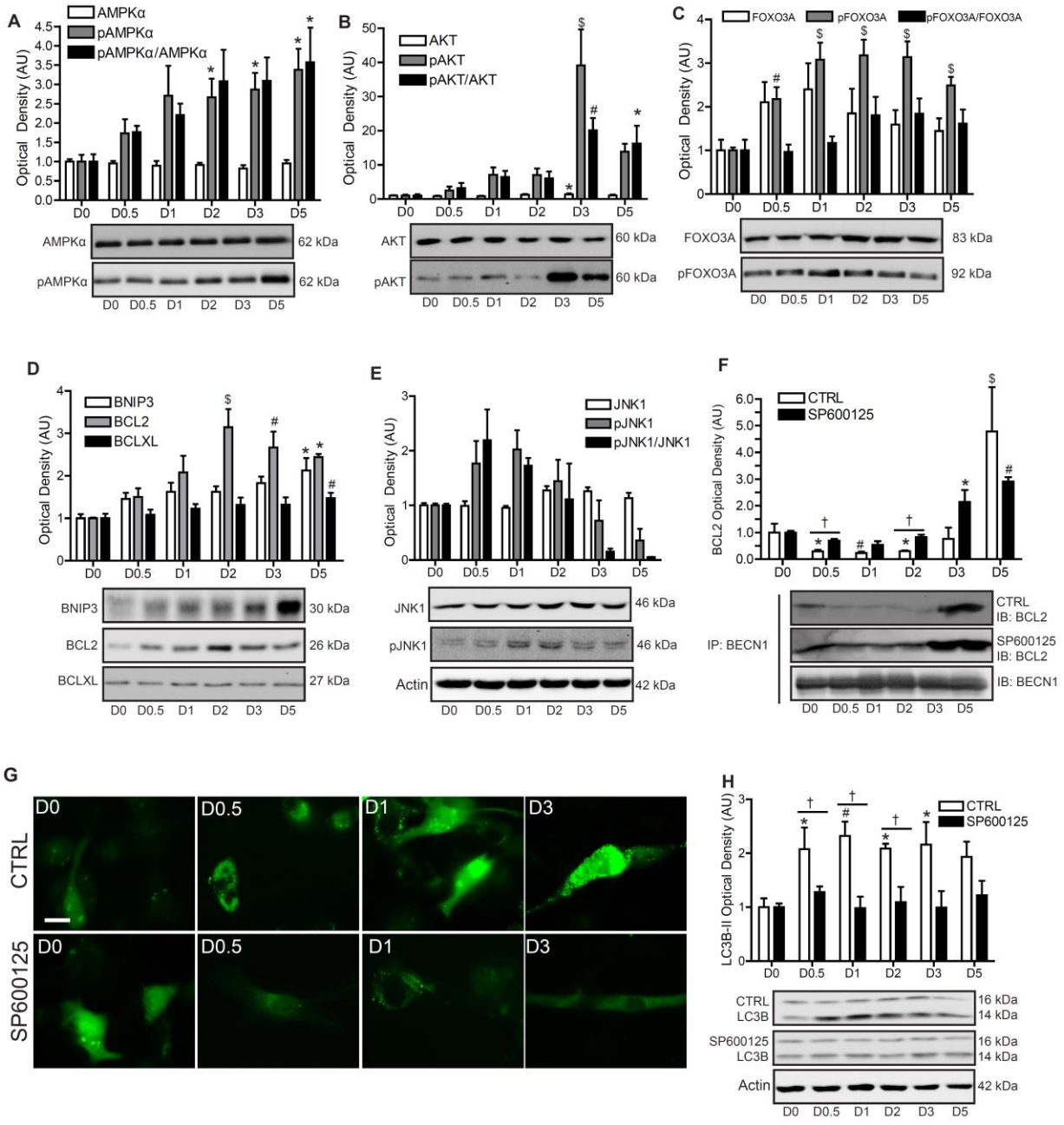

Fig. II - 3: JNK activity is required for BCL2 dissociation from BECN1 and LC3B-II formation during myoblast differentiation

(**A**) Representative immunoblots and quantitative analysis of AMPKα and pAMPKα (Thr^{172}) protein, (**B**) AKT and pAKT (Thr^{308}) protein, (**C**) FOXO3A and pFOXO3A ($Ser^{318/321}$) protein, (**D**) BNIP3, BCL2, and BCLXL protein, and (**E**) JNK1 and pJNK1 (Thr^{183}/Try^{185}) protein during C2C12 differentiation. (**F**) Representative immunoblots and quantitative analysis of BECN1:BCL2 immunoprecipitation during C2C12 differentiation in CRTL and SP600125 treated cells. (**G**) Representative images of GFP-LC3B puncta formation during C2C12 differentiation in CTRL and SP600125 treated cells. (**H**) Representative immunoblots of LC3B-I

and LC3B-II as well as quantitative analysis of LC3B-II from CTRL and SP600125 treated cells during C2C12 differentiation. LC3B CTRL and JNK inhibition experiments were conducted and blotted simultaneously. However, for representative purposes membranes are shown as separate CTRL and SP600125 images. Also shown are representative Actin loading control blots. Scale bar=10μm. A one-way ANOVA was used to examine the effect of differentiation. A Students T-Test was used to determine differences between CTRL and SP600125 groups within the same time point. $^{*}p<0.05$, $^{\#}p<0.01$, $^{\$}p<0.001$ compared to D0. $^{\dagger}p<0.05$, between treatment at same time point; (*n=2-6)*

Autophagy is required for proper myoblast differentiation

To determine if autophagy is critical for myoblast differentiation, 3MA, a specific autophagy inhibitor which mitigates the activity of the BECN1/PIK3C3 complex was used[112]. T-reatment of cells with 5mM 3MA resulted in significantly lower ($p<0.05$) LC3B-II protein and GFP-LC3B puncta compared to CTRL cells on all days of differentiation (Fig. 4A & 4B). Interestingly, inhibition of autophagy with 3MA resulted in impaired myotube formation and fewer tubes expressing myosin (Fig. 4E). More specifically, the differentiation index was significantly elevated in CTRL cells beginning on D2 ($p<0.001$) and continued throughout differentiation ($p<0.001$) (Fig. 4F). Although the differentiation index also increased in 3MA treated cells, differentiation was delayed compared to CTRL cells, reaching significance on D3 ($p<0.001$) (Fig. 4F). More importantly, 3MA treated cells had a lower differentiation index on D1, D2, D3 and D5 ($p<0.01$) compared to CTRL cells of the same day (Fig. 4F). Myoblast fusion was significantly greater by D3 ($p<0.001$) in CTRL and 3MA treated cells (Fig. 4G). However, fusion was significantly lower in 3MA compared to CTRL cells on D3 ($p<0.01$) and D5 ($p<0.001$) (Fig. 4G).

We next measured myogenin and myosin heavy chain protein content to examine if the delayed differentiation was associated with impaired expression of myogenic specific factors. In CTRL cells, myogenin protein significantly increased above D0 levels at D2 ($p<0.001$) and

remained elevated at D3 and D5 ($p<0.001$). In comparison, myogenin protein was not significantly elevated until D5 ($p<0.001$) in 3MA treated cells, and was dramatically lower ($p<0.05$) compared to CTRL cells of the same time point (Fig. 4C). Myosin heavy chain protein was significantly increased on D3 in CTRL cells ($p<0.001$) but was not significantly increased in 3MA treated myoblasts until D5 ($p<0.001$). Further, myosin heavy chain protein was dramatically lower ($p<0.05$) in 3MA treated cells compared to CTRL cells of the same time point (Fig. 4D). Collectively, these results suggest that the reduction of autophagy by 3MA impairs myoblast differentiation.

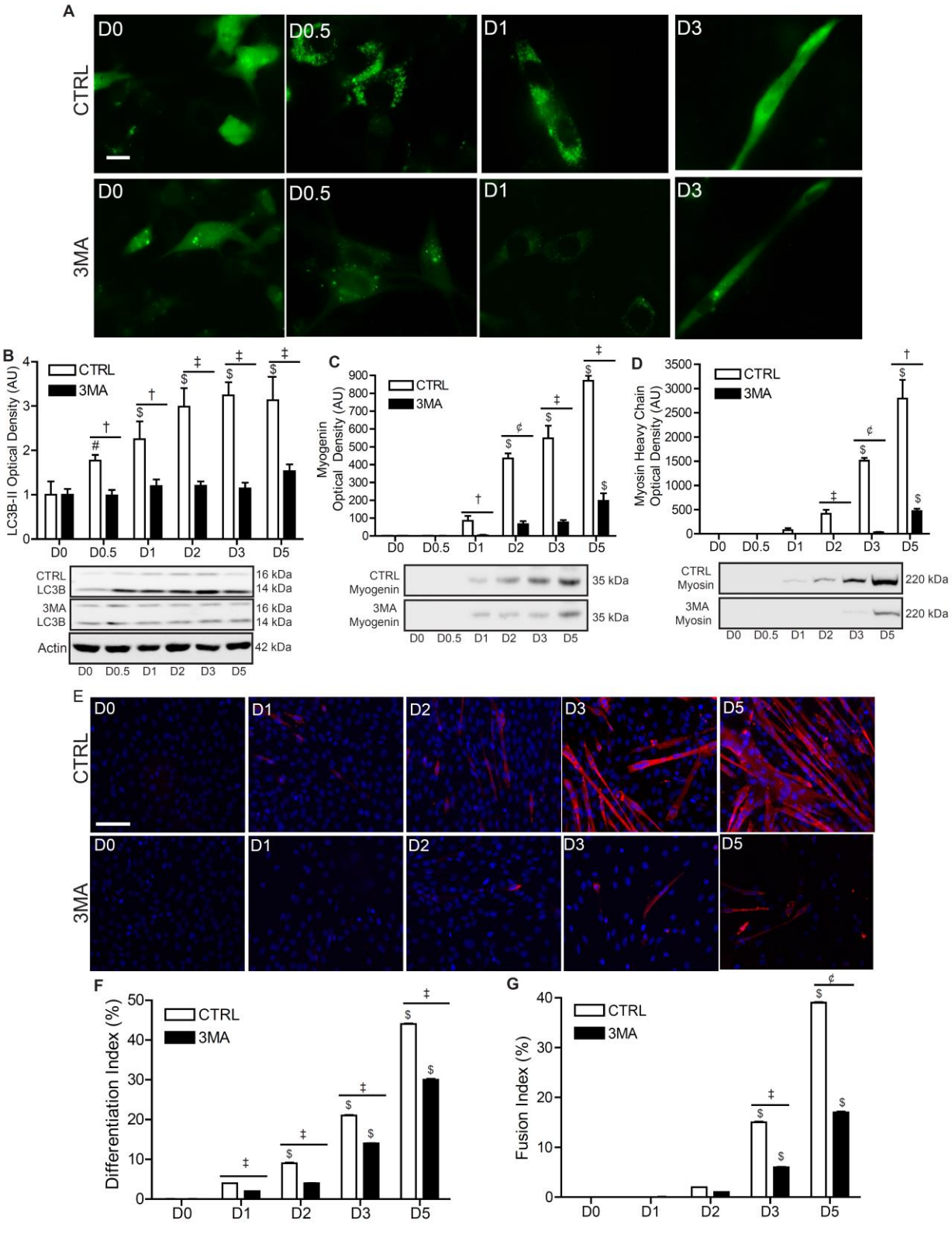
A
D0
D0.5
D1
D3
CTRL
3MA
B
LC3B-II Optical Density (AU)
CTRL
3MA
CTRL LC3B
3MA LC3B
Actin
16 kDa
14 kDa
42 kDa
C
Myogenin Optical Density (AU)
CTRL Myogenin
3MA Myogenin
35 kDa
D
Myosin Heavy Chain Optical Density (AU)
CTRL Myosin
3MA Myosin
220 kDa
E
F
Differentiation Index (%)
G
Fusion Index (%)

Fig. II - 4: Inhibition of autophagy impairs myoblast differentiation

(**A**) Representative images of GFP-LC3B puncta formation in CTRL and 3MA treated differentiating myoblasts. Scale bar=10μm. (**B**) Representative immunoblots of LC3B-I and LC3B-II as well as quantitative analysis of LC3B-II from CTRL and 3MA treated C2C12 cells during differentiation. A representative Actin immunoblot is also shown as a loading control. (**C**) Representative immunoblots and quantitative analysis of myogenin protein and, (**D**) myosin heavy chain protein in CTRL and 3MA treated C2C12 cells during differentiation. LC3B, myogenin, and myosin CTRL and 3MA experiments were conducted and blotted simultaneously within the same gel. However, for representative purposes membranes are shown as separate CTRL and 3MA images. (**E**) Representative images of C2C12 myoblast differentiation in CTRL and 3MA treated cells. Cells were stained with DAPI (blue) and MF20 (red) to image nuclei and myosin heavy chain, respectively. Scale bar=100μm. (**F**) Quantitative analysis of the differentiation index and (**G**) fusion index in CTRL and 3MA treated cells over 5 days of differentiation. A one-way ANOVA was used to examine the effect of differentiation. A Students T-Test was used to determine differences between CTRL and 3MA groups within the same time points. $^{\#}p<0.01$, $^{\$}p<0.001$ compared to D0. $^{\dagger}p<0.05$, $^{\ddagger}p<0.01$, $^{¢}p<0.001$ between treatment at same time point; (*n=3-6).*

To further confirm the role of autophagy on myoblast differentiation, we performed experiments in C2C12 cells stably transfected with ATG7 shRNA (shAtg7) or scramble shRNA (SCR). ATG7 protein was markedly reduced in shAtg7 compared to SCR cells, which remained throughout differentiation (Fig. 5A). Consistent with this, LC3B-II was dramatically lower in shAtg7 cells throughout differentiation (Fig. 5B). Consistent with our 3MA experiments, shAtg7 cells demonstrated impaired differentiation. Specifically, myosin heavy chain protein content dramatically increased throughout differentiation in SCR but not shAtg7 cells. Compared to SCR cells, myosin heavy chain expression in shAtg7 cells was significantly lower ($p<0.05$) on D1, D2, D3, and D5 (Fig. 5C). Likewise, the formation of myotubes was rare in shAtg7 cells whereas myotubes expressing myosin heavy chain were abundant in SCR cells (Fig. 5D). Together, these data support a critical role for autophagy during myoblast differentiation and myotube formation.

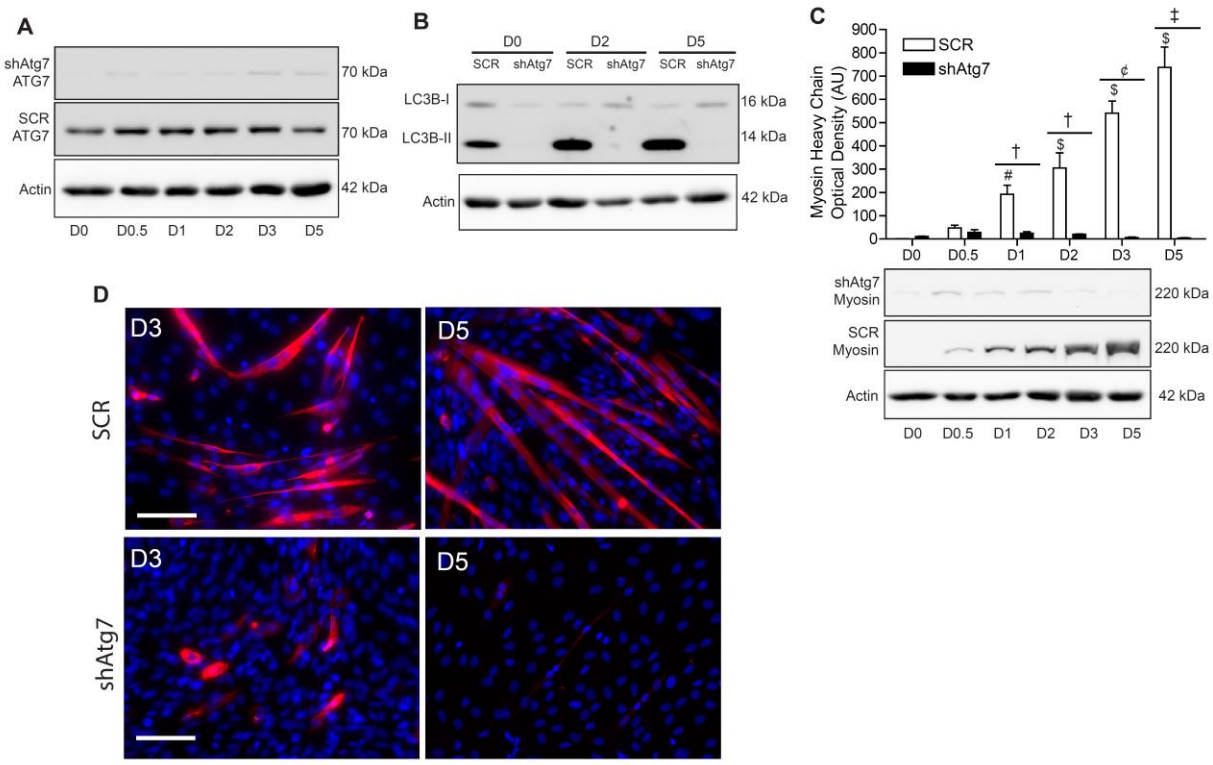

Fig. II - 5: Inhibition of autophagy by stable ATG7 knockdown inhibits myoblast differentiation

(**A**) Representative immunoblots of ATG7 protein in shAtg7 and SCR control myoblasts during differentiation. (**B**) Representative immunoblot of LC3B-I and LC3B-II from differentiating SCR and shAtg7 cells. (**C**) Representative immunoblots and quantitative analysis of myosin heavy chain protein in SCR and shAtg7 myoblasts throughout differentiation. Also shown are representative Actin loading control blots. (**D**) Representative images of myotube formation in SCR and shAtg7 cells at D3 and D5 of differentiation. ATG7 and myosin blots across groups were performed simultaneously; however, for representative purposes membranes are shown as separate SCR and shAtg7 images. Scale bar=50µm. A one-way ANOVA was used to examine the effect of differentiation. A Students T-Test was used to determine differences between CTRL and shAtg7 groups within the same time point. $^{\#}p<0.01$, $^{\$}p<0.001$ compared to D0. $^{\dagger}p<0.05$, $^{\ddagger}p<0.01$, $^{¢}p<0.001$ between treatment at same time point; (*n=3).*

Autophagy protects differentiating myoblasts from apoptosis

Throughout differentiation, we observed that 3MA treated cultures had an increase in the number of non-adherent cells that were smaller in size (4-11µm), suggesting increased apoptosis. To examine the possibility that inhibition of autophagy during myoblast differentiation results in

increased apoptosis we first examined the activity of a main death effector enzyme, CASP3[36]. Similar to previous results[2], we observed a transient increase in CASP3 activity during differentiation whereby CASP3 activity immediately increased on D0.5 ($p<0.01$) and continued to increase until D1.5 ($p<0.001$) before dropping down to baseline levels on D3 and D5 (Fig. 6A). Cells treated with 3MA also demonstrated a transient increase in CASP3 activity. However, 3MA treatment augmented CASP3 activity compared to CTRL cells on D0.5 ($p<0.01$), D1 ($p<0.001$), D1.5 ($p<0.01$), D2 ($p<0.05$), and D3 ($p<0.05$) (Fig. 6A). These data suggest that inhibition of autophagy results in a large transient activation of CASP3 during differentiation.

To further examine apoptotic events we characterized nuclei with apoptotic morphology such as chromatin condensation, a hallmark of apoptosis [36]. The percentage of apoptotic nuclei was not significantly altered in CTRL cells during differentiation. However, 3MA treatment significantly ($p<0.001$) elevated the percentage of apoptotic nuclei throughout differentiation; which was significantly higher ($p<0.05$) then CTRL cells at each time point (Fig. 6B & 6C). Moreover, quantification of DNA fragmentation via ELISA revealed higher levels ($p<0.05$) in CTRL cells on D1 which was significantly attenuated ($p<0.05$) on D3 and D5 of differentiation (Fig. 6D). In 3MA treated cells, DNA fragmentation also increased on D1 ($p<0.001$); however, higher levels were also observed on D3 and D5 ($p<0.05$). Relative to CTRL cells, inhibition of autophagy with 3MA resulted in increased DNA fragmentation on D2, D3 and D5 ($p<0.05$) (Fig. 6D). In agreement with these experiments, SCR cells displayed a transient elevation ($p<0.01$) in DNA fragmentation on D1 which declined ($p>0.05$) on D2 through to D5. In contrast, shAtg7 cells had significantly greater ($p<0.05$) DNA fragmentation throughout differentiation (Fig. 6E). Importantly, shAtg7 cells had dramatically elevated ($p<0.01$) levels of DNA fragmentation compared to SCR controls on D1 through to D5 (Fig. 6E). Overall, these results suggest that

inhibition of autophagy results in increased apoptotic events which may be contributing to impaired myoblast differentiation.

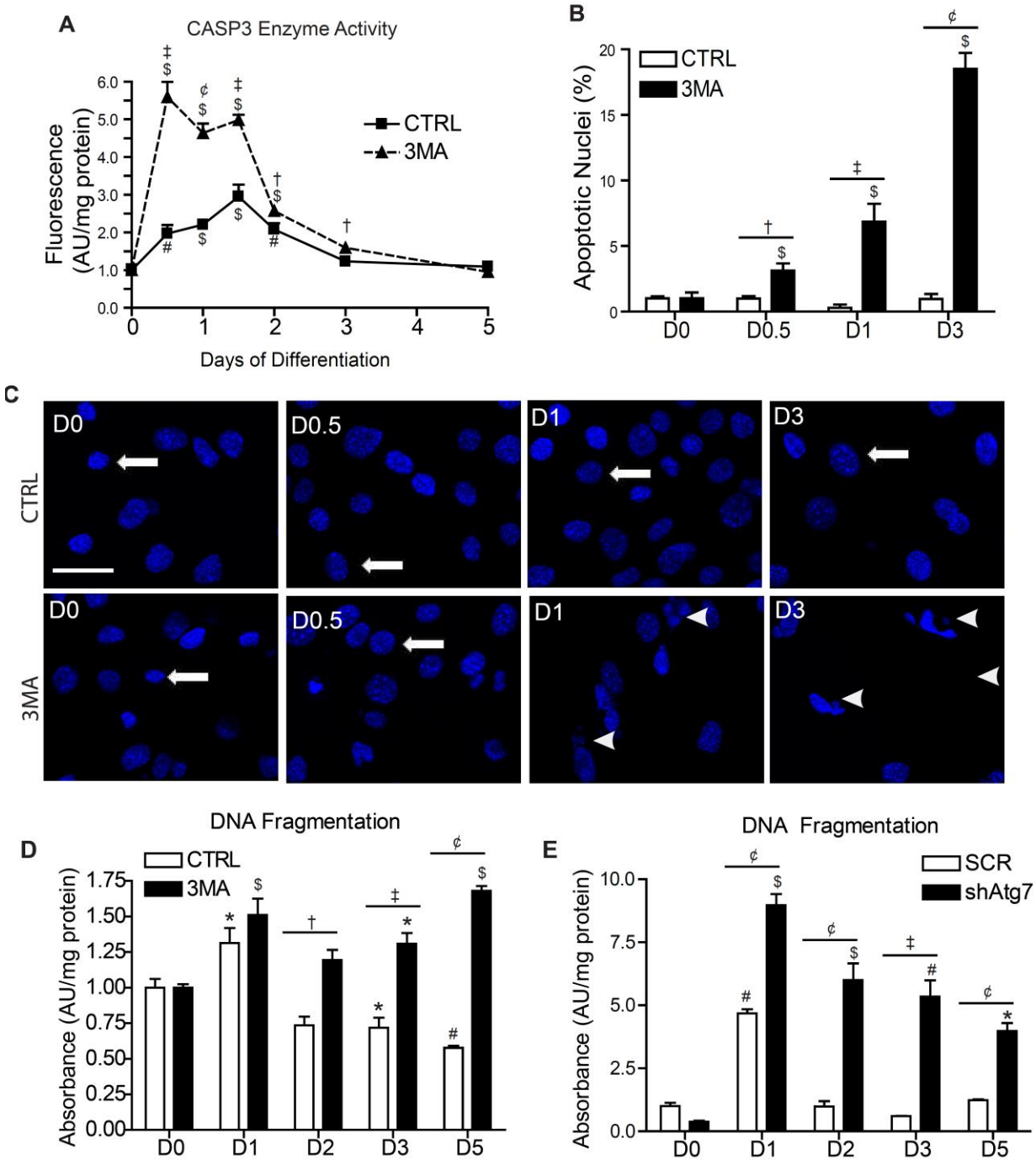

Fig. II - 6: Inhibition of autophagy leads to increased CASP3 activity and apoptosis

Quantitative analysis of (**A**) CASP3 activity, and (**B**) nuclei presenting with apoptotic features in CTRL and 3MA treated differentiating myoblasts. (**C**) Representative images of healthy (arrow) and apoptotic (arrow head) nuclei in CTRL and 3MA treated differentiating myoblasts. (**D**) Quantitative analysis of DNA fragmentation in CTRL and 3MA treated differentiating myoblasts. (**E**) Quantitative analysis of DNA fragmentation in shAtg7 and SCR myoblasts during differentiation. Scale bar=10µm. A one-way ANOVA was used to examine the effect of differentiation. A Students T-Test was used to determine differences between CTRL and shAtg7 or CTRL and 3MA groups within the same time point. $^{*}p<0.05$, $^{\#}p<0.01$, $^{\$}p<0.001$ compared to D0. $^{\dagger}p<0.05$, $^{\ddagger}p<0.01$, $^{¢}p<0.001$ between treatment at same time point; (*n=3-4*)

DISCUSSION

Myogenesis involves the terminal differentiation of muscle precursor cells and the fusion of mononucleated myoblasts into long syncytial cells[15,16]. Although this process is associated with increased protein synthesis and organelle biogenesis/remodeling[51,201], an increase in catabolic processes are required for the execution of the differentiation program and the formation of mature myotubes[2,186,202]. Accordingly, our data demonstrate the appearance of GFP-LC3B puncta, and that autophagic markers such as LC3B-II is elevated while SQSTM1 protein is depressed during myoblast differentiation. Importantly, inhibition of lysosomal degradation resulted in a significant accumulation of LC3B-II protein and GFP-LC3B puncta in differentiating myoblasts, supporting increased autophagic activity during this process. This confirms previous research which also shows an increase in LC3B-II in association with myoblast differentiation[138]. Similar to skeletal muscle, other cell types which undergo dramatic remodeling during differentiation also require the induction of autophagy[188,200,203]. Therefore, it stands to reason that autophagy may be rapidly induced upon myoblast differentiation to facilitate the elimination of pre-existing structures and proteins in order to promote differentiation and remodeling.

The ubiquitin-like conjugation systems involving ATG4B, ATG7 and ATG12-5 as well as both the BECN1/PIK3C3 and ULK1 kinase complexes are required for the formation of autophagosomes[188,203,204]. Accordingly, we found that changes to these autophagy regulatory proteins mirrored the induction of autophagy, further supporting the role of autophagy in myoblast differentiation. In agreement, Jacquel et al. demonstrated that silencing of ATG5, ATG7, BECN1 and ULK1 can inhibit the production of LC3B-II as well as impair macrophagic differentiation[203].

Myoblast differentiation requires the coordinated expression and activity of myogenic regulatory factors[16]. For example, impaired myogenin expression can inhibit terminal differentiation as well as delay markers of myotube formation[22,25,205]. We found that chemical inhibition of autophagy with 3MA delayed myogenin and myosin heavy chain expression, as well as impaired myoblast fusion and differentiation. Previous work has shown that targeted knockdown of ATGs in myogenic factor 5 expressing cells results in smaller myotubes along with reduced myogenic regulatory factor mRNA[206]. In agreement with these finding, we found that ATG7 knockdown resulted in dramatically lower myosin heavy chain protein expression as well as impaired myotube formation during differentiation. Thus, these data confirm that autophagy is required for proper muscle differentiation. Interestingly, there is also evidence that too much autophagy during muscle differentiation is detrimental[207]. Together with our results, this highlights the importance of regulated autophagy during myoblast differentiation.

The activation of several common signaling cascades regulates both muscle differentiation and autophagy. Myoblast differentiation requires the activation of the phosphoinositide 3-kinase-AKT axis for the promotion of myogenic regulatory factor activity and suppression of FOXO transcriptional activity[46,208]; however, FOXO3A also promotes the

transcription of several autophagy related genes[3,192]. AKT can also inhibit autophagy by increasing MTOR activity[3,209]. Although several reports confirm the requirement of MTOR activity in skeletal muscle differentiation, Tanida et al. found that increased MTOR activity occurs despite an elevation in LC3B-II content in differentiating C2C12 myoblasts[138]. Similarly, despite observing a gradual increase in AKT and FOXO3A phosphorylation during myoblast differentiation in this study, an increase in autophagy was observed. We suggest that the elevated AKT signaling along with increased pFOXO3A at D3 may be important in mitigating a further increase in autophagy; thus, contributing to a fine balance between too much and too little autophagy during myoblast differentiation.

MAPKs play an important role in both myoblast differentiation and autophagy[13,37]. In the current study we observed a transient increase in JNK1 phosphorylation which coincided with the dissociation of BCL2 from BECN1. JNK1 can promote autophagy by phosphorylating BCL2 which results in its dissociation from BECN1 allowing for enhanced activity of PIK3C3[125]. Accordingly, an increase in BCL2 has previously been shown to inhibit autophagy by suppressing the activity of the BECN1 complex[116,117]. In this study, the temporal pattern of JNK phosphorylation was similar to the dissociation of BCL2 from BECN1. This also corresponded to an increase in LC3B-II protein content and GFP-LC3B puncta during differentiation. Moreover, chemical inhibition of JNK activity resulted in higher BECN1:BCL2 association and a reduction in LC3B-II protein and GFP-LC3B puncta. Similarly, the induction of JNK activity in differentiating macrophages was shown to mediate the dissociation of BECN1 and BCL2 as well as contribute to the induction of autophagy and monocyte survival[200]. Collectively, our data supports a role for JNK1 in promoting autophagy during myoblast differentiation through the disassociation of BECN1:BCL2 complexes.

Apoptotic signaling has been shown to play an important regulatory role in promoting myoblast differentiation. For example, the transient activation of CASP3 is essential for the formation of myotubes [2]. However, the induction of apoptotic signaling must be highly regulated in order to avoid the loss of cell viability[210]. Previous work has shown that autophagy can protect cells from apoptosis by regulating the induction of caspase activity[12]. The present results suggest that autophagy may regulate CASP3 activation during myoblast differentiation and thus may influence cell viability. Specifically, we found that inhibition of autophagy using 3MA significantly elevated CASP3 activity, increased the percentage of nuclei with apoptotic morphology, and augmented DNA fragmentation throughout differentiation. Knockdown of ATG7 also increased DNA fragmentation confirming that autophagy is required to protect differentiating myoblasts from cell death. In agreement with our results, autophagy is required to protect against cell death during monocyte-macrophage differentiation[200]. Interestingly, JNK inhibition not only impairs monocyte differentiation, but results in lower autophagy and increased cell death[200]. Collectively, our data suggests that autophagy protects myoblasts from apoptosis during differentiation.

In conclusion, the induction of autophagy-related proteins and autophagic flux throughout the differentiation period demonstrates a role for autophagy in myoblast differentiation. This study demonstrates that the induction of autophagy occurs and is required for myoblast differentiation; a process which involves JNK-mediated regulation of BECN1:BCL2 signaling. Importantly, the inhibition of autophagy not only impairs myoblast differentiation and fusion, but is associated with increased apoptotic signaling, including elevated CASP3 activity, DNA fragmentation, and nuclear condensation. We propose that impaired myoblast differentiation in the absence of autophagy is likely due to diminished cell

viability. Together, the results of this work demonstrate a critical role for autophagy during myoblast differentiation.

CHAPTER III – Autophagy regulates mitochondrial-mediated apoptosis during myoblast differentiation

OVERVIEW

Autophagy is an essential degradative process involved in myoblast differentiation. We have previously shown that the inhibition of autophagy results in increased apoptosis and impaired myotube formation. The purpose of the present study was to further examine the role of autophagy in myoblast differentiation with particular emphasis on mitochondrial stress/apoptotic signaling. Similar to previous results, an increase ($p<0.05$) in LC3B-II and ATG7 protein was observed early during differentiation. Furthermore, the induction of myoblast differentiation was associated with an increase ($p<0.05$) in GFP-LC3:pDsRed2-Mito co-localization and LC3B-II protein content in mitochondrial-enriched fractions. shRNA-mediated knockdown of ATG7 resulted in an increase ($p<0.05$) in CASP3 activity, Annexin V staining, and a decrease of mitophagy markers. Inhibition of autophagy increased ($p<0.05$) CAPN activity, HSP70 protein content, mitochondrial permeability transition pore formation, as well as reduced mitochondrial membrane potential. We also observed an increase in mitochondrial-mediated apoptotic signaling events such as increased ($p<0.05$) cytosolic CYTO C protein and CASP9 activity in shAtg7 cells. Attenuation ($p<0.05$) of CASP3 activity in shAtg7 cells early during differentiation partially restored ($p<0.05$) MHC protein content, as well as differentiation and fusion indexes. Together, this data demonstrates a role for autophagy in protecting differentiating myoblasts from mitochondrial-mediated apoptotic signaling.

INTRODUCTION

The formation of mature skeletal muscle requires mononucleated myoblasts to endure tremendous levels of cell stress[29,31,211]. In fact, skeletal muscle development requires the induction of potentially lethal apoptotic signaling[2]. During apoptosis the cleavage of numerous intracellular proteins results in regulated cellular dismantling and packaging of cellular material into apoptotic bodies which are subsequently removed by immune cells[4]. However, apoptotic events such as phosphatidylserine exposure and submaximal/transient caspase (CASP) activation are integral for normal myoblast differentiation and myotube formation[2,58,60].

How apoptotic signaling is induced during skeletal muscle differentiation and how it contributes to cell specialization instead of cell death is inconclusive[210]. Evidence suggests that canonical apoptotic pathways may be involved in CASP3 activation[2], including the apoptotic proteases CASP12 and CASP8[29,212]. Of particular interest is the observation that CASP9 activity has been shown to contribute to the activation of CASP3 during myogenesis[211]; although its involvement has recently been disputed[42]. Typically, engagement of the mitochondrial-mediated pathway of apoptosis and the activation of CASP9 is considered a point of no return in cell death signaling[89]. Mitochondrial-mediated apoptotic signaling often requires a decline in mitochondrial membrane potential, a loss of mitochondrial membrane integrity, and full release of CYTO C[89]. As a result, the cell undergoes a rapid loss of ATP followed by the activation of cell death amplification loops[89]. However, some research suggests that the activation of mitochondrial-mediated pathways may not be an all or nothing event[210]. For example, during lens cell differentiation, a submaximal release of CYTO C results in the activation of caspases below the threshold required to induce cell death[213]. Similarly, active CASP12, CASP9 and CASP3 is detected in myoblasts which continue to differentiate[29,30]; however, their levels are significantly

greater in myoblasts which have undergone developmentally regulated apoptosis[29,30]. Together, these results suggest that the level of caspase activity and apoptotic stress must be maintained at sub-apoptotic levels in cells which progress through the myogenic program. Recent evidence suggests that CASP9 may not be directly involved in myoblast differentiation[42]. However, additional observations demonstrate that CASP12 and CASP9 are elevated in dead differentiating myoblasts suggesting that the level of mitochondrial-mediated apoptotic signaling occurring during myoblast differentiation must be regulated to protect myoblasts from cell death. Therefore, factors which control mitochondrial viability and integrity may be essential in the regulation of apoptotic signaling and cell death during myoblast differentiation.

Autophagy is a degradative process intimately involved with the cells stress response[12]. Accordingly, autophagy is induced by the stress related kinase JNK during myoblast differentiation[214]. Interestingly, recent work in our lab demonstrates that a loss of autophagy via 3MA administration or knockdown of ATG7 impairs myoblast differentiation and result in cell death[214]. Therefore, autophagy plays a critical role in regulating cell death signaling during myoblast differentiation. Although autophagy was originally characterized as a bulk degradation system, autophagy is now understood to be far more sophisticated, being able to target and selectively remove damaged, superfluous or dysfunctional proteins and organelles[12]. The clearance of mitochondria through autophagic processes is known as mitophagy and occurs as a protective response to mitochondrial damage [215,216]. The removal of damaged mitochondria prior to the induction of mitochondrial-mediated apoptotic signaling has been shown to regulate the promotion of cell death and mitigation of cell stress[12]. Therefore, we hypothesize that autophagy may protect myoblasts from apoptosis by regulating the level of caspase activity and cellular

stress which occurs during myogenesis specifically through the regulation of mitochondrial-mediated apoptotic signaling which has not yet been investigated.

METHODS

Transfections and Cell culturing

Mouse C2C12 skeletal myoblasts (ATCC) were plated at a low passage in polystyrene cell culture dishes (BD Biosciences) in growth media (GM) consisting of low-glucose Dulbecco's Modified Eagles Medium (DMEM; Hyclone, Thermo Scientific) containing 10% fetal bovine serum (FBS; Hyclone, Thermo Scientific) with 1% penicillin/streptomycin (Hyclone, Thermo Scientific) and incubated at 37ºC in 5% CO_2. Myoblast differentiation was induced once C2C12 myoblasts reached 80-90% confluence by replacing GM with differentiation media (DM) consisting of DMEM supplemented with 2% horse serum (Hyclone, Thermo Scientific) and 1% penicillin/streptomycin. Subconfluent myoblasts were collected prior to the addition of DM (D0) as well as at 12 hrs (D0.5), 24 hrs (D1), 36 hrs (D1.5), 48 hrs (D2), 72 hrs (D3) and 120 hrs (D5) following the addition of DM.

C2C12 cells stably expressing shRNA against ATG7 or scramble control sequence (SCR) CTRL were generated as previously described[214]. Stably transfected C2C12 cells were co-transfected with GFP-LC3B (generously provided by Dr. Terje Johansen, Institute of Medical Biology; University of Tromsø) and pDsRed2-Mito (generously provided by Dr. D. R. Green, St Jude's Children's Research Hospital, Memphis, Tennessee) plasmid DNA to investigate the percentage of cell with co-localization of autophagic puncta with mitochondria during differentiation. Cells were transfected upon reaching 60-70% confluence on gelatin coated glass

coverslips, and induced to differentiate 36 hr following transfection. Transfections were performed with Lipofectamine 2000 (Life Technologies) optimized according to the manufactures instructions. Glass coverslips with co-transfected cells were removed from culture dishes, washed in warm PBS and mounted on glass slides using Prolong Gold Antifade Reagent (Life Technologies) prior to imaging on an Axio Observer Z1 fluorescent microscope equipped with a Apotome/structured-illumination system (Carl Zeiss). Co-localization analysis was conducted using AxioVision Software.

Attenuation of caspase activity was achieved with either CASP3 inhibitor (Ac-DEVD-CHO; Enzo Life Sciences) or CASP9 inhibitor (Ac-LEHD-CHO; Enzo Life Sciences). Both inhibitors are cell permeable and have been documented to effectively inhibit the activity of CASP3 directly or indirectly via inhibition of upstream CASP9 activity. CASP3 activity was attenuated in shAtg7 CTRL cells using 1.5 μM and 1 μM of CASP9 and CASP3 inhibitors, respectively. Differentiating myoblasts were exposed to caspase inhibitors or equal volumes of DMSO in DM during all days of differentiation and replaced with new media/drug every 24 hours.

Cell Isolations and Acquisition of Enriched Subcellular Fractions

For whole cell lysates**,** cells were removed from culture dishes by trypsinization (0.25% trypsin with 0.2g/L EDTA; Thermo Scientific), and collected by centrifugation (800 x g for 5 min). Cell pellets were resuspended and washed in ice cold PBS, centrifuged (800 x g for 5 min) and then frozen at -80°C until further analysis.

Fresh cells were separated into cytosolic-, mitochondrial- and nuclear-enriched subcellular fractions. Briefly, cells were resuspended and incubated in digitonin buffer (PBS with

250 mM sucrose, 80 mM KCl, and 50 µg/mL digitonin, Sigma Aldrich) for 5 min on ice. Cells were then centrifuged at 1000 x g for 10 min, the supernatant was then centrifuged at 16,000 x g for 10 min to pellet mitochondrial contamination. The supernatant was removed and frozen as the cytosolic-enriched fraction. The pellet from the 1000 x g spin was resuspended in ice cold PBS and centrifuged at 1000 x g for 5 min. The pellet was then resuspended in lysis buffer (20 mM HEPES, 10 mM NaCl, 1.5 mM MgCl, 1 mM DTT, 20% glycerol and 0.1% Triton X-100; pH 7.4) and incubated on ice for 5 min before centrifugation at 1000 x g for 10 min. The supernatant containing mitochondria was isolated and centrifuge for 10 min at 1000 x g to remove nuclear contamination. The resulting supernatant was removed and frozen as the mitochondrial-enriched fraction. The pellet was resuspended in lysis buffer, centrifuged at 1000 x g for 10 min. The pellet was resuspended in lysis buffer and sonicated for 20 seconds and frozen as the nuclear-enriched fraction. Protein content of whole cell and subcellular fractions was determined using the BCA protein assay. Purity of subcellular fractions was determined through immunoblotting for CuZnSOD (SOD1) (cytosol), MnSOD (SOD2) (mitochondria), and histone H2B (nucleus).

Immunoblotting

Immuoblotting was conducted as previously described[214]. Briefly, cells were lysed in ice cold lysis buffer with or without protease inhibitor (Roche Applied Sciences). Equal amounts of cell lysates were loaded and separated on 7.5-15% SDS-PAGE gels, transferred onto PVDF membranes (Bio-Rad Laboratories), and blocked for 1 hr at room temperature or overnight at 4°C with 5% milk-Tris-buffered saline-Tween 20 (milk-TBST). Membranes were incubated either overnight at 4°C or for 1 hr at room temperature with primary antibodies against: BECN1, ATG7, LC3B (Cell Signaling Technology); BCL2, BAX, ARC, CYTO C, AIF (Santa Cruz

Biotechnology); Myogenin (MYOG), myosin heavy chain (MYH) (Developmental Studies Hybridoma Bank); BNIP3, Actin (Sigma-Aldrich); Catalase (CAT), HSP70, SOD2, SOD1 (Stressgen Bioreagents); histone H2B (Enzo Life Sciences); and 4-HNE (Abcam). Membranes were then washed with TBST, incubated with the appropriate horseradish peroxidase (HRP)-conjugated secondary antibodies (Santa Cruz Biotechnology) for 1 hr at room temperature, washed with TBST, and bands visualized using enhanced chemiluminescence western blotting detection reagents (BioVision) and the ChemiGenius 2 Bio-Imaging System (Syngene). The approximate molecular weight for each protein was estimated using Precision Plus Protein WesternC Standards and Precision Protein Strep-Tactin HRP Conjugate (Bio-Rad Laboratories). Equal loading and quality of transfer was confirmed by staining membranes with Ponceau S (BioShop).

Flow Cytometry

Cells were collected and washed/resuspended in Hank's Balanced Salt Solution (HBSS). Mitochondrial membrane depolarization was monitored by changes in the JC-1 red:green fluorescence ratio. A decreased ratio is indicative of decreased mitochondrial membrane potential. Briefly, cells were incubated with 2 μM JC-1 (Life Technologies) in HBSS for 15 min at 37 °C. Following incubation, cells were washed by centrifugation and resuspended in HBSS.

Calcein AM was used to measure the formation of the mitochondrial permeability transition pore (mPTP). The fluorescent dye calcein AM which accumulates in intact mitochondria is quenched by cobalt following mitochondrial membrane permeabilization. Thus, a decrease in calcein fluorescence is indicative of mPTP formation. Briefly, cells were incubated with 1 μM calcein AM (Life Technologies) and 1 mM $CoCl_2$ in HBSS for 15 min at 37°C. Following incubation, cells were washed by centrifugation and resuspended in 500 μl HBSS.

For analysis of phosphatidylserine (PS) exposure Annexin V staining was performed. Briefly, cells were washed in PBS then resuspended in buffer (10 mM HEPES/NaOH, 150 mM NaCl, 1.8 mM $CaCl_{2;}$ pH 7.4). Cells were then incubated with 5 µl of Annexin V-FITC (BioVision) for 20 min at room temperature. All analyses were performed on a flow cytometer (BD FACSCalibur) equipped with Cell Quest Pro software (BD Bioscience) as previously described[93].

Proteolytic Enzyme Activity Assay and ROS Generation

Enzymatic activity of CASP3 and CASP9 was determined using the substrates Ac-DEVD-AMC and Ac-LEHD-AMC (Enzo Life Sciences), respectively, as previously described[93,214]. Enzymatic activity of calpain (CAPN) was assessed using the fluorogenic substrate Suc-LLVY-AMC (Enzo Life Sciences) as previously described[93]. Measurement of ROS generation was conducted as previously demonstrated using 5 µM DCFH-DA (Life Technologies)[217]. CASP, CAPN and DCF fluorescence was normalized to total protein content and expressed as arbitrary units (AU) per milligram protein.

Fluorescence Microscopy

Immunofluorescence analysis of MYH expression was determined on cells grown on glass coverslips in culture dishes following their removal at indicated time points as previously described[214]. Briefly, coverslips were washed 2 x 5 min with PBS. Cells were fixed with 4% formaldehyde in PBS for 10 min at room temperature, and washed 2 x 5 min with PBS. Cells were permeabilized for 10 min with 0.5% Triton X-100, and then washed 2 x 5 min in PBS. Cells were blocked with 10% goat serum (Sigma-Aldrich) (in PBS) for 30 min, then incubated with a primary antibody against MYH (Developmental Studies Hybridoma Bank; MF20) diluted in blocking solution for 2 hr, and washed 2 x 5 min with PBS. An anti-mouse PE-conjugated

secondary antibody (Santa Cruz) was made in 10% goat serum blocking solution. Cells were incubated in secondary solution for 1 hr, washed 2 x 5 min in PBS, counterstained with DAPI nuclear stain (Life Technologies) for 5 min, then washed 2 x 5 min in PBS. Coverslips were mounted with Prolong Gold Antifade Reagent (Life Technologies). Slides were visualized with an Axio Observer Z1 fluorescent microscope equipped with standard Red/Green/Blue filters, an AxioCam HRm camera, and AxioVision software (Carl Zeiss). The fusion index was calculated as a percentage of nuclei present in multinucleated (two or more nuclei) cells relative to total nuclei present and represents the formation of nascent myotubes. The differentiation index was calculated as the percentage of cells expressing MYH relative to total number of cells.

Statistics

A One-Way repeated measure ANOVA was used to assess the effect of differentiation. If a main effect of differentiation was observed, Tukey's post hoc test was used to determined differences from D0. Differences between time-matched SCR and shAtg7 cells were assessed using a Students T-Test. A Two-Way ANOVA was used to assess the effects of differentiation in caspase inhibitor experiments with the use of a Tukey's post-hoc test where appropriate. For all experiments $p<0.05$ was considered statistically significant.

RESULTS

Inhibition of autophagy impairs myoblast differentiation and myoblast fusion

C2C12 myoblasts stably transfected with a scramble control plasmid (SCR) had significantly elevated ($p<0.05$) LC3B-I and LC3B-II protein content throughout differentiation compared to D0 (Fig. 1A, B). Interestingly, the LC3B-II/I ratio was only elevated ($p<0.05$) on

D0.5 and D5 ($p<0.01$; Fig. 1A, B). Autophagosome formation requires the assembly and activation of several protein complexes which direct its creation and substrate targeting[9]. Similar to previous results[214], ATG7 protein content was increased ($p<0.05$) during differentiation beginning on D1 (Fig. 1B, C). Additionally, the protein levels of BECN1 and BNIP3 were elevated ($p<0.05$) on D3 and D5 compared to D0. These results support our previous findings demonstrating increased autophagy during myoblast differentiation[214].

Consistent with our previous report[214], stable knockdown of ATG7 (shAtg7) resulted in impaired differentiation compared to SCR cells (Fig. 1E). MYOG was elevated ($p<0.05$) in SCR cells but was decreased ($p<0.05$) throughout differentiation in shAtg7 cells (Fig.1F). This resulted in dramatically lower MYOG protein during differentiation in shAtg7 cells compared to SCR cells (Fig 1F). In agreement with our previous results, ATG7 knockdown attenuated the formation of myosin-positive myotubes during differentiation (Fig. 1E). Accordingly, shAtg7 cells displayed significantly decreased ($p<0.01$) cell fusion and differentiation indexes on D3 ($p<0.01$) and D5 ($p<0.001$) compared to SCR cells (Fig. 1G & 1H).

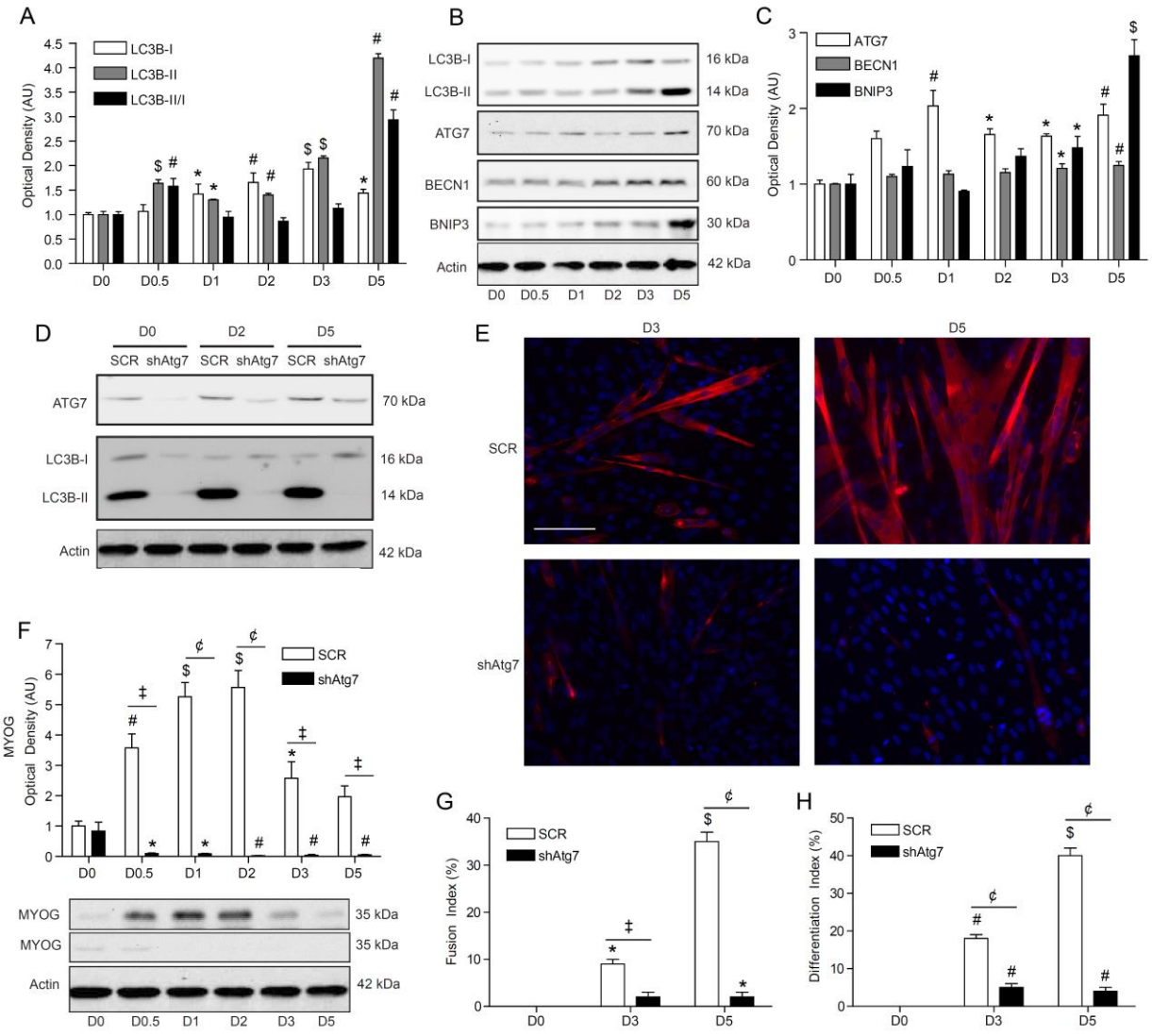

Fig. III - 1: Autophagy is induced during and required for myoblast differentiation

(A) Quantitative analysis of LC3B-I, LC3B-II and LC3B-II/I protein ratio during myoblast differentiation. **(B)** Representative immunoblots of LC3B-I, LC3B-II, ATG7, BECN1, and BNIP3 protein in differentiating myoblasts. **(C)** Quantitative analysis of ATG7, BECN1 and BNIP3 protein during myoblast differentiation. **(D)** Representative immunoblots of ATG7, LC3B-I and LC3B-II protein in SCR and shAtg7 cells. **(E)** Representative images of C2C12 myotube formation in SCR and shAtg7 cells at D3 and D5 of differentiation. Cells were stained with DAPI (blue) and MF20 (red) to image nuclei and MYH, respectively. Scale bar=100 µm. **(F)** Representative immunoblots and quantitative analysis of MYOG protein in SCR and shAtg7 myoblast cells during differentiation. Quantitative analysis of the **(G)** fusion index and **(H)** differentiation index in SCR and shAtg7 cells on D0, D3 and D5 of differentiation. Also shown are representative Actin loading control blots. Representative immunoblots of MYOG were blotted simultaneously. However, for representative purposes membranes are shown as separate SCR and shAtg7 images. A one-way ANOVA was used to examine the effect of differentiation. A Students T-Test was used to determine differences between CTRL and shAtg7 groups within

the same time point. *p<0.05, #p<0.01, $p<0.001 compared to D0. †p<0.05, ‡p<0.01, ¢p<0.001 between treatment at same time point; (*n=3-5).*

Inhibition of autophagy during myoblast differentiation results in apoptotic features

Inhibition of autophagy during myoblast differentiation results in increased DNA fragmentation, a hallmark of apoptosis[200,214]. In the current study we add to this finding by demonstrating that ATG7 knockdown results in increased (p<0.05) Annexin staining early (p<0.05) and throughout (p<0.001) differentiation in shAtg7 cells (Fig 2A). Interestingly, Annexin levels were higher (p<0.05) in SCR on D0 compared to shAtg7 cells; however, Annexin staining was greater (p<0.05) in shAtg7 cells throughout differentiation. An increase (p<0.05) in CASP3 activity was observed in both SCR and ATG7 cells during differentiation[214] (Fig 2B); however, levels were significantly greater in shAtg7 compared to SCR at each time point (p<0.01) (Fig 2B). In addition, shAtg7 cells displayed increased (p<0.01) CAPN proteolytic activity early during differentiation (D0.5, D1, D1.5 and D2) compared to SCR cells (Fig. 2C). However, CAPN activity was reduced (p<0.05) below D0 levels in SCR and shAtg7 cells on D3 and D5 (Fig. 2C).

Changes to BCL2 family proteins often occur during the induction of apoptosis[68]. Interestingly, neither SCR nor shAtg7 myoblasts demonstrated a change (p>0.05) in BAX protein levels during differentiation (Fig 2D); however, levels were higher in shAtg7 cells on D2 and D3 (Fig 2D). BCL2 protein was increased (p<0.05) on D1 and D2 in SCR but not shAtg7 cells (Fig 2E). Accordingly, significantly higher (p<0.01) BCL2 protein levels were observed in SCR compared to shAtg7 cells on D0.5, D1, D2 and D3 (Fig 2E). In addition, the BAX:BCL2 ratio was lower (p<0.05) on D1, D2 and D5 compared to D0 in SCR but not shAtg7 cells (Fig 2F).

The anti-apoptotic protein, ARC, increased ($p<0.01$) on D5 compared to D0 in SCR but not shAtg7 cells (Fig 2H). Further, ARC content was significantly greater ($p<0.01$) on D0.5, D1, and D2 of differentiation in SCR compared to shAtg7 cells (Fig 2H). Interestingly, HSP70 decreased ($p<0.05$) throughout differentiation in SCR cells (Fig. 2G). In contrast, shAtg7 cells demonstrated a robust increase ($p<0.05$) in HSP70 protein content during differentiation, resulting in dramatically higher ($p<0.01$) levels at each time point when compared to SCR cells (Fig. 2G). Together, the elevated Annexin staining, increased CASP3 activity, and changes to critical anti-apoptotic proteins support our previous findings of altered cellular stress and apoptosis in autophagy-deficient myoblasts during differentiation.

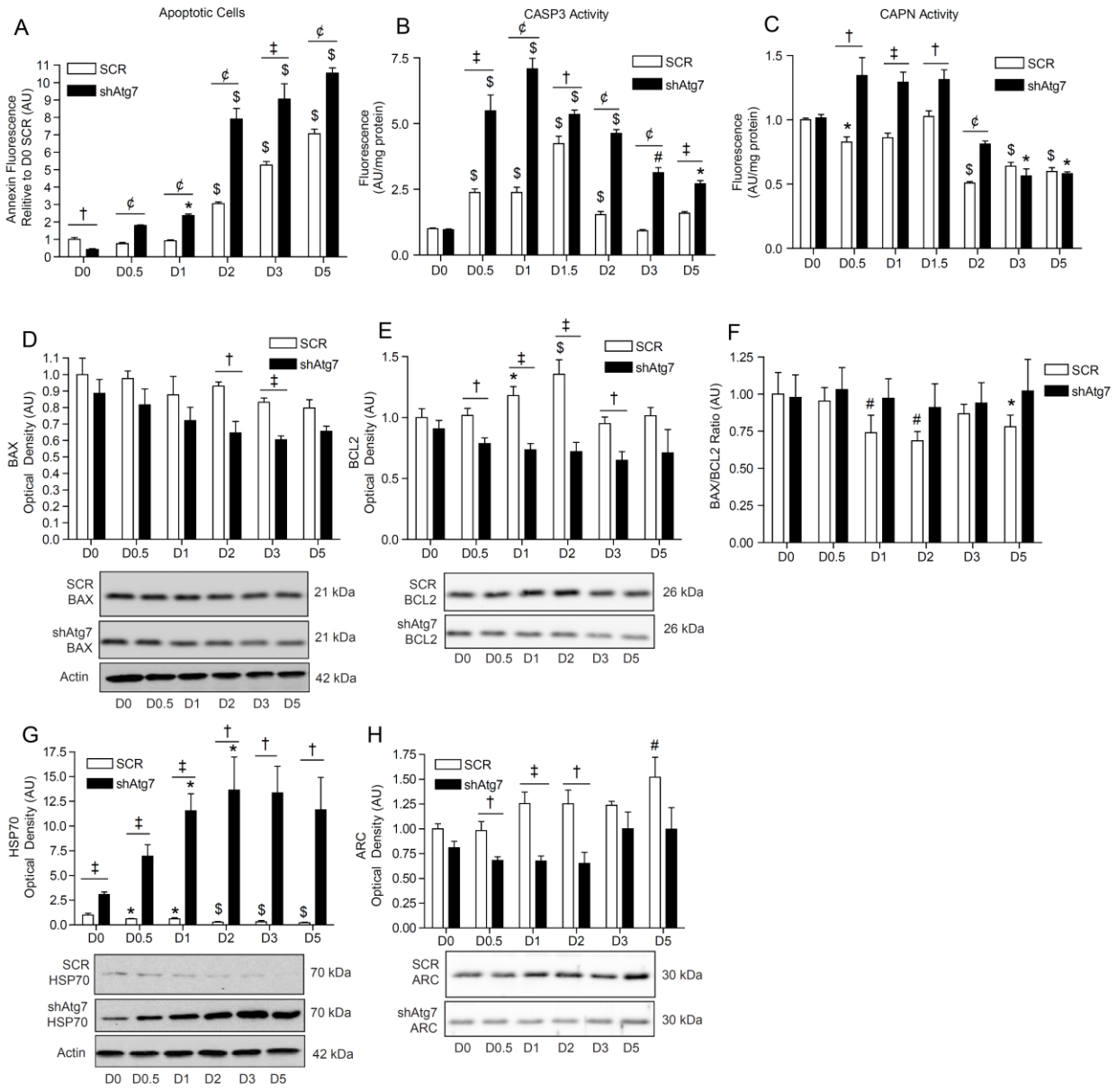

Fig. III - 2: Inhibition of autophagy during myoblast differentiation alters proteolytic activity and apoptotic protein content

(A) Quantitative analysis of Annexin staining in SCR and shAtg7 differentiating myoblasts. **(B)** CASP3 activity and **(C)** CAPN activity in SCR and shAtg7 cells during differentiation. Representative immunoblots and quantitative analysis of **(D)** BAX protein and **(E)** BCL2 protein content and **(F)** BAX/BCL2 protein ratio in SCR and shAtg7 myoblast cells during differentiation. Representative immunoblots and quantitative analysis of **(G)** HSP70 and **(H)** ARC protein in SCR and shAtg7 myoblast cells during differentiation. Also shown are representative Actin loading control blots. Representative immunoblots of BAX, BCL2, HSP70, ARC and Actin protein in SCR and shAtg7 cells were blotted simultaneously. However, for representative purposes membranes are shown as separate SCR and shAtg7 images. A one-way

ANOVA was used to examine the effect of differentiation. A Students T-Test was used to determine differences between CTRL and shAtg7 groups within the same time point. *$p<0.05$, $^{\#}p<0.01$, $^{\$}p<0.001$ compared to D0. $^{\dagger}p<0.05$, $^{\ddagger}p<0.01$, $^{¢}p<0.001$ between treatment at same time point; (*n=3-5).*

Autophagy prevents oxidative damage and ROS generation in myoblasts and differentiating myocytes

Previous reports have shown that in the absence of autophagy, changes to the redox environment can contribute to cellular stress and apoptosis[216]. Here, SCR myoblasts showed reduced ($p<0.01$) ROS generation beginning on D2 of differentiation (Fig 3A). However, shAtg7 cells displayed increased ($p<0.05$) whole-cell ROS generation on D1, D1.5 and D5 (Fig 3A). As a result, shAtg7 cells displayed greater ($p<0.01$) ROS generation compared to SCR cells beginning on D1 (Fig 3A). In response to increased ROS generation, oxidative stress and cell damage can occur if antioxidant defences are not sufficient[216]. In both SCR and shAtg7 cells, CAT protein content was decreased ($p<0.05$) during differentiation (Fig. 3B). Interestingly, shAtg7 cells had higher ($p<0.01$) CAT expression than SCR cells on D0 (Fig 3B). Conversely, levels of CAT in SCR cells were greater than shAtg7 cells on D1 ($p<0.001$), D3 ($p<0.01$) and D5 ($p<0.01$) (Fig 3B). SOD1 expression was increased ($p<0.05$) on D5 in SCR cells but did not change throughout differentiation in shAtg7 cells (Fig. 3C). However, SOD1 levels were higher ($p<0.05$) in shAtg7 compared to SCR cells on D0 and D0.5 (Fig. 3C). SOD2 protein expression increased ($p<0.01$) in shAtg7 cells by D2 and continued to rise throughout differentiation (Fig. 3C). Similarly, SCR myoblasts displayed increased ($p<0.05$) SOD2 on D3 and D5 compared to D0 (Fig. 3C). Interestingly, SOD2 content was greater ($p<0.01$) in shAtg7 compared to SCR cells on D2, D3 and D5. The levels of lipid peroxidation in mitochondrial-enriched fractions of SCR cells was greater ($p<0.05$) than D0 from D1 throughout differentiation (Fig. 3E & F).

However, in shAtg7 myoblasts, the level of lipid peroxidation in mitochondrial-enriched fractions was significantly greater ($p<0.001$) than SCR on D0 and D0.5 but declined their after to levels similar to SCR cells (Fig. 3E & F). Collectively, the inhibition of autophagy resulted in altered ROS defences as well as markers of oxidative damage during differentiation.

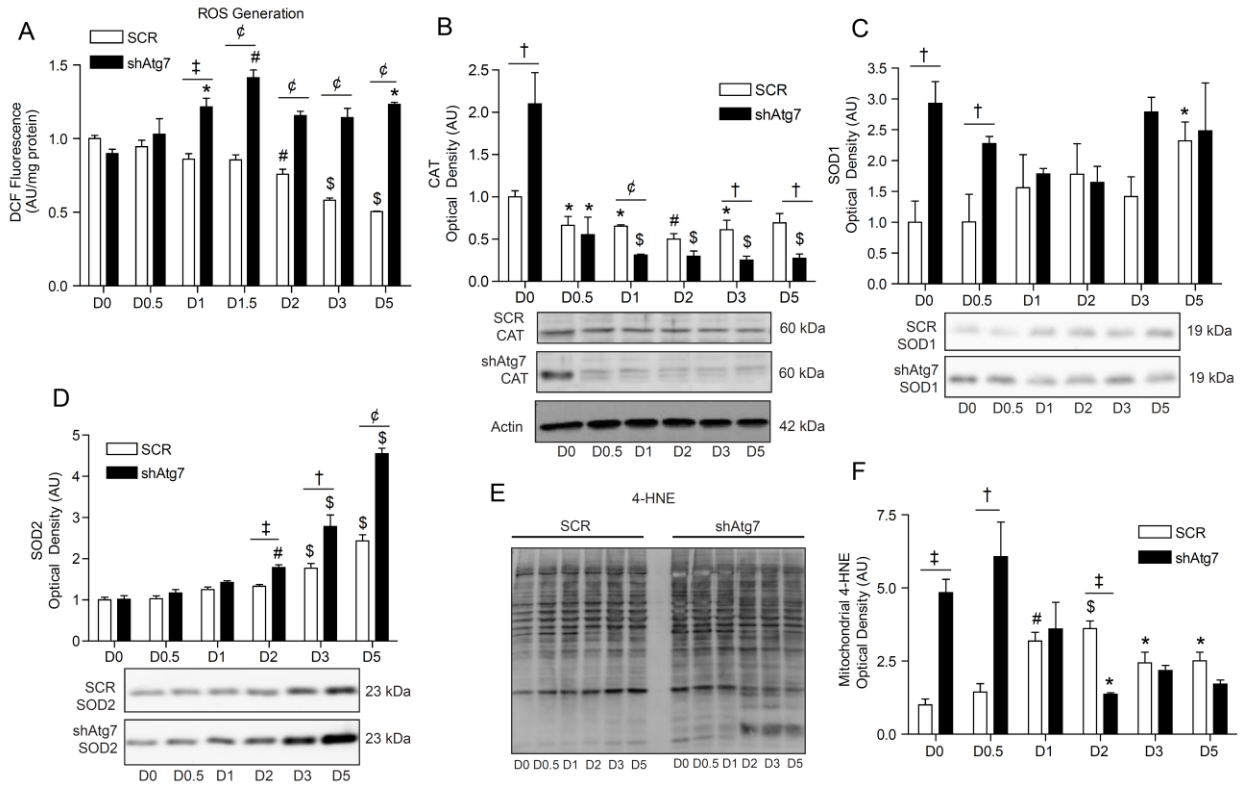

Fig. III - 3: Inhibition of autophagy during myoblast differentiation alters the expression of antioxidant and ROS generation

(A) Quantitative analysis of ROS generation in SCR and shAtg7 myoblasts during differentiation. Representative immunoblots and quantitative analysis of **(B)** CAT**, (C)** SOD1, and (**D)** SOD2 in SCR and shAtg7 myoblast cells during differentiation. **(E)** Representative immunoblot and **(F)** quantitative analysis of 4-HNE content from mitochondrial-enriched fractions of SCR and shAtg7 myoblasts during differentiation. Also shown are representative Actin loading control blots. Representative immunoblots of CAT, SOD1, SOD2 and Actin protein in SCR and shAtg7 cells were blotted simultaneously. However, for representative purposes membranes are shown as separate SCR and shAtg7 images. A one-way ANOVA was used to examine the effect of differentiation. A Students T-Test was used to determine differences between CTRL and shAtg7 groups within the same time point. *$p<0.05$, $^{\#}p<0.01$, $^{\$}p<0.001$ compared to D0. $^{\dagger}p<0.05$, $^{\ddagger}p<0.01$, $^{¢}p<0.001$ between treatment at same time point; (*n=3-4).*

Markers of mitophagy are altered during myoblast differentiation

The removal of damaged mitochondria may regulate apoptotic signaling during muscle differentiation. However, mitophagy has not been previously studied in this context. Our results show increased ($p<0.01$) co-localization of mitochondria and autophagic puncta on D0.5 compared to D0 in SCR cells (Fig. 4D & E). This effect remained ($p<0.001$) on D1 but subsided by D2, indicating the co-localization of mitochondria and autophagosomes in C2C12 cells is rapid and transient during differentiation (Fig. 4D & E). Compared to shAtg7 cells, the level of co-localization was greater ($p<0.01$) in SCR cells at each time point (Fig. 4D & E). In addition, we observed increased ($p<0.05$) LC3B-II protein content in mitochondrial-enriched subcellular fractions of SCR cells on all days of differentiation compared to D0 (Fig. 4B). LC3B-II protein in mitochondrial fractions was not altered during differentiation in shAtg7 cells, and was also dramatically reduced ($p<0.05$) compared to SCR cells (Fig. 4B). These results support the induction of mitophagy during myoblast differentiation.

Mitophagy is regulated by a diverse array of signaling events originating at the mitochondria[215]. One of the initiators of mitophagy is the reduction in mitochondrial membrane potential[215]. Early during differentiation both SCR and shAtg7 myoblast showed reduced ($p<0.001$) mitochondrial membrane potential compared to D0 levels. However, compared to SCR cells, shAtg7 cells had significantly reduced ($p<0.001$) membrane potential at all-time points (Fig. 4C). Together, this data demonstrates that myoblast differentiation results in changes to mitochondrial membrane potential, which may participate in the induction of mitophagy.

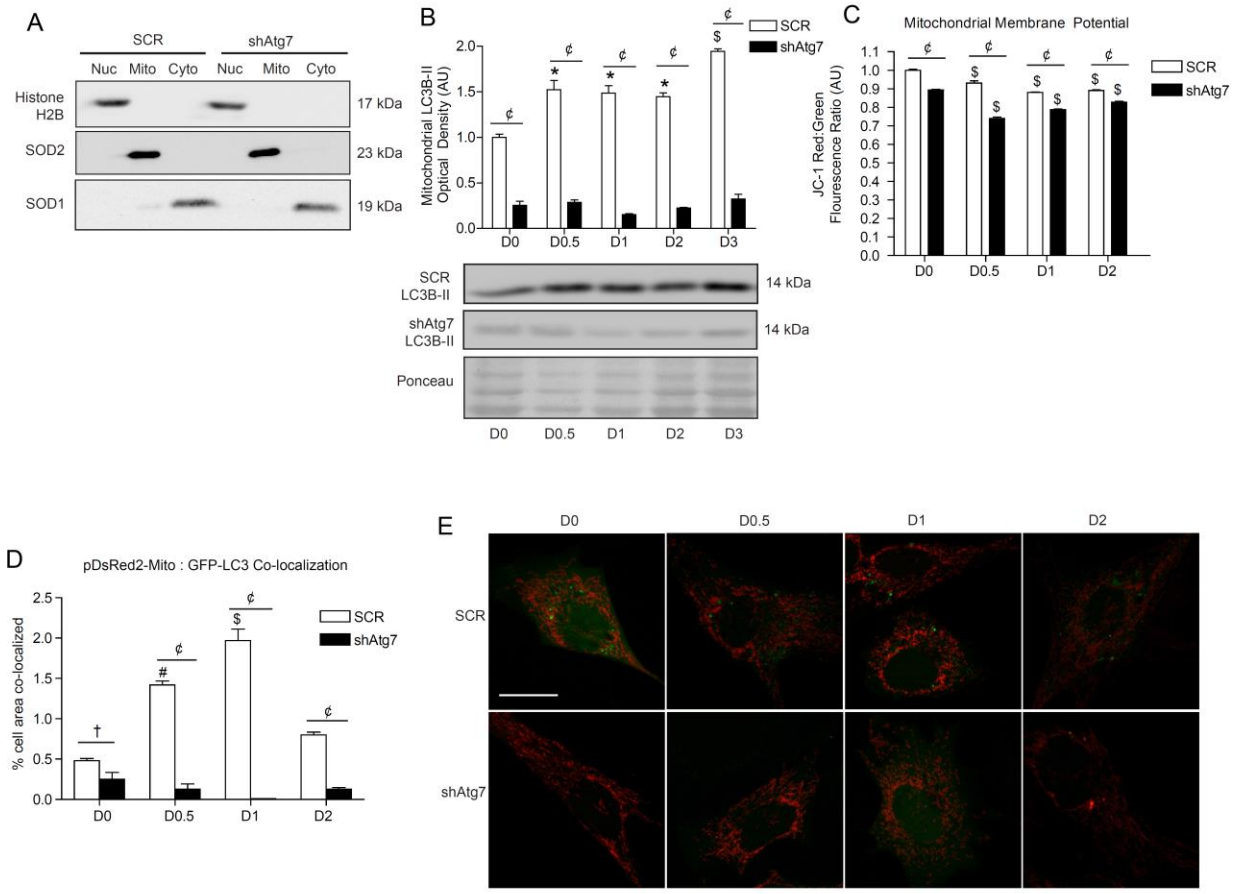

Fig. III - 4: Myoblast differentiation is associated with increased markers of mitophagy which are inhibited in the absence of ATG7

(A) Representative immunoblots of histone H2B, SOD1 and SOD2 protein in nuclear- (nuc) mitochondrial- (mito) and cytosolic-enriched (cyto) subcellular fractions. **(B)** Representative immunoblots and quantitative analysis of LC3B-II protein in mitochondrial-enriched subcellular fractions. Also shown is a representative ponceau stained membrane to display equal protein loading and quality of transfer. **(C)** Quantitative analysis of the JC-1 red:green fluorescence ratio in SCR and shAtg7 myoblasts during differentiation. **(D)** Quantitative analysis of GFP-LC3B and pDsRed2-Mito co-localization. Scale bar=25 µm. **(E)** Representative images of GFP-LC3B and pDsRed2-Mito co-transfected SCR and shAtg7 myoblasts during early time points of differentiation. Representative immunoblots of LC3B protein in SCR and shAtg7 cells were blotted simultaneously. However, for representative purposes membranes are shown as separate SCR and shAtg7 images. A one-way ANOVA was used to examine the effect of differentiation. A Students T-Test was used to determine differences between CTRL and shAtg7 groups within the same time point. *$p<0.05$, $^{\#}p<0.01$, $^{\$}p<0.001$ compared to D0. $^{\dagger}p<0.05$, $^{¢}p<0.001$ between treatment at same time point; (*n=2-3).*

Inhibition of autophagy results in increased mitochondrial-mediated apoptotic signaling during myoblast differentiation

Mitochondrial apoptotic signaling begins with the loss of mitochondrial membrane integrity through processes such as opening of the mitochondrial permeability transition pore[89] . Decreased ($p<0.05$) calcein fluorescence (indicative of mPTP formation) was observed on D1, D2 and D3 compared to D0 in shAtg7 cells (Fig. 5A). In contrast, SCR cells displayed increased ($p<0.001$) calcein fluorescence from D1 to D3 of differentiation (Fig. 5A). Interestingly, the level of calcein fluorescence was lower ($p<0.001$) in shAtg7 at all measured time points, indicating a more permeable mitochondrial membrane in autophagy-deficient myocytes. Following the permeabilization of mitochondrial membranes, the release of proteins such as CYTO C and AIF can promote the induction of apoptosis[36]. Both SCR and shAtg7 cells had a transient increase ($p<0.05$) in cytosolic CYTO C during differentiation (Fig. 5 & D). However, the level of cytosolic CYTO C protein content was greater ($p<0.01$) in shAtg7 compared to SCR cells during all days of differentiation (Fig. 5B & D). The release of mitochondrial CYTO C promotes the activation of CASP9[99]. In contrast to SCR cells, shAtg7 cells displayed elevated ($p<0.05$) CASP9 activity early during differentiation (Fig. 5E). Mitochondrial disruption can also contribute to caspase-independent forms of cell death through AIF-induced DNA fragmentation[36]. Cytosolic AIF was greater ($p<0.05$) on D3 than D0 in SCR cells (Fig. 5C & D). Interestingly, the level of cytosolic AIF was significantly greater ($p<0.01$) in shAtg7 than SCR myoblasts on D0 and D0.5 (Fig. 5C & D). For AIF to promote DNA fragmentation, it must translocate to the nucleus. While nuclear AIF levels increased ($p<0.05$) on D3 of differentiation in SCR cells, this increase ($p<0.05$) occurred on D0.5 in shAtg7 cells (Fig 5F & G). Collectively,

this data demonstrates that autophagy contributes to the regulation of mitochondrial-mediated apoptotic signaling during myoblast differentiation.

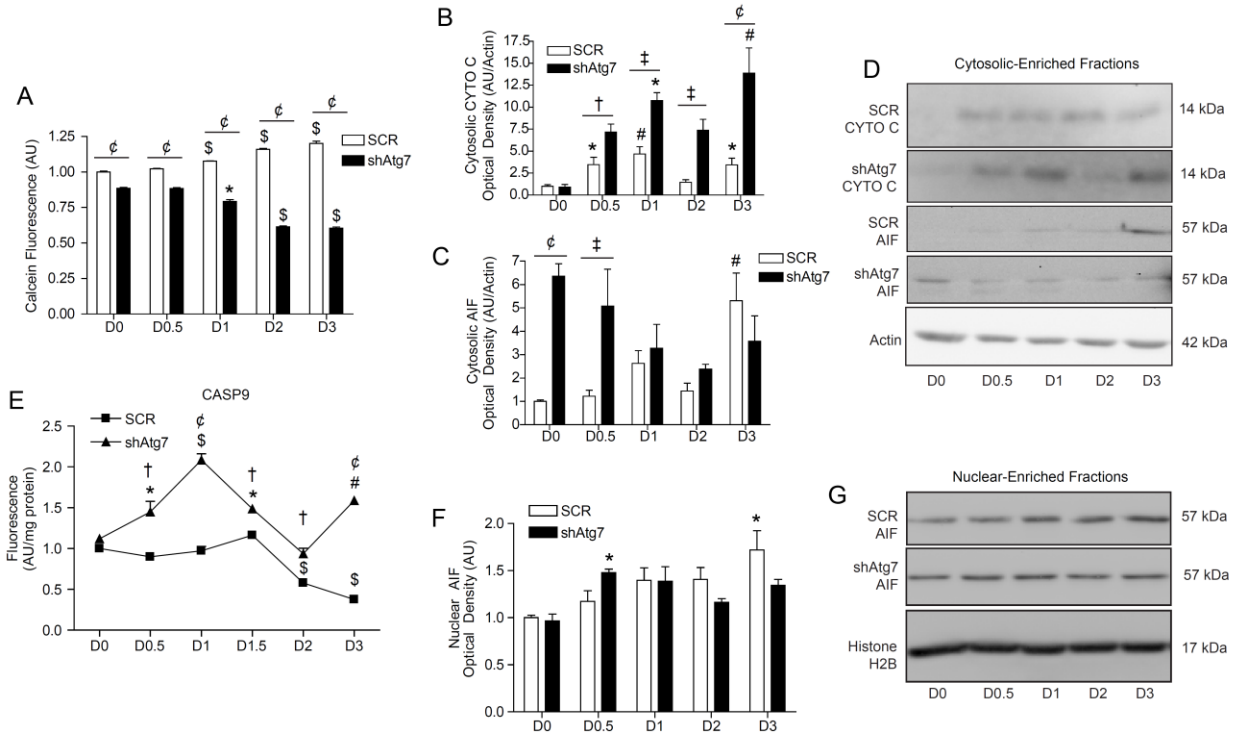

Fig. III - 5: Inhibition of autophagy during myoblast differentiation promotes increased mitochondrial-mediated apoptotic signaling

(A) Qualitative analysis of calcein fluorescence (where a decrease is indicative of mitochondrial permeability transition pore formation) in SCR and shAtg7 myoblasts during early differentiation. Quantitative analysis of cytosolic **(B)** CYTO C and **(C)** AIF protein as well as **(D)** representative immunoblots of cytosolic CYTO C and AIF protein in SCR and shAtg7 myoblasts during early differentiation. **(E)** Quantitative analysis of CASP9 activity in SCR and shAtg7 myoblasts during early differentiation. **(F)** Quantitative analysis of AIF protein content and **(G)** representative immunoblots of AIF and histone H2B protein in nuclear-enriched fractions from SCR and shAtg7 myoblasts during early differentiation. Also shown are representative Actin and histone H2B loading control blots. Representative immunoblots of CYTO C, AIF, histone H2B and Actin protein in SCR and shAtg7 cells were blotted simultaneously. However, for representative purposes membranes are shown as separate SCR and shAtg7 images. A one-way ANOVA was used to examine the effect of differentiation. A Students T-Test was used to determine differences between CTRL and shAtg7 groups within the same time point. $^{*}p<0.05$, $^{\#}p<0.01$, $^{\$}p<0.001$ compared to D0. $^{\dagger}p<0.05$, $^{\ddagger}p<0.01$, $^{¢}p<0.001$ between treatment at same time point; (*n=3-5).*

Inhibition of CASP9 and CASP3 partially recover markers of myoblast differentiation

Cell types which require caspase activity to accomplish cellular differentiation are at risk of cell death[210]. In our previous work we demonstrated that 3MA administration resulted in increased CASP3 activity and cell death in differentiating myoblasts[214]. To test whether elevated caspase activity is linked to the impaired myoblast differentiation observed in autophagy-deficient cells, shAtg7 cells were treated with a CASP3 or CASP9 inhibitor to limit caspase activity near to that observed in SCR cells. At the concentrations used, both CASP inhibitors reduced ($p<0.05$) CASP3 activity in shAtg7 myoblasts on D0.5 and D1 compared to non-treated shAtg7 cells (Fig. 6A). Attenuated CASP3 activity in shAtg7 cells resulted in increased ($p<0.05$) MYH protein content on D2 and D5 of differentiation compared to D0 in shAtg7 myocytes (Fig. 6B). However, MYH protein was not fully recovered to levels observed in SCR cells. Attenuation of CASP3 activity in shAtg7 myoblasts resulted in increased ($p<0.05$) fusion and differentiation indexes on D2 and D5 compared to non-treated shAtg7 cells (Fig. 6D & C). Overall, these results suggest that increased CASP3 activity is partially linked to impaired differentiation in autophagy-deficient myoblasts; an effect mediated by CASP9 activation.

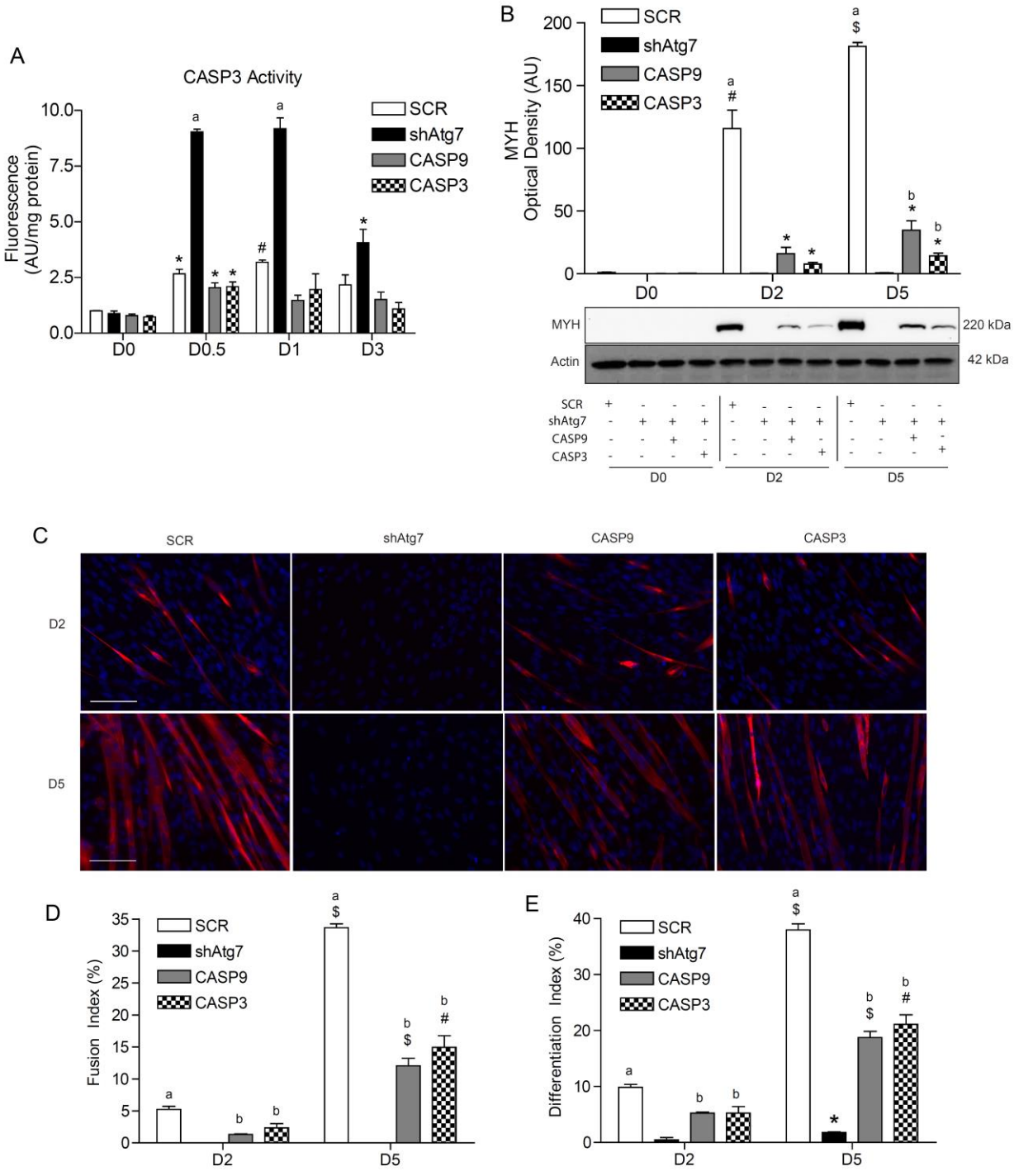

Fig. III - 6 Attenuation of CASP3 activity in shAtg7 myoblasts partially recovers myogenic markers and myotube formation

(A) Quantitative analysis of CASP3 activity in SCR, shAtg7, and shAtg7 myoblasts treated with caspase inhibitors during differentiation. **(B)** Quantitative analysis and representative immunoblot of MYH protein content in SCR, shAtg7, and treated shAtg7 myoblasts during

differentiation. **(C)** Representative images of myotube formation in SCR, shAtg7, and treated shAtg7 cells at D2 and D5 of differentiation. Cells were stained with DAPI (blue) and MF20 (red) to image nuclei and MYH, respectively. Scale bar=100 μm. Quantitative analysis of the **(D)** fusion index and **(E)** differentiation index in SCR, shAtg7, and treated shAtg7 myoblasts on D2 and D5 of differentiation. SCR and shAtg7: cells treated with DMSO vehicle; CASP9: shAtg7 cells treated with Ac-LEHD-CHO; CASP3: shAtg7 cells treated with Ac-DEVD-CHO. A two-way ANOVA with appropriate post hoc test was used to examine differences between treatment groups and differentiation.*$p<0.05$, $^{\#}p<0.01$, $^{\$}p<0.001$ compared to D0. a, significantly different than all ($p<0.05$), b, significantly different than shAtg7 ($p<0.05$).

DISCUSSION

Autophagy is required for myoblast differentiation and protects against apoptosis.

The formation and regeneration of myofibers involves the differentiation of myoblasts, followed by their fusion with other mononucleated myoblasts to form nascent myotubes or fusion with mature myofibers for regeneration[16,218]. We previously reported that autophagy increased during differentiation and was required for C2C12 differentiation. Furthermore, pharmacologic inhibition of autophagy increased DNA fragmentation and morphological features of apoptosis during differentiation[214]. In line with our previous study, inhibition of autophagy through stable knockdown of ATG7 reduced myotube formation and significantly increased apoptotic signaling and phosphatidylserine exposure. Although previous studies have shown that phosphatidylserine is required for the formation of myotubes[35], the presence of elevated CASP3 activity and mitochondrial-mediated cell death signaling suggests that this increase in phosphatidylserine exposure represents a cell death event in this context.

The loss of autophagy increases ROS generation, oxidative damage and CAPN activity

Our data suggests that ATG7 knockdown resulted in elevated oxidative stress in myoblasts prior to the induction of differentiation as supported by increased antioxidants such as SOD1 and CAT, and augmented ROS generation[219-221]. Although elevated SOD1 and CAT could

protect cells against oxidative damage, this is likely not the case here as 4HNE levels were elevated in shAtg7 cells during early differentiation. 4HNE can also contribute to ROS generation through oxidative modification of other proteins and lipids as well as by damaging ETC proteins [222]. Since the inhibition of autophagy in shAtg7 cells impaired mitophagy, it is likely that the inability to clear damaged mitochondria resulted in increased oxidative stress and susceptibility to cell death signaling upon the induction of differentiation.

Autophagy can also attenuate oxidative and ER-stress by degrading aggregated/misfolded proteins[12,156]. Previous work has demonstrated that damaged proteins can accumulate in the absence of autophagy [1]. In response to this, molecular chaperones such as HSP70 are upregulated to prevent proteotoxicity [223]. As such we observed a robust increase in HSP70 in shAtg7 cells which may have been an attempt to process damaged or misfolded proteins. HSP70 has also been shown to respond to apoptotic stress by sequestering and inhibiting pro-apoptotic proteins such as BAX and AIF [88,224]. Therefore, increased HSP70 may be a compensatory response to autophagy impairment. Together, the increased HSP70 protein content and CAPN activity in autophagy-deficient cells at the onset of differentiation suggests elevated ER-stress[28,156,225]. Interestingly, when induced in myoblasts prior to differentiation, ER-stress has been shown to promote skeletal myotube formation[30]. However, ER-stress and CAPN activity can also participate in CASP12 activation, cleavage of several muscle-specific contractile proteins, impair AKT signaling, and directly contribute to the induction of mitochondrial-mediated apoptotic pathways[226-229]. Accordingly, these factors may have contributed to the induction of apoptosis during myoblast differentiation. Collectively, the damage caused by oxidative and possibly ER stress early during the differentiation process likely promoted mitochondrial-mediated death signaling during differentiation.

Autophagy regulates mitochondrial-mediated apoptotic signaling during myoblast differentiation

In the absence of autophagy, reduced mitochondrial membrane potential was associated with the formation of mPTP. Increased ROS, lipid peroxidation, ER-stress, and reduced BCL2 and ARC protein have all been shown to promote mitochondrial-mediated apoptosis associated with the formation of the mPTP[67,77,230-232]. Considering that all these occurred in the absence of autophagy during differentiation, it is likely that one or more contributed to the formation of mPTP. This would suggest that autophagy can attenuate cellular stress and mitigate the formation of mPTP; a key event in mitochondrial-mediated apoptosis. Consistent with our results, inhibition of autophagy has been shown to promote the induction of mitochondrial-mediated apoptosis through the loss of mitochondrial membrane integrity[233].

The formation of mPTP promotes the release of CYTO C and AIF into the cytosol where they contribute to the induction of mitochondrial-mediated apoptotic signaling[67]. We observed higher levels of cytosolic CYTO C in autophagy-deficient myoblasts during differentiation. Once in the cytosol, CYTO C promotes the induction of apical CASP9 which leads to CASP3 activation and cell death[63]. Importantly, increased cytosolic CYTO C was associated with elevated CASP9 activity in shAtg7 cells during differentiation. This augmented CASP9 activity in shAtg7 cells promoted cell death signaling and associated events above levels observed in SCR control cells. Together, these data demonstrate that autophagy is required to protect from caspase-dependent, mitochondrial-mediated apoptotic signaling and cellular stress events. In addition, autophagy may also protect against caspase-independent apoptotic signaling (AIF) early during myoblast differentiation.

In control cells, differentiation resulted in a small reduction in mitochondrial membrane potential and a submaximal increase in cytosolic CYTO C. Interestingly, these events did not result in increased CASP9 activity. The maintenance of sub-apoptotic cytosolic CYTO C and reduced mitochondrial membrane potential observed in control cells during differentiation may have been due to normal regulation of mitophagy. During mitophagy, mitochondria can be sequestered and degraded in response to decreased mitochondrial membrane potential, mitochondrial lipid peroxidation, and/or increased ROS[234], all factors observed in control myoblasts during differentiation. The induction of mitophagy and selective sequestration of mitochondria with lower membrane potential and dysfunction acts as a quality control mechanisms removing these aberrant organelles before they promote apoptotic signaling[235]. It is therefore likely that the inability to clear dysfunctional mitochondria in shAtg7 myoblasts via mitophagy led to the initiation of mitochondrial-mediated apoptotic signaling during differentiation. Additional work should be designed to further study the direct influence of mitophagy during myoblast differentiation and to ascertain why and how certain mitochondria may be selected for degradation.

Autophagy regulates the magnitude of CASP activity during myoblast differentiation

Compared to cells which die during differentiation, adherent myocytes display low levels of cleaved CASP12, CASP9, and CASP3 suggesting that these enzymes may contribute to non-cell death signaling events[29,30]. Furthermore, this data indicates that the magnitude of CASP3 activity is essential in the balance between the induction of physiological apoptosis-related signaling and apoptotic cell death during myoblast differentiation[210]. In the current study, we postulate that ATG7 knockdown induced mitochondrial apoptotic signaling that exceeded a threshold set for CASP9 and CASP3. Rather than causing physiological adaptation, the high

level of upstream signaling resulted in apoptotic cell death. Similarly, autophagy is required to protect from caspase-mediated cell death during monocyte to macrophage specialization, and during endothelial cell precursor cell differentiation[200,236]. In addition, the current results demonstrate that autophagy regulates caspase activity during myoblast differentiation by attenuating the level of mitochondrial cell death signaling.

Impaired myoblast differentiation is directly involved in increased caspase activity

We found that the caspase inhibitors used to reduce CASP3 activity in shAtg7 cells to levels observed in untreated control cells partially recovered the loss of MYH expression and morphological indices. These data demonstrate that increased CASP3 activity is partially linked to the reduction in myoblast differentiation observed in the absence of autophagy and points to a critical role of autophagy in regulating the magnitude of CASP3 activity during myoblast differentiation. Furthermore, treating shAtg7 cells with a CASP9 inhibitor during differentiation reduced CASP3 activity to levels similar to cells treated with a CASP3 inhibitor. This finding suggests that the rise in CASP3 activity observed in shAtg7 myocytes during differentiation is mediated by CASP9. Together, these data provide evidence that autophagy plays a critical role in regulating the quantity of apoptotic signaling during myoblast differentiation. It should be noted that differentiation was not fully recovered in shAtg7 cells with attenuated CASP3 activity, suggesting that autophagy regulates other elements of myoblast differentiation in addition to apoptotic signaling. This may include the regulation of amino acid or fatty acid availability for organelle biogenesis and protein accretion. Furthermore, autophagy may be required for the degradation of specific signaling molecules required for myoblast differentiation. However, further research will be required to identify these roles.

The induction of catabolic processes such as autophagy and apoptotic signaling is required for normal differentiation and formation of skeletal muscle[2,210,211]. We recently observed increased autophagy-related proteins and markers of autophagosome content during C2C12 differentiation[214]. Furthermore, we found that inhibition of autophagy impaired differentiation and increased markers of cell death. We now show that mitochondrial-mediated apoptosis and mitochondrial stress are elevated in the absence of autophagy during myoblast differentiation and are associated with impaired mitophagy. Moreover, the impairments observed in myoblast differentiation due to inhibition of autophagy were linked to increased caspase activity, suggesting that autophagy helps regulate the level of apoptotic signaling during myoblast differentiation.

CHAPTER IV: Autophagy is required to protect against apoptotic signaling during and following CisPT injury

OVERVIEW

Both apoptosis and autophagy are associated with muscle atrophy and dysfunction. However, the interplay between these two "cell death" processes is complex and has not been directly investigated in skeletal muscle. The purpose of this study was to examine the cross-talk between autophagy and apoptosis in response to the cell death and muscle atrophy inducer cisplatin (CisPT). Our data demonstrates that in C2C12 myotube cultures CisPT causes a reduction ($p<0.05$) in myotube diameter and elevation ($p<0.05$) of autophagy markers LC3B-II, BNIP3, BECN1, CTS as well as apoptotic measures, BAX, BAX/BCL2, CASP3, and DNA fragmentation. Interestingly, when autophagy is inhibited during submaximal levels of apoptotic stress, apoptotic hallmarks such as mPTP formation, CASP9 and CASP3 activity, and DNA fragmentation are further augmented ($p<0.05$). However, inhibition of autophagy during CisPT exposure does not alter myotube diameter. To examine the role of autophagy in the recovery following stress, CisPT was removed from C2C12 myotube cultures after 24hrs of exposure and replace with fresh media or media with 3MA for 48hr. Following the removal of CisPT, myotube recovery required autophagy to mitigate ($p<0.05$) CASP9 and CASP3 activity. Autophagy is also required to attenuate ($p<0.05$) mPTP formation, restore ($p<0.05$) mitochondrial membrane potential, and increase differentiation and fusion indexes during recovery. Together, this data supports an anti-apoptotic role for autophagy during muscle atrophy induced by CisPT. In addition, autophagy is required to promote the recovery of damaged myotubes following CisPT-induced apoptotic stress.

INTRODUCTION

The interplay between autophagic and apoptotic processes in skeletal muscle remains unresolved and is complex. Hindlimb unloading, denervation, and the administration of chemotherapeutic agents have been shown to induce apoptotic signaling in skeletal muscle; moreover, they have also been shown to alter autophagic signaling[6,104,106,123,237]. Some skeletal muscle literature has hypothesized that autophagy is a cell death system which promotes muscle atrophy[11,123,157,181]. In contrast, evidence is accumulating which demonstrates that autophagy plays an important pro-survival role in the cell stress response[12]. For example, following a cellular insult resulting in damaged mitochondria, mitophagy, a form of selective autophagy, can specifically target damaged mitochondria and promote their degradation through the lysosome. In effect, dysfunctional mitochondria are removed thus preserving mitochondrial function and preventing the release of pro-apoptotic proteins[235,238,239]. Further, autophagy has as a well-established role in the removal of aggregated proteins, which can also promote pro-apoptotic signaling and compromise cellular function[12,156,240]. Together, these data suggest that autophagy is present during periods of skeletal muscle apoptosis and atrophy but could protect the myofiber from stress.

Apoptotic signaling in skeletal muscle results in the cleavage of structural/contractile proteins, destruction of organelles, and loss of nuclei within the myofiber[241]. Collectively, this promotes the remodeling of the entire myofiber resulting in atrophy of the cell and tissue[4,36,241,242]; however, the cell remains intact and functional, albeit at a lower capacity[6,58]. Research shows, that degradative processes can be stimulated by apoptotic signaling and contribute to the removal of apoptotic debris[242]. In skeletal muscle, autophagic proteins are altered during the recovery from apoptotic inducing events such as hindlimb suspension and

crush injury[243,244]; suggesting that autophagy may also respond to apoptotic signaling by clearing damaged protein and organelles once the stress has been removed. Thus, the ability of the muscle to recover from apoptotic events is associated with altered markers of autophagy, yet the role of autophagy in these processes has not been specifically investigated.

Cisplatin (CisPT) is a commonly used chemotherapeutic drug due to its ability to induce cell death through multiple mechanisms in several cancer cell types[245]. CisPT is highly effective at promoting cell death in cancer cells; however, non-target tissues such as skeletal muscle are also adversely effected[246]. Although CisPT treatment in skeletal muscle cultures results in an alteration to both autophagic and apoptotic processes and both are associated with a loss in cell size[247-249], the role of autophagy in cell death signaling and the interplay between apoptosis and autophagy are not known. Furthermore, following the cessation of CisPT treatments the muscle must recover from the cytotoxicity/injury[246]. In order to recover muscle mass, inhibiting degradative pathways has been suggested[250]; however, how or what affect this may have on muscle viability and regeneration after CisPT treatments is unknown.

METHODS

Cell culturing and drug administration

Mouse C2C12 skeletal myoblasts (ATCC) were plated at a low passage in polystyrene cell culture dishes (BD Biosciences) in growth media (GM) consisting of low-glucose Dulbecco's Modified Eagles Medium (DMEM; Hyclone, Thermo Scientific) containing 10% fetal bovine serum (FBS; Hyclone, Thermo Scientific) with 1% penicillin/streptomycin (Hyclone, Thermo Scientific) and incubated at 37ºC in 5% CO_2. Myoblast differentiation was

induced once C2C12 myoblasts attained 80-90% confluence by replacing GM with differentiation media (DM) consisting of DMEM supplemented with 2% horse serum (Hyclone, Thermo Scientific) and 1% penicillin/streptomycin following 3 washes in warm phosphate buffered saline (PBS; Hyclone, Thermo Scientific).

To investigate the effects of CisPT on differentiated myotubes, C2C12 myotubes at day 4 of differentiation were exposed to vehicle (0.9% $NaCl^-$ solution) or CisPT (made in vehicle) for 24 hr at various doses as indicated in the results. To examine myotube recovery following CisPT injury, myotubes at day 4 of differentiation were given 50 µM of CisPT for 24 hr. After 24 hr of CisPT cells were either immediately collected (0 hr recovery cells), or given fresh DM with or without 5 mM of 3MA and collected at various time points up to 48 hr. Inhibition of autophagosome formation was achieved with 5 mM doses of 3MA as previously described over 24 hr periods[214]. Inhibition of autophagic flux was achieved using 10 µM of chloroquine (CQ) for 12 hr.

Cells were removed from culture dishes by trypsinization (0.25% trypsin with 0.2 g/L EDTA; Thermo Scientific), and collected by centrifugation (800 x g for 5 min). Cell pellets were resuspended and washed in ice cold PBS, centrifuged (800 x g for 5 min), and frozen at -80°C until further analysis. Protein concentrations were determined using the BCA protein assay.

Immunoblotting

Immuoblotting was conducted as previously described[214]. Briefly, cells were lysed in ice cold buffer (20 mM HEPES, 10 mM NaCl, 1.5 mM MgCl, 1 mM DTT, 20% glycerol and 0.1% Triton X100; pH 7.4) with protease inhibitor (Roche Applied Sciences). Equal amounts of cell protein was loaded and separated on 7.5-15% SDS-PAGE gels, transferred onto PVDF membranes (Bio-Rad Laboratories), and blocked for 1 hr at room temperature or overnight at

4°C with 5% milk-Tris-buffered saline-Tween 20 (milk-TBST). Membranes were incubated overnight at 4°C or for 1 hr at room temperature with primary antibodies against: BECN1, ATG7, LC3B (Cell Signaling Technology); BCL2, BAX (Santa Cruz Biotechnology); BNIP3 and Actin (Sigma-Aldrich). Membranes were washed with TBST, incubated with the appropriate horseradish peroxidase (HRP)-conjugated secondary antibodies (Santa Cruz Biotechnology) for 1 hr at room temperature and washed with TBST. Bands were visualized using enhanced chemiluminescence western blotting detection reagents (BioVision) and the ChemiGenius 2 Bio-Imaging System (Syngene). The approximate molecular weight for each protein was estimated using Precision Plus Protein WesternC Standards and Precision Protein Strep-Tactin HRP Conjugate (Bio-Rad Laboratories). Equal loading and quality of transfer was confirmed by staining membranes with Ponceau S (BioShop).

Flow cytometry

To measure mitochondrial-membrane potential, cells were washed in Hank's Buffered Salt Solution (HBSS) and then incubated with 2 μM JC-1 (Life Technologies) for 15 min at 37°C. Following incubation, cells were washed, centrifuged, and resuspended in HBSS. To measure the formation of the mitochondrial permeability transition pore (mPTP) cells were incubated with 1 μM calcein AM (Life Technologies) and 1 mM $CoCl_2$ in HBSS for 15 min at 37°C, washed, centrifuged, and resuspended in HBSS. All analyses were performed on a flow cytometer (BD FACSCalibur) equipped with Cell Quest Pro software (BD Bioscience) as previously described[93].

Proteolytic enzyme activity and ROS generation

Enzymatic activity of CASP3 (CASP3) and CASP9 (CASP9) was determined in cells lysates using the substrate Ac-DEVD-AMC and Ac-LEHD-AMC (Enzo Life Sciences),

respectively, as previously described[93,214]. Enzymatic activity of cathepsin (CTS) was assessed using the fluorogenic substrate z-FR-ARC (Enzo Life Sciences) as previously described[251]. CASP and CTS enzymatic activity was normalized to total protein content and expressed as fluorescence intensity in arbitrary units (AU) per milligram protein.

DNA fragmentation was determined using the Cell Death Detection ELISA^{PLUS} Kit (Roche Diagnostics) as previously described[214]. Briefly, cells were homogenized in the supplied lysis buffer and centrifuged at 200 g for 10 min at room temperature. 20 µl of supernatant was incubated with 80 µl of anti-histone-biotin/anti-DNA-POD reagent in a streptavidin-coated microplate for 2 hr at room temperature with gentle shaking. Each well was washed several times followed by the addition of 100 µl of ABTS substrate solution. Absorbance was measured with a SPECTRAmax Plus spectrophotometer (Molecular Devices), normalized to total protein content, and expressed as AU per mg protein.

Fluorescence microscopy

Myosin heavy chain (MYH) immunofluorescence analysis was conducted on cells grown on glass coverslips in culture dishes[214] to determine myotube size as well as differentiation and fusion indexes. Coverslips were first washed with PBS, fixed with 4% formaldehyde-PBS for 10 min at room temperature, and washed with PBS. Cells were permeablized for 10 min with 0.5% Triton X100, and washed in PBS. Cells were then blocked with 10% goat serum (Sigma-Aldrich) for 30 min, incubated with a primary antibody against MYH (Developmental Studies Hybridoma Bank; MF20) for 2 hr, washed with PBS, and incubated with an anti-mouse PE-conjugated secondary antibody (Santa Cruz). Cells were washed in PBS, counterstained with DAPI nuclear stain (Life Technologies) for 5 min, washed min in PBS, and mounted with Prolong Gold Antifade Reagent (Life Technologies). Slides were visualized with an Axio Observer Z1

fluorescent microscope equipped with Red/Green/Blue filters, an AxioCam HRm camera, and AxioVision software (Carl Zeiss). Myotube diameter was quantified as the average diameter of 3 random areas of each myotube per field (between 4-5 images per sample). The fusion index was calculated as the percentage of nuclei present in multinucleated (two or more nuclei) cells relative to total nuclei. The differentiation index was calculated as the percentage of cells expressing MYH relative to total cell number.

To visualize lysosomal and mitochondrial content, live cells were incubated with either LysoTracker Red (LTR; 75nM) (Life Technologies) and/or MitoTracker Green (MTG; 50nM) (Life Technologies) for 30 min at 37ºC in 5% CO_2. Cells were then washed in PBS, fixed with 4% formaldehyde, and counterstained with Hoescht NucBlue (Life Technologies) for 5 min at room temperature to visualize nuclei. LTR fluorescence and LTR:MTG co-localization was determined in multinucleated cells (2 or more nuclei within a single cell) using Image J software.

Statistics

A One-Way repeated measure ANOVA was used to assess the dose response of CisPT. If a main effect was observed, Tukey's post hoc test was used to determine differences. A Two-Way ANOVA was used to assess the effects of treatment over time, along with the Tukey's post-hoc test. For all experiments $p<0.05$ was considered statistically significant.

RESULTS

CisPT induces dose-dependent changes to autophagy and apoptosis in C2C12 myotubes.

To investigate autophagy and apoptosis in response to CisPT exposure, C2C12 myotubes were incubated with vehicle, 25 µM, 50 µM, 100 µM, or 200 µM CisPT for 24 hours. LC3B-II

and LC3B-I increased ($p<0.05$) in response to CisPT. Moreover, the LC3B-II/I protein ratio was elevated ($p<0.05$) in response to 200 µM CisPT (Fig. 1A). We also observed changes to key autophagy-related proteins which regulate the formation of the autophagosome. BNIP3 and BECN1 protein were elevated ($p<0.05$) at various doses of CisPT, but not ATG7 protein (Fig. 1B). CTS activity is required for the degradation of autophagosomal cargo, and showed a dose-dependent change to CisPT ($p<0.01$) (Fig. 1C).

CisPT also induced several changes to apoptosis-related proteins, including up-regulating ($p<0.05$) BAX and down-regulating ($p<0.001$) BCL2 (Fig. 1D). As such, the BAX/BCL2 protein ratio was significantly increased ($p<0.001$) at 25 µM, 50 µM, and 100 µM CisPT (Fig. 1D). Interestingly, the BAX/BCL2 protein ratio during 50 µM CisPT was greater ($p<0.001$) than all other doses. CASP3 activity increased ($p<0.01$) in a dose-dependent manner in response to CisPT (Fig. 1E). Activation of downstream apoptotic signaling enzymes such as CASP3 promotes DNA fragmentation, a hallmark of late stages of apoptosis[36]. As such, DNA fragmentation was increased ($p<0.001$) in response to 50 µM, 100 µM, and 200 µM CisPT (Fig. 1F).

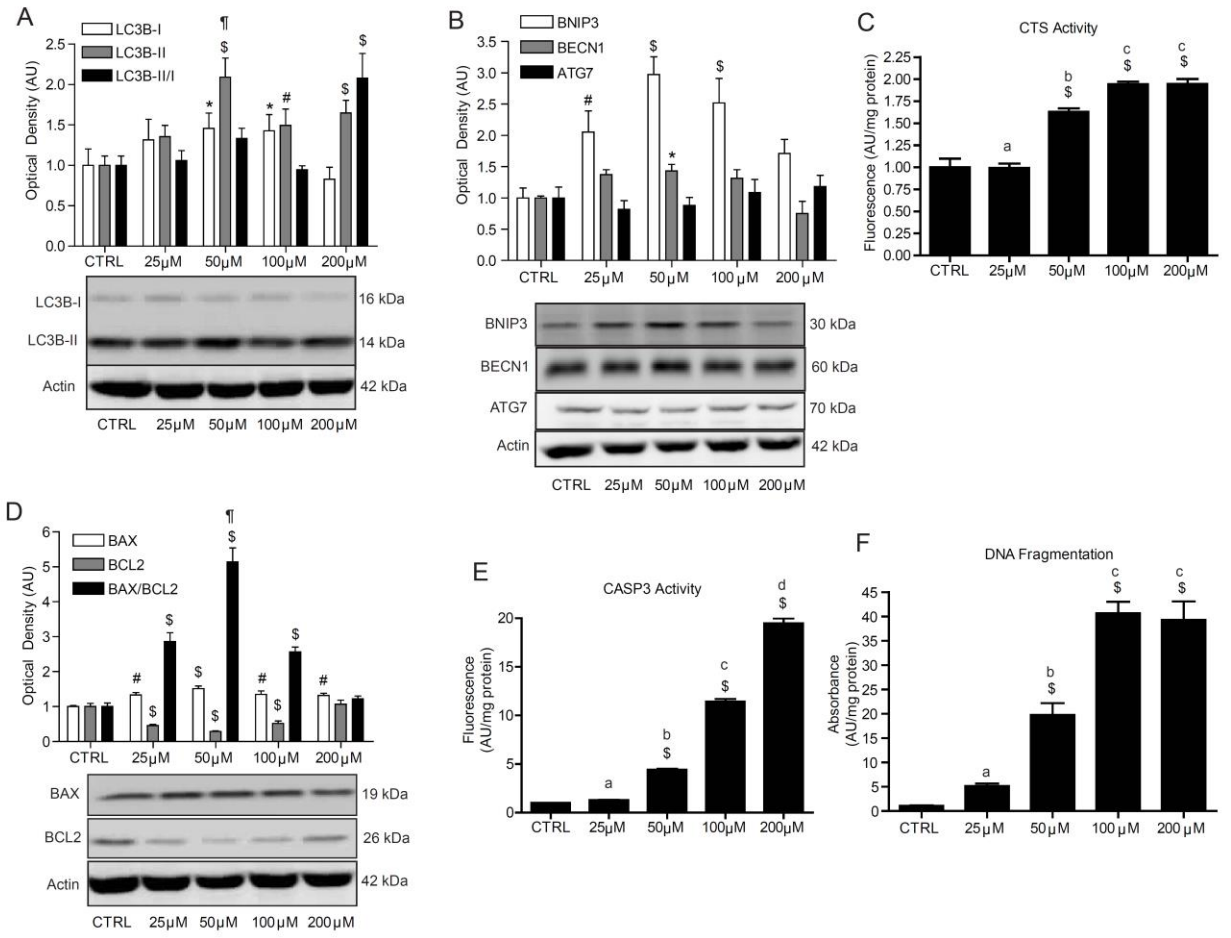

Fig. IV - 1: Autophagic and apoptotic dose response to CisPT

Quantitative analysis and representative immunoblots of **(A)** LC3B-I and LC3B-II protein as well as LC3B-II/I protein ratio, and **(B)** BNIP3, BECN1, and ATG7 protein in response to various doses of CisPT after 24 hr. Quantitative analysis of **(C)** CTS activity and **(D)** quantitative analysis and representative immunoblots of BAX and BCL2 protein as well as the BAX/BCL2 protein ratio in response to various doses of CisPT after 24 hr. Quantitative analysis of **(E)** CASP3 activity and **(F)** DNA fragmentation in response to various doses of CisPT after 24 hr. Also shown are representative Actin loading control blots. A one-way ANOVA was used to examine the effect of dose. *$p<0.05$, $^{\#}p<0.01$, $^{\$}p<0.001$ compared to non-treated CTRL. ¶ $p<0.05$ compared to all. a, b, c, d $p<0.05$ compared to non-matching letters; (*n=3-5).*

To ensure changes observed to markers of autophagy represented increased autophagic flux we administered 50 μM and 200 μM CisPT to C2C12 myotubes along with 5 μM of chloroquine (CQ), a commonly used inhibitor of lysosomal enzymes. LC3B-II protein

accumulation in CQ treated cells was significantly greater ($p<0.01$) at both 50 µM and 200 µM doses of CisPT relative to CTRL (Fig 2C & D). These results suggest that the increase in autophagy markers during CisPT exposure is due to increased autophagic flux.

Increased proteolytic activity in skeletal muscle can contribute to muscle atrophy[59]. Accordingly CisPT caused a dose-dependent decline ($p<0.01$) in myotube diameter. Interestingly, myotube diameter did not differ between 100 µM and 200 µM CisPT (Fig. 2A & B).

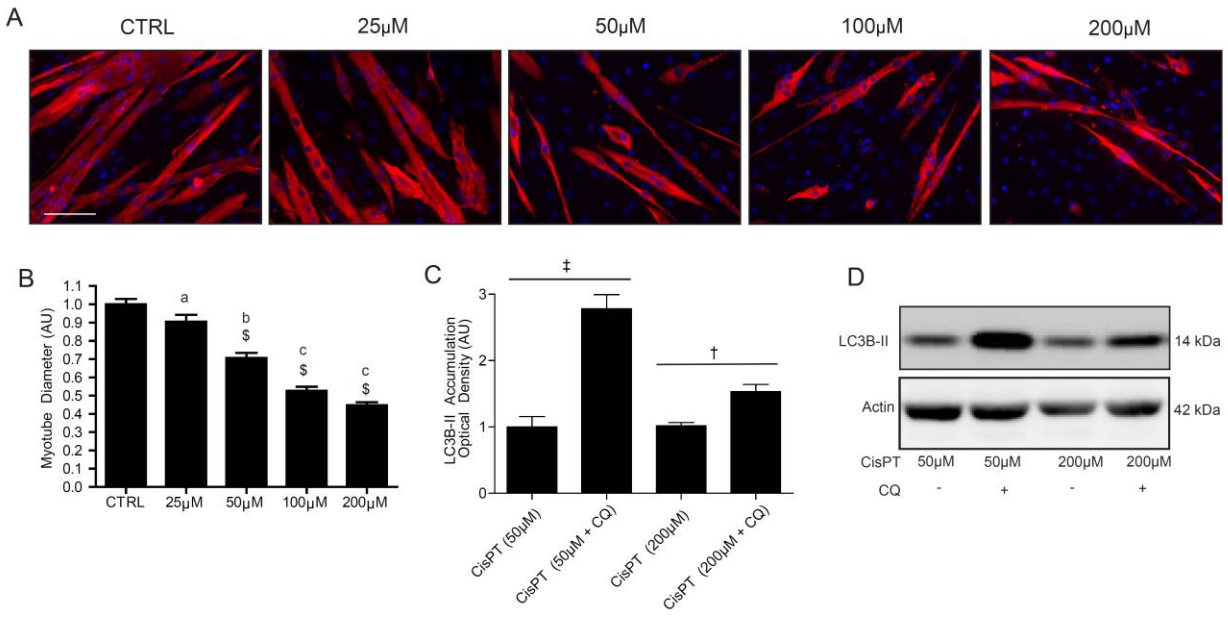

Fig. IV - 2: CisPT induces myotube atrophy and an increase in autophagic flux

(A) Representative images of myotubes exposed to CisPT after 24 hr. Cells were stained with DAPI (blue) and MF20 (red) to image nuclei and MYH, respectively. Scale bar=100µm. **(B)** Quantitative analysis of myotube diameter. **(C)** Quantitative analysis and **(D)** representative immunoblot of LC3B-II in CisPT and CisPT + CQ exposed cells after 24 hr of incubation. Also shown is a representative Actin loading control blot. A one-way ANOVA was used to examine the effect of dose. A Students T-Test was used to determine differences between CisPT and CQ groups. $^{\$}p<0.001$ compared to non-treated CTRL. $^{\dagger}p<0.05$, $^{\ddagger}p<0.01$ compared to treatment at same dose point. a, b, c, d $p<0.05$ compared to non-matching letters. (*n=3).*

Time-course analysis of autophagy- and apoptosis-related markers over 24 hr of CisPT exposure

We next examined the temporal kinetics of autophagy and apoptosis over a 24 hr period to submaximal (50 μM) and maximal (200 μM) levels of CisPT. CASP3 activity was elevated ($p<0.01$) at 12 hr and 24 hr in response to 200 μM CisPT but only at 24 hr ($p<0.001$) in myotubes treated with 50 μM CisPT (Fig. 3A). CASP3 activity was greater to 200 μM than 50 μM CisPT beginning at 6 hr (Fig. 3A). BAX protein increased ($p<0.05$) at 12 hr and 24 hr in cells incubated with 200 μM CisPT (Fig. 3B). Similarly, 50 μM CisPT increased ($p<0.05$) BAX protein at 3 hr, 12 hr, and 24 hr (Fig. 3B). Furthermore, BAX protein was higher ($p<0.05$) with 200 μM compared to 50 μM CisPT at 24 hr (Fig. 3B). BCL2 protein was also significantly ($p<0.05$) reduced with CisPT at 12 hr (50 μM) and 24 hr (200 μM) (Fig. 3C).

CTS activity was elevated ($p<0.05$) from 6 hr to 24 hr in myotubes incubated with 200 μM CisPT but only at 24 hr ($p<0.05$) to 50 μM CisPT (Fig. 3D). LC3B-II increased ($p<0.01$) at 3 hr and remained elevated at 24 hr in response to 50 μM of CisPT; however, in response to 200 μM LC3B-II levels increased only at 12 hr. Compared to 50 μM, LC3B-II was greater ($p<0.05$) at 3hr, 6 hr, and 24 hr to 200 μM (Fig. 3E). BECN1 levels were increased ($p<0.05$) at 3 hr and 6 hr in both 50 μM and 200 μM CisPT groups; as well as at 24 hr in 50 μM CisPT (Fig. 3G). BNIP3 increased ($p<0.001$) at 24 hr in response to both 50 μM and 200 μM CisPT. Interestingly, both BECN1 and BNIP3 protein were greater ($p<0.05$) with 50 μM compared to 200 μM CisPT at 24 hrs (Fig. 3H). ATG7 protein increased ($p<0.01$) at 3 hr and 6 hr in response to 50 μM CisPT (Fig. 3I).

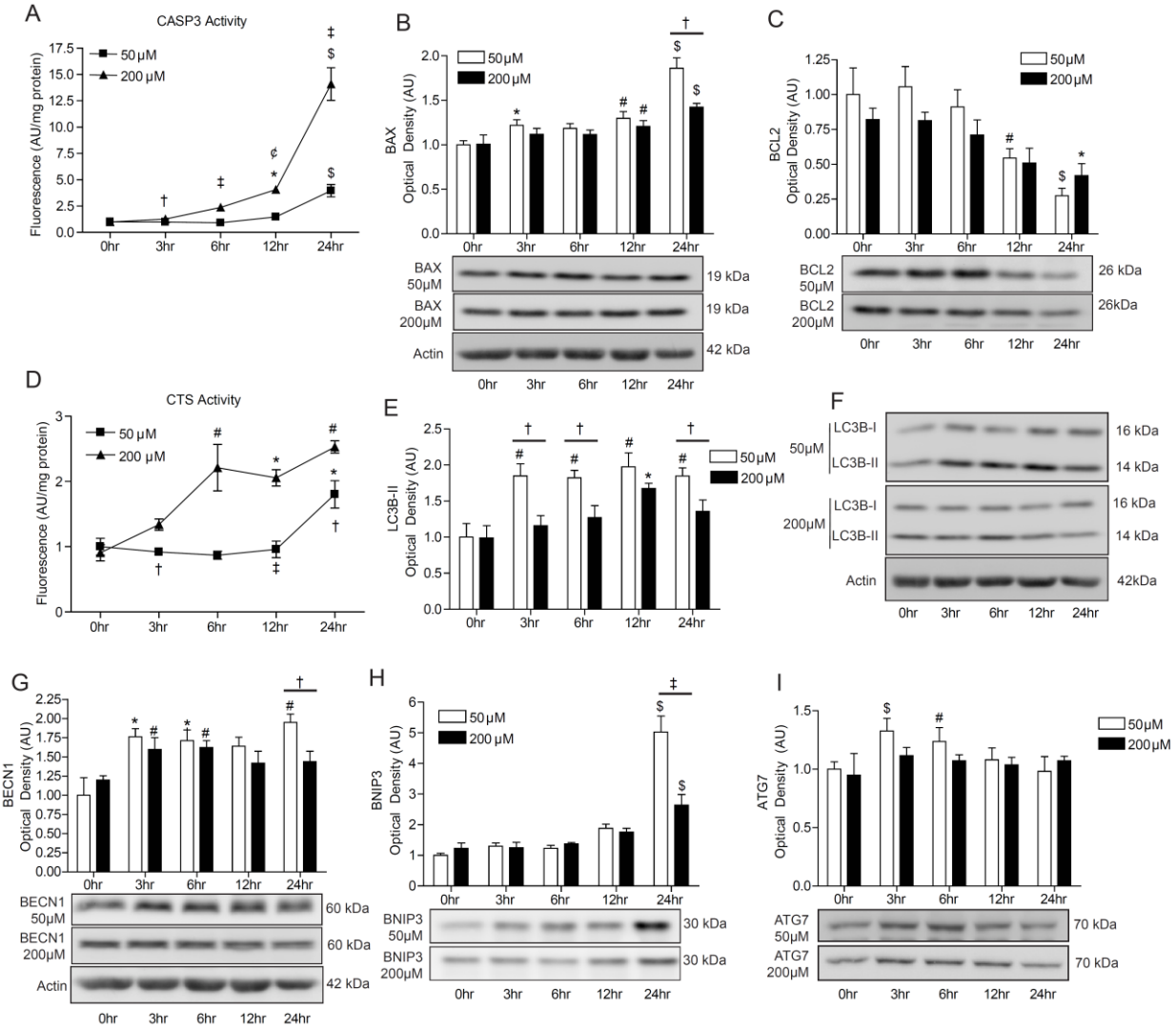

Fig. IV - 3: Time course analysis of apoptotic and autophagic responses to 50 µM and 200 µM of CisPT over 24 hrs

(A) Quantitative analysis of CASP3 activity. Quantitative analysis and representative immunoblots of **(B)** BAX and **(C)** BCL2 protein. **(D)** Quantitative analysis of CTS activity. **(E)** Quantitative analysis of LC3B-II protein, and **(F)** representative immunoblots of LC3B-I and LC3B-II protein. Quantitative analysis and representative immunoblots for **(G)** BECN1, **(H)** BNIP3 and **(I)** ATG7 protein. Also shown are representative Actin loading control blots. A one-way ANOVA was used to examine the effect of time or doses independently. A Students T-Test was used to determine differences between 50µM and 200µM groups within a single time point. *$p<0.05$, $^{\#}p<0.01$, $^{\$}p<0.001$ compared to 0 hr CTRL. $^{\dagger}p<0.05$, $^{\ddagger}p<0.01$, compared between 50 µM and 200 µM doses at same time point; (*n=3-4).*

Pharmacological inhibition of autophagy with 3MA increases apoptosis

To test whether the induction of autophagy was promoting or mitigating apoptotic signaling we attenuated the formation of the autophagosome with 3MA[214,248]. Experiments were performed with 50 µM of CisPT given that we observed a large increase in autophagy and submaximal levels of apoptosis. 3MA effectively attenuated ($p<0.05$) LC3B-II protein during CisPT exposure (Fig. 4A). Although CisPT affected BAX, BCL2 and the BAX:BCL2 ratio at later time points ($p<0.05$), 3MA had little effect (Fig. 4B, C & D). In contrast, the elevated CASP3 and DNA fragmentation caused by CisPT was further augmented ($p<0.05$) by 3MA treatment (Fig 4E & F).

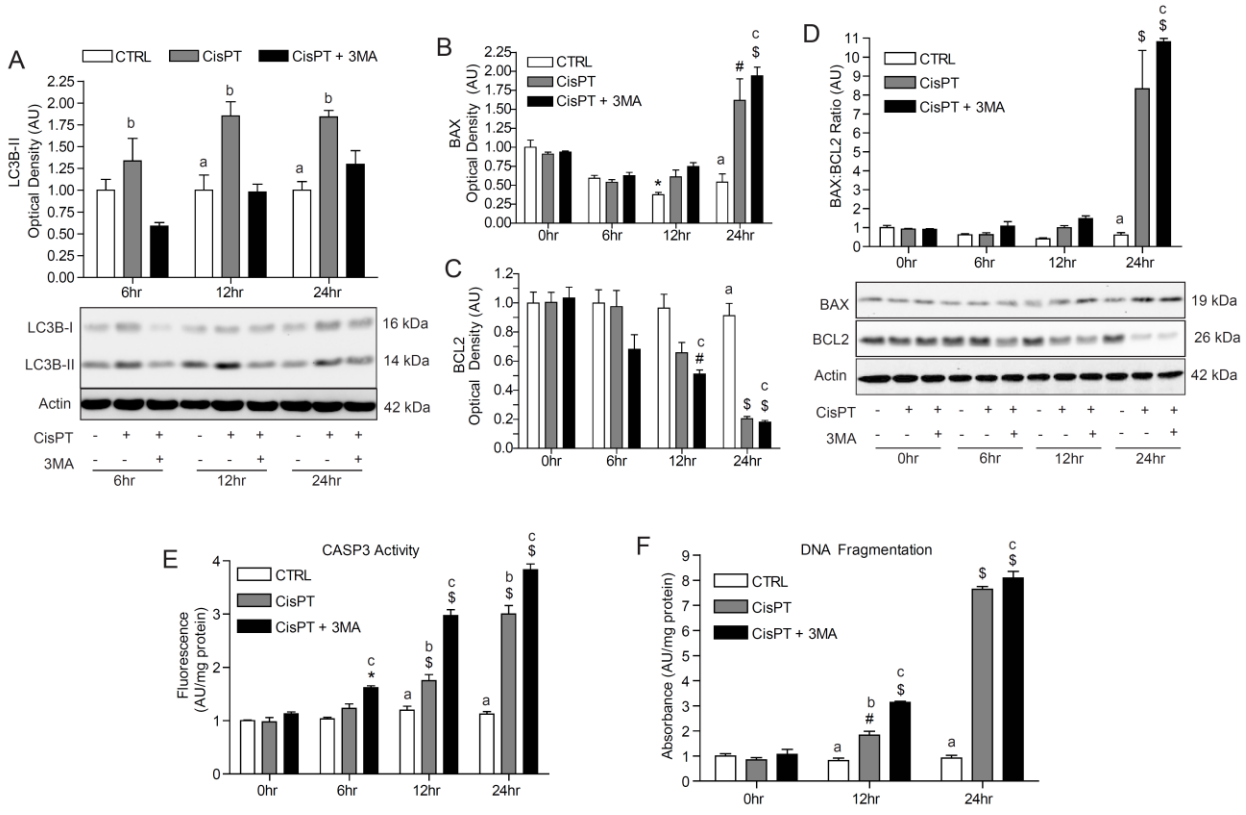

Fig. IV - 4: Effect of 3MA-mediated inhibition of autophagy on apoptotic signaling

(A) Quantitative analysis of LC3B-II protein as well as representative immunoblots of LC3B-I and LC3B-II protein in response to CisPT and CisPT + 3MA at 6 hr, 12 hr, and 24 hr of incubation. Quantitative analysis of **(B)** BAX protein, **(C)** BCL2 protein, **(D)** BAX:BCL2 protein

ratio as well as, representative immunoblots of BAX and BCL2 protein, **(E)** CASP3 activity and, **(F)** DNA fragmentation in response to CisPT and/or CisPT + 3MA over 24 hr of treatment. Also shown are representative Actin loading control blots. Differences were examined with a two-way ANOVA with post hoc analysis if significant interactions were found. *$p<0.05$, $^{\#}p<0.01$, $^{\$}p<0.001$ compared to 0 hr CTRL. a, time matched CTRL $p<0.05$ compared to CisPT. b, CisPT $p<0.05$ compared to CisPT + 3MA. c, CisPT + 3MA $p<0.05$ compared time matched CTRL; *(n=3-4)*.

Inhibition of autophagy during CisPT treatment induces mitochondrial-mediated apoptotic events

Autophagy has been shown to attenuate mitochondrial-mediated apoptotic signaling through the degradation of mitochondria presenting with low membrane potential[239]. MTG:LTR co-localization increased ($p<0.05$) in CisPT treated myotubes compared to non-treated controls; an effect which was attenuated ($p<0.05$) with 3MA (Fig. 5A & B). LTR fluorescence increased ($p<0.05$) with CisPT at 12 hr and 24 hr but was not affected by 3MA treatment (Fig. 5C).

The induction of mitochondrial-mediated apoptotic events is often associated with a loss of mitochondrial membrane potential[67]. While CisPT increased ($p<0.05$) the number of cells with low mitochondrial membrane potential, this effect was further exacerbated ($p<0.05$) by 3MA (Fig. 5D). Cell stress can promote the formation of the mitochondrial permeability transition pore (mPTP) which can result in the loss of mitochondrial membrane integrity, release of apoptotic factors and induction of CASP9[67]. There was greater ($p=0.11$) mPTP formation at 24 hr following CisPT treatment but this did not reach statistical significance. However, this was further elevated ($p<0.05$) during 3MA administration (Fig. 5E). Moreover, the CisPT-induced increase ($p<0.05$) in CASP9 was further augmented ($p<0.03$) with 3MA (Fig. 5F).

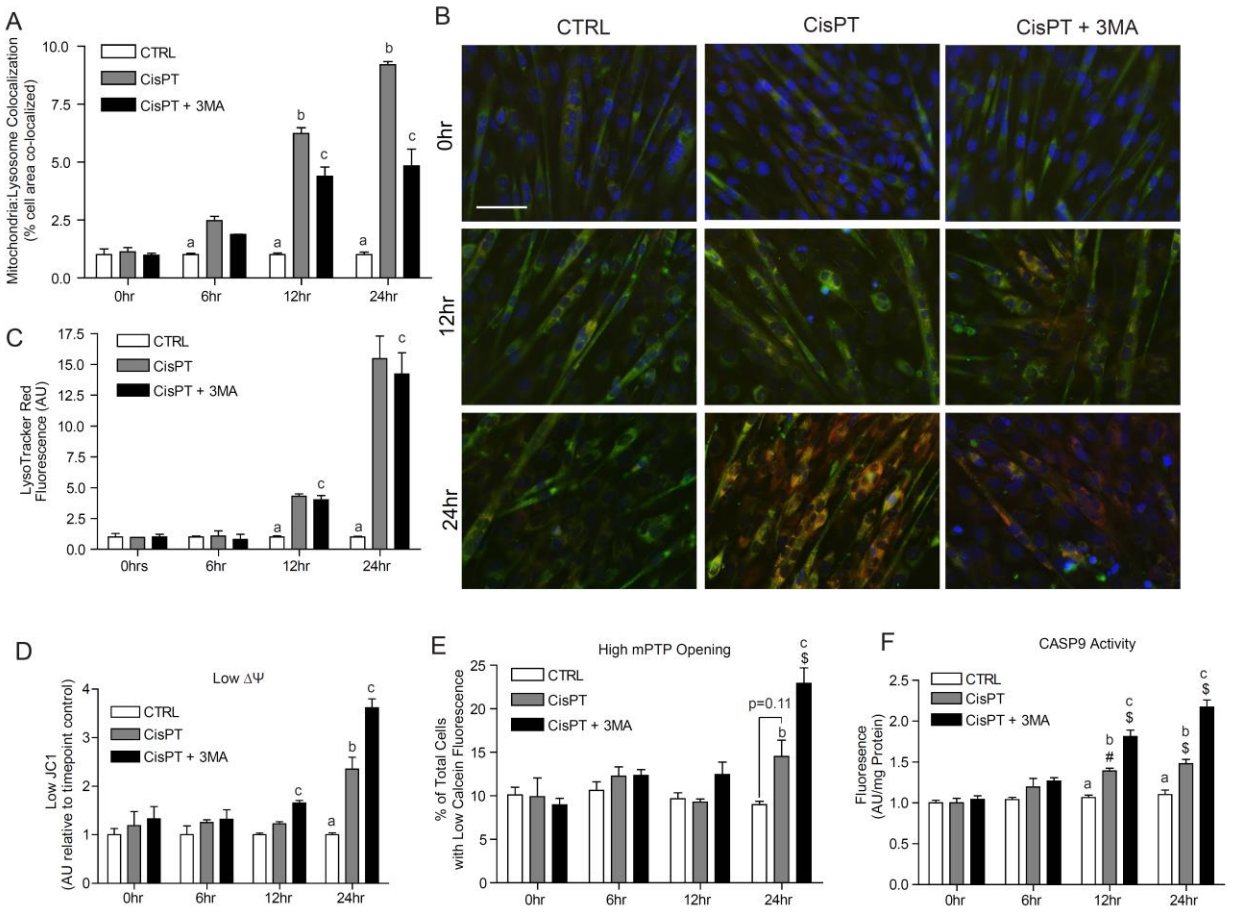

Fig. IV - 5: Effect of autophagy inhibition on mitochondrial-mediated apoptotic signaling events in response to CisPT over a 24 hr time course

(A) Quantitative analysis of MTG:LTR co-localization. **(B)** Representative images of mitochondrial content (MTG: green) lysosomal content (LTR: red), and MTG:LTR co-localization (orange). **(C)** Quantitative analysis of LTR fluorescence, **(D)** JC-1 staining **(E)** calcein fluorescence, and **(F)** CASP9 activity. Scale bar=100µm. Differences were examined with a two-way ANOVA with post hoc analysis if significant interactions were found. *$p<0.05$, $^{\#}p<0.01$, $^{\$}p<0.001$ compared to 0 hr CTRL. a, time matched CTRL $p<0.05$ compared to CisPT. b, CisPT $p<0.05$ compared to CisPT + 3MA. c, CisPT + 3MA $p<0.05$ compared time matched CTRL; *(n=3-4).*

With respect to morphological characteristics, myotube diameter was lower ($p<0.001$) after 24 hr of CisPT. Interestingly, despite the differences in mitochondrial-mediated events between CisPT and CisPT+3MA, myotube diameter was not further affected by 3MA (Fig. 6A & B).

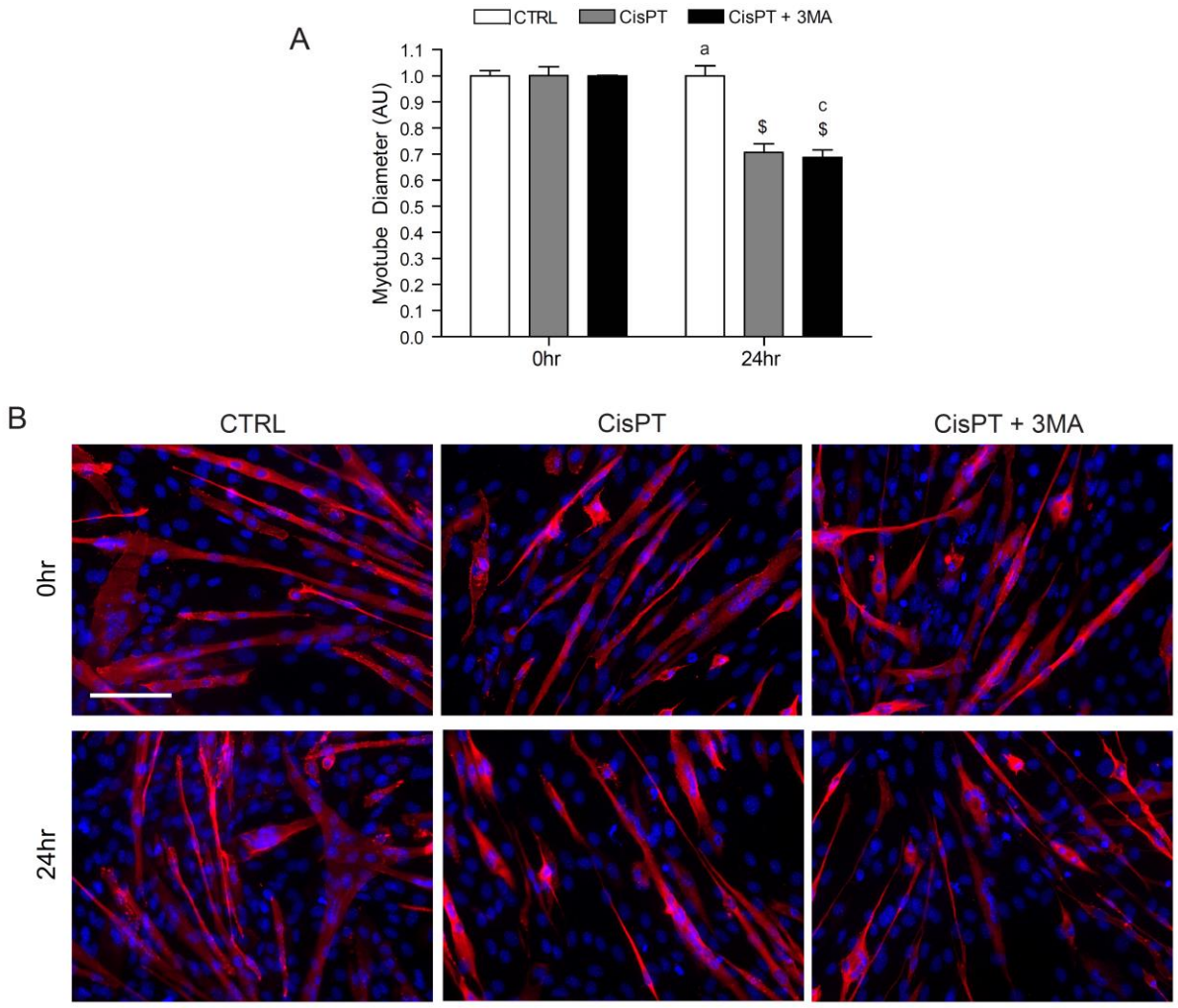

Fig. IV - 6: Effect of inhibition of autophagy on myotube atrophy during CisPT exposure

(A) Quantitative analysis of myotube diameter. **(B)** Representative images of myotube size. Cells were stained with DAPI (blue) and MF20 (red) to image nuclei and MYH, respectively. Scale bar=100µm. Differences were examined with a two-way ANOVA with post hoc analysis if significant interactions were found. $^{\$}p<0.001$ compared to non-treated CTRL. a, time matched CTRL $p<0.05$ compared to CisPT. c, CisPT + 3MA $p<0.05$ compared time matched CTRL. *(n=4).*

Autophagic flux increases following the removal of CisPT

To better understand if autophagy is involved in the recovery of muscle viability and integrity following CisPT-induced apoptotic signaling, we removed CisPT treated media after 24

hr and replaced it with fresh DM. Addition of fresh media caused a reduction ($p<0.01$) in LC3B-II content at 24 hr and 48 hr of recovery (Fig. 7A). We observed elevated ($p<0.001$) levels of BNIP3 protein at 0 hr and 24 hr of recovery (Fig. 7B). Interestingly, the level of BNIP3 dropped significantly to CTRL levels by 48 hr (Fig. 7B). To determine the cause of reduced LC3B-II levels we treated recovering cells with 5 μM of CQ for 12 hr to examine autophagic flux. We found that LC3B-II and SQSTM1 levels dramatically accumulated ($p<0.05$) in the presence of CQ during recovery, suggesting that the decrease in LC3B-II and SQSTM1 was due to increased lysosomal degradation (Fig. 7D, E & F).

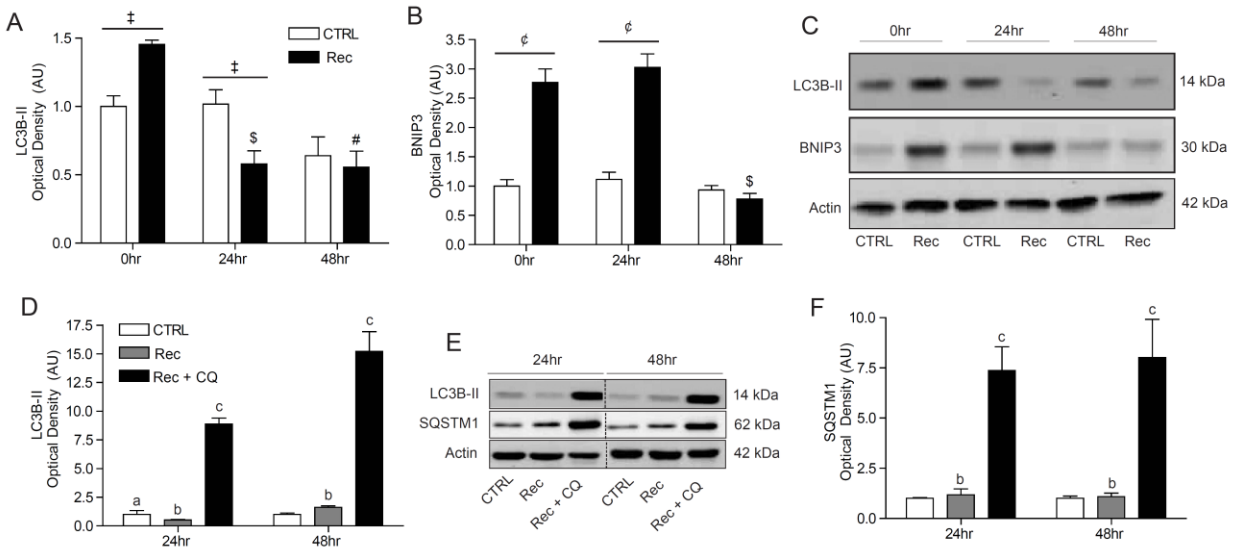

Fig. IV - 7: Alterations to autophagic proteins and flux during 48 hr of recovery from CisPT injury

(A) Quantitative analysis of LC3B-II protein content at 0 hr, 24 hr, and 48 hr of recovery (Rec). **(B)** Quantitative analysis of BNIP3 protein. **(C)** Representative immunoblots of LC3B-II and BNIP3 protein. **(D)** Quantitative analysis of LC3B-II accumulation. **(E)** Representative immunoblots of LC3B-II and SQSTM1 accumulation and **(F)** quantitative analysis of SQSTM1 accumulation after CQ treatment at 24 hr and 48 hr of recovery. Also shown are representative Actin loading control blots. A one-way ANOVA was used to examine differences over time within independent groups (A and B). A Students T-Test was used to examine differences between CTRL and Rec groups within a time point (A and B). Differences between CTRL, Rec and Rec + CQ over time and within groups were examined with a two-way ANOVA with post hoc analysis if significant interactions were found. $^{\$}p<0.001$ compared to non-treated CTRL.

‡p<0.01, ¢p<0.001 between groups at same time point. a, time matched CTRL p<0.05 compared to CisPT. c, CisPT + CQ p<0.05 compared time matched CTRL. *(n=3-4).*

The reduction in apoptotic signaling during recovery is dependent on autophagy

To examine if autophagy is required for recovery following CisPT-induced apoptotic signaling we added 5 mM of 3MA for 24 hours prior to the collection of cells at 24 hr and 48 hr into recovery. 3MA treatment successfully reduced (p<0.05) LC3B-II protein content at 24 hr and 48 hr (Fig 8A).

The BAX/BCL2 ratio was elevated (p<0.001) in recovery cells at 24 hr. Interestingly, the BAX/BCL2 ratio was increased (p<0.05) further in 3MA exposed cells at both 24 hrs and 48 hrs (Fig. 8B). While CASP3 activity remained elevated (p<0.001) at 24 hr and returned to baseline by 48 hr in recovery cells, 3MA exposed cells displayed a further elevation (p<0.05) in CASP3 activity at 24 hr, which remained higher (p<0.05) at 48 hrs (Fig. 8C).

Similarly, DNA fragmentation remained elevated at 24 hr of recovery then dropped (p<0.001) towards baseline at 48 hr; however, DNA fragmentation was elevated (p<0.05) with 3MA at both time points (Fig. 8D).

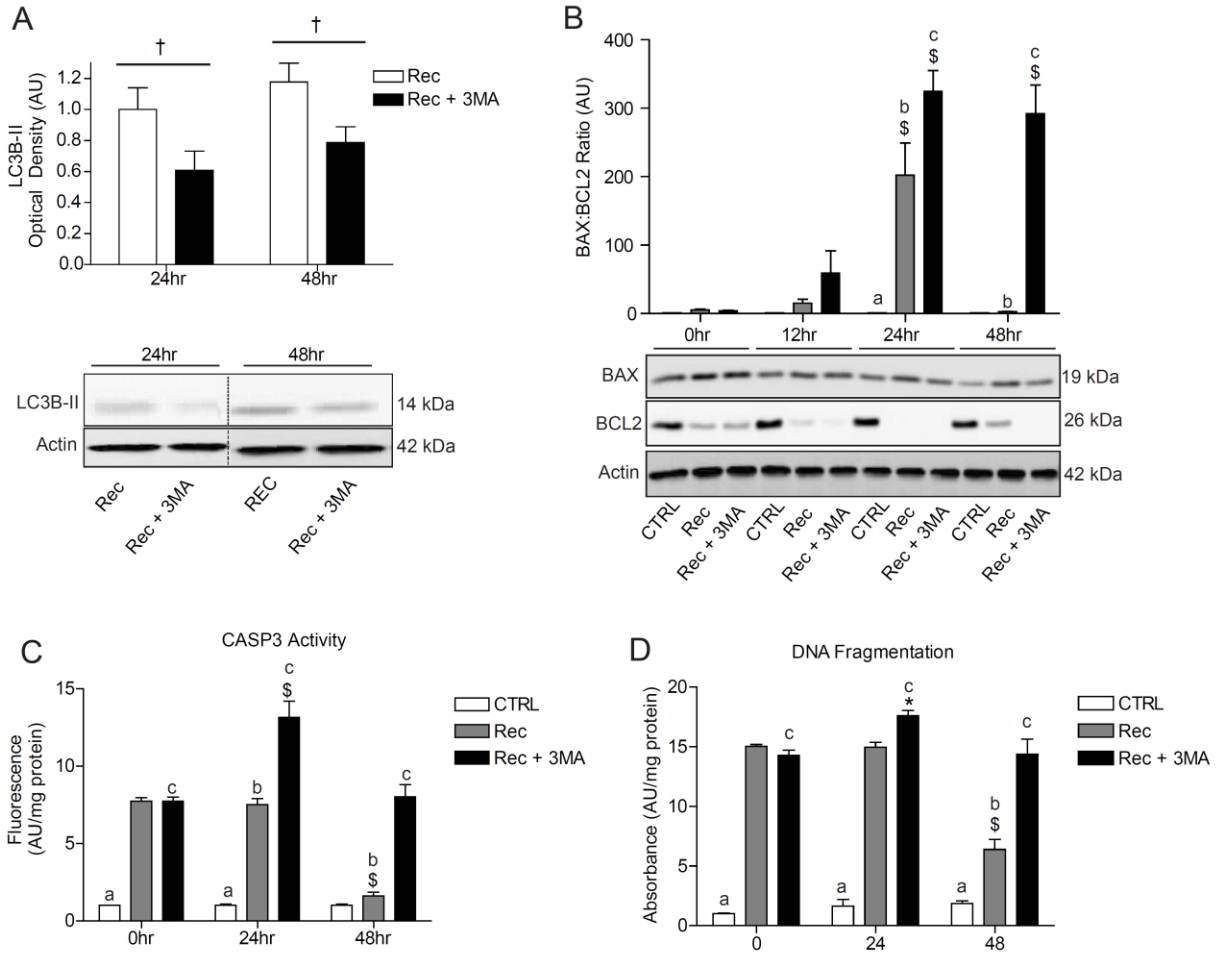

Fig. IV - 8: Effect of inhibition of autophagy on apoptotic markers during 48 hr of recovery from CisPT injury

(A) Quantitative analysis of LC3B-II protein and representative immunoblots of LC3B-II protein. **(B)** Quantitative analysis of BAX/BCL2 protein ratio as well as representative immunoblots to BAX and BCL2 protein. **(C)** Quantitative analysis of CASP3 activity, and **(D)** DNA fragmentation. Also shown is a representative Actin loading control blot. A Students T-Test was used to examine differences between Rec and Rec + 3MA (A). Differences were examined with a two-way ANOVA with post hoc analysis if significant interactions were found (B, C, D). $^{\$}p<0.001$ compared to 0 hr CTRL. $^{\dagger}p<0.05$, between groups at the same time point. a, time matched CTRL $p<0.05$ compared to Rec. b, Rec $p<0.05$ compared to Rec + 3MA. c, Rec + 3MA $p<0.05$ compared time matched CTRL; *(n=3-4)*.

Inhibition of autophagy during recovery leads to mitochondrial-mediated apoptotic signaling

Next, we examined the effects of autophagy on mitochondrial viability and apoptotic signaling during recovery. The elevated MTG:LTR co-localization was somewhat maintained ($p<0.05$) at 24 hr; however, 3MA restored levels to baseline. A similar trend was shown at 48 hrs (Fig. 9A & B). While LTR fluorescence was restored at 48 hr, levels were higher in cells treated with 3MA (Fig. 9B & C). We then investigated the ability of mitochondrial membrane potential to recovery following CisPT treatment. Although CisPT decreased membrane potential, this declined ($p<0.05$) during recovery (Fig. 9D). In contrast, the number of cells with lower membrane potential was dramatically more evident ($p<0.05$) into recovery with 3MA (Fig. 9D). While CisPT caused mPTP formation ($p<0.05$), there was recovery by 48 hrs. In contrast, mPTP formation continued to increase ($p<0.001$) throughout recovery in the presence of 3MA (Fig. 9E). Accordingly, the elevated CASP9 levels in response to CisPT declined ($p<0.05$) during recovery, but continued to increase ($p<0.05$) in cells treated with 3MA (Fig. 9F).

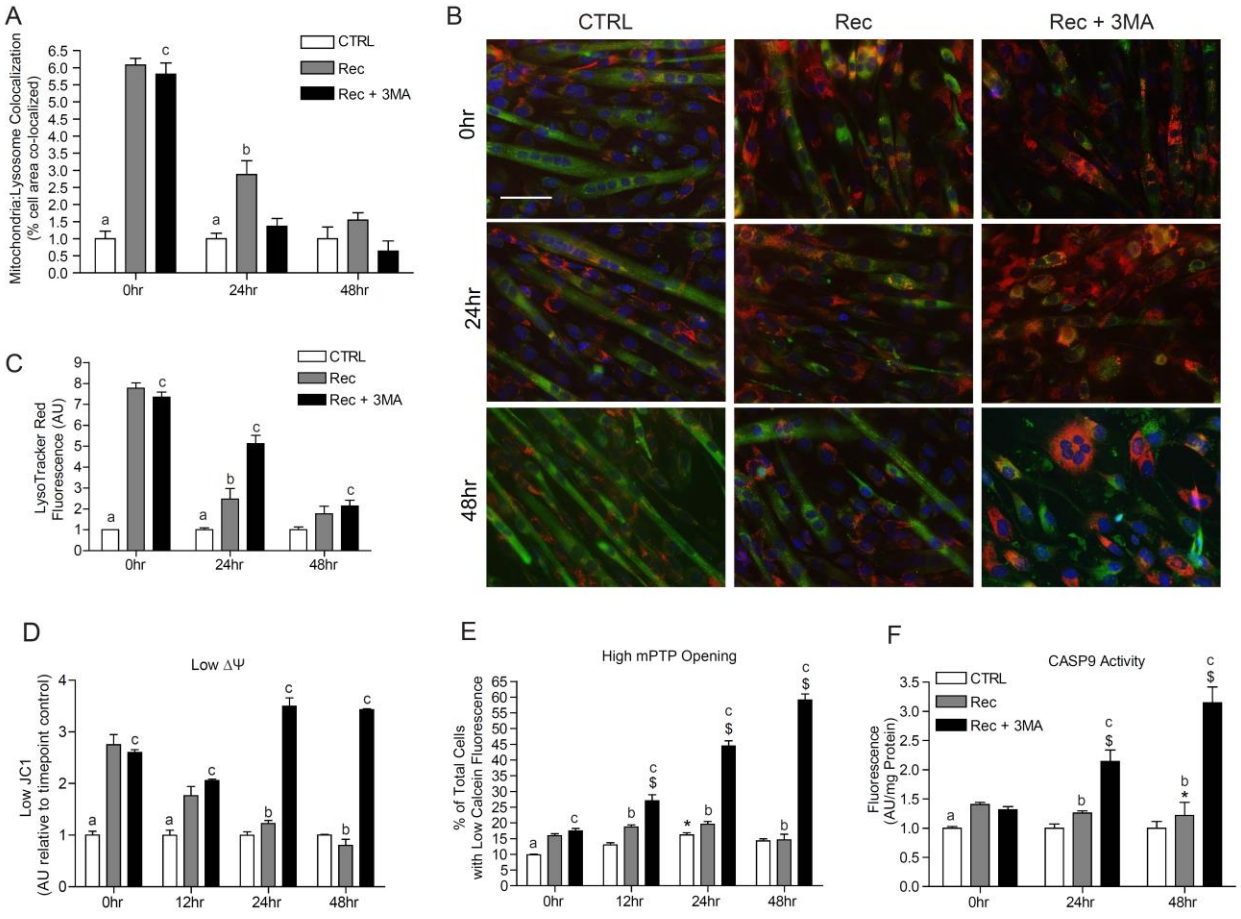

Fig. IV - 9: Effect of inhibition of autophagy on mitochondrial apoptotic signaling during recovery from CisPT injury

(A) Quantitative analysis of MTG:LTR co-localization over 48 hr of recovery from CisPT injury with or without 3MA. **(B)** Representative images of MTG, LTR, and MTG:LTR co-localization. **(C)** Quantitative analysis of LTR over 48 hr of recovery from CisPT injury with or without 3MA. Quantitative analysis of **(D)** JC-1 staining, **(D)** calcein fluorescence and, **(E)** CASP9 activity. Scale bar=100µm. Differences were examined with a two-way ANOVA with post hoc analysis if significant interactions were found. *$p<0.05$, $^{\$}p<0.001$ compared to 0 hr CTRL. a, time matched CTRL $p<0.05$ compared to Rec. b, Rec $p<0.05$ compared to Rec + 3MA. c, Rec + 3MA $p<0.05$ compared time matched CTRL; *(n=3-4).*

Autophagy is required for regenerative processes

We next determined the importance of autophagy in the recovery of myotube morphology from CisPT. As previously shown, 24 hr of 50 µM CisPT decreased ($p<0.05$)

myotube diameter (Fig. 10A & D). However, both recovery with or without 3MA had no effect on myotube diameter (Fig. 10A & D).

We decided to examine if the lack of change to myotube diameter was a result of impaired differentiation and fusion of the reserve myoblasts remaining following the removal of CisPT. We observed a significant reduction ($p<0.05$) in the number of differentiated and fused cells immediately after CisPT exposure. Both differentiation and fusion increased ($p<0.05$) during recovery in both CTRL and recovery cells (Fig. 10 B, C & D). In contrast, differentiation and fusion not only lower with 3MA, but tended to be reduced throughout recovery (Fig. 10B, C & D).

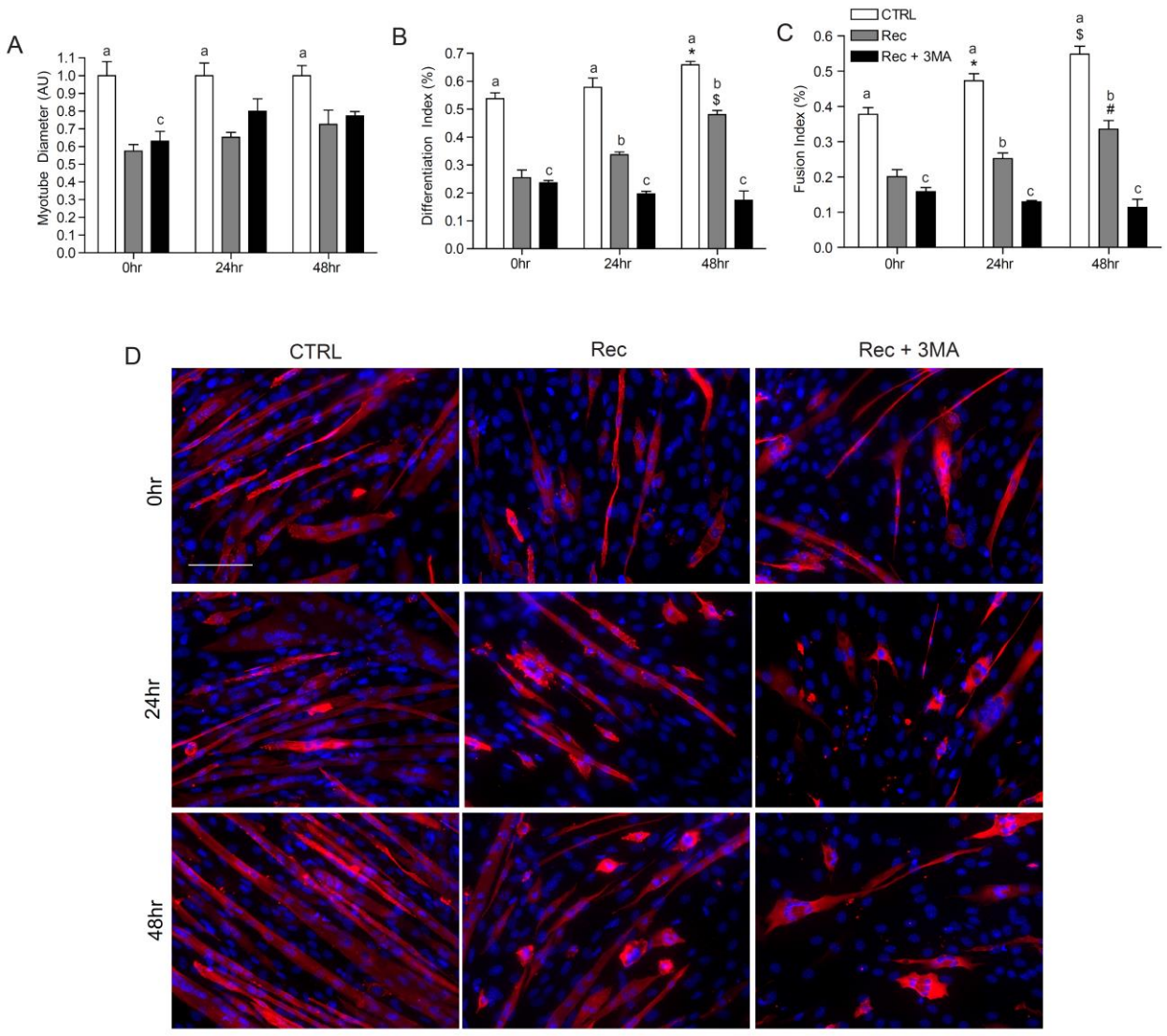

Fig. IV - 10: Effect of inhibition of autophagy on myotube size and regenerative capacity during recovery from CisPT injury

(A) Quantitative analysis of myotube diameter over 48 hr of recovery from CisPT injury with or without 3MA. Quantitative analysis of the **(B)** differentiation index and **(C)** fusion index over 48 hr of recovery from CisPT injury with or without 3MA. (D) Representative images of myotube size in response to drug exposure after 24 hr. Cells were stained with DAPI (blue) and MF20 (red) to image nuclei and MYH, respectively. Scale bar=100µm. Differences were examined with a two-way ANOVA with post hoc analysis if significant interactions were found. *$p<0.05$, $^{\#}p<0.01$, $^{\$}p<0.001$ compared to 0 hr CTRL. a, time matched CTRL $p<0.05$ compared to Rec. b, Rec $p<0.05$ compared to Rec + 3MA. c, Rec + 3MA $p<0.05$ compared time matched CTRL; *(n=3-4)*

DISCUSSION

CisPT-induced myotube atrophy is associated with autophagy, apoptosis, and proteolytic activity

Our results demonstrate that CisPT induces an increase in apoptotic proteolytic enzyme activity, DNA fragmentation, and autophagy along with decreases in myotube size. In support of our results, Stacchiotti et al. found an increase in apoptosis, autophagy, and myotube atrophy in myotubes exposed to 50 μM CisPT after 24 hr[248], implicating these processes as contributing factors to muscle atrophy. The induction of apoptosis results in the destruction of genomic material and the loss of myonuclei[58,60]. According to Allen et al. this loss of myonuclei can promote muscle atrophy by reducing the transcriptional potential of the remaining myotube[58,60]. Thus, increased DNA fragmentation could be responsible, at least in part, for the reduction in myotube diameter at submaximal doses. Interestingly, we observed a plateau in muscle atrophy at high doses of CisPT which was associated with a plateau in DNA fragmentation suggesting that the further reduction in myotube size may depend upon the level of DNA fragmentation. Other apoptotic signaling mechanisms can result in the destruction of myofibrillar proteins and organelles which may contribute to the altered morphology and function[241,242]. The degradation of such proteins and organelles is orchestrated by degradative systems such as the UPS and likely autophagy[241]. We observed an increase in autophagy as noted by increased LC3B-II, BNIP3, and BECN1 protein content as well as altered autophagic flux following 24 hr of 50 μM CisPT. Interestingly, CisPT doses greater than 50 μM caused a decline in autophagy-related proteins, and augmented CASP3 activity. CASP3 activity can promote the loss of autophagic protein stability and as a result impairing the induction of autophagy[252]. Interestingly, at higher doses of CisPT when CASP3 activity was greatest and autophagy was attenuated, there were no

further decrements in myotube size. Therefore, it is possible that for the muscle to continue to undergo remodeling a further induction of autophagy is required. As such, inhibition of autophagy using 3MA did not result in further loss of myotube size even though an increase in CASP3 was observed. Our results contribute to previous evidence suggesting that inhibition of autophagy and autophagic signaling can preserve muscle size in the presence of cell stress[106,250]

Autophagy is required to attenuate mitochondrial-mediated apoptotic signaling induced by submaximal doses of CisPT

Observations of both apoptotic and autophagic processes in similar models of skeletal muscle stress have promoted a theory suggesting that autophagy contributes to cell death signaling and atrophy in muscle[6,192,241]. We found that autophagy is required to mitigate the magnitude and induction kinetics of apoptotic signaling in C2C12 myotubes. For example, inhibition of autophagy augmented and more rapidly induced CASP3 activity. Interestingly, DNA fragmentation was greater in CisPT exposed cells when autophagy was inhibited at 12 hr but not at 24 hr. This suggests that autophagy can slow down the induction of DNA fragmentation but not inhibit it completely. It is possible that caspase independent modes of cell death are occurring simultaneously in addition to caspase-mediated apoptotic signaling [59,245]. Collectively, these data demonstrate that the induction of autophagy can mitigate apoptotic proteolytic activity and DNA fragmentation in skeletal muscle.

The promotion of CASP3 activity and apoptosis can be achieved through the mitochondrial-mediated activation of apical CASP9[67]. In response to CisPT we observed a reduction in mitochondrial membrane potential, the formation of the mPTP, and the activation of CASP9, which strongly suggests mitochondrial-mediated apoptotic signaling likely contributed to the increase in cell death signaling and apoptosis. Interestingly, inhibition of autophagy

resulted in cells with lower mitochondrial membrane potential, likely due to impaired mitochondrial clearance[235]. Mitophagy can maintain mitochondrial viability by selectively degrading damaged mitochondria prior to their participation in apoptotic signaling thus, protecting the cell[235,239]. BNIP3 and other mitophagy-related proteins co-localize with mitochondria during mitochondrial stress and induce mitochondrial membrane depolarization or simply respond to mitochondria with low membrane potential in order to promote their degradation[238]. During CisPT exposure, the induction of autophagy occurred with increased BNIP3 and MTG:LTR co-localization as early as 6 hr after treatment suggesting that mitochondrial degradation occurs at submaximal apoptotic doses of CisPT. Interestingly, 3MA attenuated MTG:LTR co-localization and elevated mitochondrial-mediated cell death signaling. Similarly, it has been previously shown that 3MA impairs mitochondrial degradation through inhibition of autophagosome-lysosome co-localization resulting in the accumulation of impaired mitochondria and increased cell death[233]. Furthermore, we found that inhibition of autophagy increased mPTP formation and augmented CASP9. Collectively, this data demonstrates that degradation of mitochondria via autophagic processes is critical in regulating mitochondrial-mediated apoptotic signaling. Similarly, previous work has shown that the forced induction of autophagy in muscle can attenuate levels of apoptotic signaling[176,179,238].

Recovery from CisPT toxicity involves altered autophagic flux and autophagy-dependent recovery from mitochondrial-mediated apoptotic signaling

Recovery from muscle wasting and damage is relevant in a number of stress and disease states. We found that following the removal of CisPT, myotubes begin to recover; a process that occurs with increased autophagic flux. It is peculiar that we observed an increase in LC3B-II protein content during incubation with CisPT and a decrease in LC3B-II protein content during

recovery even though both were associated with increased flux. These results demonstrate the importance of investigating autophagic flux as autophagy is highly dynamic system[9,112]. To date, few studies have characterized the induction or flux of autophagy during recovery from muscle stress[243,244].

Evidence suggests that during recovery from muscle injury, CASP activity and cell death signaling is attenuated over time, a phenomena which largely depends on the type, duration, and magnitude of the injury[15]. In agreement with this, myotubes allowed to recover following CisPT exposure displayed reduced CASP3 activity and DNA fragmentation. Teng et al. observed a decrease in apoptotic signaling along with a moderate increase in autophagy markers and improved muscle morphology, suggesting a relationship between apoptosis and autophagy may exist in recovering skeletal muscle[244]. In the present work, inhibiting autophagy by 3MA during the recovery form CisPT augmented apoptotic markers such as the BAX:BCL2 ratio, CASP3 activity, and DNA fragmentation. In addition, 3MA treated recovering myotubes had lower mitochondrial membrane potential, greater mPTP formation, and elevated CASP9 activity suggesting that autophagy can improve the cellular environment following stress. In support of this, the forced induction of autophagy in dystrophic mice promoted the recovery of mitochondria morphology and attenuation of cell stress[14,179]. Previous work has shown that autophagy can target damaged mitochondria for degradation and in doing so likely improve the function and viability of the available mitochondrial population[238,253]. Cells treated with 3MA had reduced mitochondrial-lysosomal co-localization suggesting a reduction in mitochondrial degradation and the accumulation of damaged mitochondria. These results demonstrate that autophagy is required to regulate apoptotic events and signaling via promotion of mitochondrial viability in myotubes recovering from injury.

Autophagy is required to promote regenerative processes in recovering myotubes

Following myotrauma the differentiation of myogenic precursor cells is followed by their fusion into the damaged myofiber or *de novo* synthesis of new myotubes[16]. We have previously shown that autophagy is required for myoblast differentiation and myotube formation[214]. In the current study we observed an increase in markers of differentiation and fusion by 48 hr of recovery, processes which were also dependent upon autophagy. The increase in both fusion and differentiation are factors which can contribute to the increase in myotube size, complexity, and anti-apoptotic profile[254]. Interestingly, we did not see any significant changes to myotube size during recovery. However, skeletal muscle regeneration has been shown to take several days in mammalian models of muscle injury[15]. Furthermore, the lack of immune cell presence in the myotube cultures would be expected to delay recovery[255]. Overall these, our results demonstrate that autophagy is required for increasing the regenerative potential within cultures of differentiated C2C12 myocytes by promoting differentiation and fusion.

Autophagy is required to suppress cell death signaling and delay the induction of muscle cell death events that occur during and following recovery to CisPT exposure. More specifically, autophagy is vital in this apoptotic response through regulation of mitochondrial-mediated cell death signaling and health. Furthermore, autophagy is required to promote an increase in regenerative potential in C2C12 myotubes following the removal of CisPT. In conclusion, these data suggest that autophagic processes are critical in maintaining muscle viability and regenerative potential.

CHAPTER V: THESIS DISCUSSION

SUMMARY

Autophagic processes are required to maintain basal cell viability and contractile function in skeletal muscle[1,256]. Acting as a quality control system, autophagy can target and promote the degradation of damaged cellular constituents before they pose a risk to cell health[180,181,257]. As such, several models presenting with muscle dysfunction, associated with an accumulation of damaged/dysfunctional proteins and organelles, have been shown to have diminished levels of autophagy[179,181]. Importantly, the integrity of the muscle can be improved in these conditions through the forced induction of autophagy[14,175,176]. In contrast, several models including denervation, nutrient deprivation, sarcopenia, unloading, cachexia, and myopathies such as Pompe disease and Danones disease are associated with impaired muscle function and atrophy[181,184]. In these conditions the induction of autophagy has been suggested to contribute to muscle atrophy[104,157,182,184]. Based on the available literature the role of autophagy in skeletal muscle health is complex.

Autophagy is often observed in dying cells and many studies have suggested this "autophagic cell death" occurs in models of skeletal muscle atrophy and disease. For example, O'Leary et al. observed an increase in LC3B-II protein content in whole cell and mitochondrial fractions of denervated skeletal muscle. Since denervation also induces atrophy and apoptotic events/signaling, the induction of autophagy was interpreted as a "cell death inducing" mechanism[157]. Furthermore, Smuder et al; reported an increase in skeletal muscle apoptotic signaling and muscle atrophy in response to the chemotherapeutic drug doxorubicin. In a follow up study this group reported an increase in autophagy and atrophy in response to doxorubicin. Interestingly, this study demonstrated that exercise training can mitigate the autophagy following doxorubicin exposure. Ultimately the authors concluded that the induction of autophagy was a

mechanism contributing to skeletal muscle cell death processes and that exercise mitigated cell death and muscular atrophy through the suppression of autophagy[123].

Despite these reports, autophagy has never been shown to be the direct cause of cell death in skeletal muscle. Only associative evidence exists. Recently, accumulating evidence points to a pro-survival role of autophagy through the disposal of damaged organelles, clearance of proteotoxicity factors, and recycling of nutrients to conserve energy under starvation conditions[181]. Skeletal muscle apoptotic signaling is directly linked to muscle atrophy and contractile dysfunction; however, it is also required for physiological remodeling and developmental processes[59,66]. Therefore, understanding the role of autophagy in skeletal muscle will improve our basic understanding of the interplay between autophagy and apoptosis, and allow us to better understand processes which regulate cell death processes.

Autophagy is required to protect differentiated myotubes from apoptosis

The induction of skeletal muscle apoptosis is associated with the increase in autophagy and muscle atrophy[181]. As such, the present work reveals that autophagy occurs prior to the induction of apoptotic signaling in response to submaximal apoptotic stress. Previous reports have concluded that this association suggests that autophagy is a cell death mechanism[123,157]. Importantly, these data also demonstrates that when autophagy is inhibited at a submaximal dose, the level of apoptotic signaling increases sooner and at a greater magnitude compared to controls. Therefore, we suggest that the induction of autophagy prior to apoptotic signaling at submaximal levels of stress is protective. Underlying this protective response is the ability of autophagy to promote the maintenance of mitochondrial viability. The clearance of damaged mitochondria through autophagic processes such as mitophagy protects the cell from the induction of mitochondrial- mediated apoptosis[235,238-240]. Furthermore, the induction of

mitophagy has been shown to improve mitochondrial energy production and allow for rapid recovery of energy during cell stress[258,259]. In this work, the loss of membrane potential, reduction in mitochondrial membrane integrity, and increase in CASP9 activity was observed in the absence of autophagy during CisPT exposure. Therefore, our data strongly suggests that autophagy mitigates apoptotic signaling through the maintenance of mitochondrial viability in response to submaximal levels of apoptotic stress. However, autophagy may also protect against cell death through the degradation of damaged proteins and nuclear remodeling, thereby attenuating ER-stress and genomic-stress induced apoptotic signaling[12,252]. Thus, an examination of the role of autophagy in the regulation of these pathways of apoptotic stress should be examined in future research.

Relative to submaximal levels of apoptotic stress, the rapid induction of apoptotic signaling at high doses of CisPT was not associated with the same autophagic response. Cell death has become better understood as dynamic processes in which several death-related processes compete for the determination of cell fate[12,252,259]. Interestingly, caspase signaling is one of the main conversation points determining the influence of autophagy and apoptosis on cell fate. For example, the immediate upregulation of autophagy-related proteins such as ATG7 has been shown to inhibit the activity of CASP9[260]. Furthermore, autophagic processes can hijack CASP activation sites such as the DISC and promote autophagy over apoptosis[173]. In contrast, the activation of CASP3 has been shown to dismantle autophagic proteins such as BECN1 and ATG4D; converting them into pro-apoptotic proteins and inhibiting autophagy[261,262]. In this thesis we also observed an attenuation of ATG's such as BECN1, ATG7, and BNIP3 when elevated levels of apoptotic signaling were observed. Therefore, it is possible that in skeletal muscle the rapid induction of CASP3 due to high levels of cell stress from CisPT can result in

cleavage of ATG's and mitigate the induction of autophagy. Regardless, the inability to induce an autophagic response during high levels of apoptotic stress may have favoured a pro-apoptotic balance thus increasing cell death and remodeling.

Taken together these experiments demonstrate that autophagy occurs along with apoptosis and muscle atrophy as previously shown. However, these cell death-associated events are not one in the same. The induction of autophagy during submaximal levels of apoptotic stress does not promote the induction of apoptosis, but rather acts as a pro-survival system removing factors which can stimulate apoptotic cell death. Conversely, conditions with significant and rapid increase in apoptotic signaling may impair the pro-survival response of autophagy and promote apoptotic cell death.

Autophagy is a required process in the recovery from apoptotic stress in myotubes

Observations in skeletal muscle show that autophagic puncta rapidly appear during stress and persist for days after the stress has been removed[180]. This suggests that autophagy may be required in recovery and repair processes in skeletal muscle. Skeletal muscle is a remarkable tissue due to its ability to evade complete cell death[247,254]. This is an essential component of skeletal muscle as it is a terminally differentiated, long lived, multinucleated cell type[59]. The ability to resist cell stress is dependent upon a robust stress response system which includes a rapid increase in molecular chaperone proteins such as HSP70, antioxidant systems, and autophagy. Furthermore, skeletal muscle can ward off apoptotic insults due to high levels of anti-apoptotic proteins such as ARC and BCL2. Interestingly, skeletal muscle can also mitigate cell stress through the ability to upregulate and mobilize mitochondria for ROS, and Ca^{2+} buffering[59,197,214,263]. However, one of the most remarkable features of skeletal muscles resistance against total cell death/loss is its multinucleated nature.

In mononucleated cell types, cell stress which breaches a certain threshold can elicit apoptotic signaling to destroy the cell through a highly regulated process which results in the removal of the mutated, damaged, and/or stressed cell[36]. In contrast, following apoptotic signaling skeletal muscle fibers are not removed by immune cells; instead they can undergo dramatic remodelling[58]. It is important to note that following apoptotic signaling the elongated myotube, which shares a common cytosol, is at risk of cell stress being propagated throughout the myotube. The induction of degradative systems such as the UPS has been shown to contribute to the degradation of cleaved and damaged proteins mediated by CASP in skeletal muscle[264] suggesting that degradative processes may clean up after cell death events. Furthermore, an increase in autophagic markers has been found in skeletal muscle several days after crush injury and following unloading[243,244]. Our results also support that this autophagic process occurs following the removal of apoptotic stresses and during cell recovery. More interestingly, our observations add to this knowledge by demonstrating that autophagy is essential for the maintenance of mitochondrial viability and attenuation of CASP activity during recovery from apoptotic stress. Similar to the observations made in cells undergoing stress, the induction of autophagy during recovery from stress was required to promote the restoration of the mitochondrial population. It is possible that the induction of autophagy may provide metabolic building blocks for intermediary metabolism during times when mitochondria are damaged, such as following mitochondrial apoptotic signaling. Importantly, this could provide energy potential to sustain other remodeling processes such as protein synthesis and mitochondrial biogenesis. Although interesting, these potential actions of autophagy require further investigation. Regardless, the removal of damaged mitochondria would help preserve myotube viability by limiting the spread of impaired mitochondrial function throughout the

mitochondrial network[253]. In support of this, myotubes recovering with impaired autophagy showed increased cell death, associated with sustained CASP activity and mitochondrial damage.

Skeletal muscle is continuously under conditions in which sub-apoptotic stress occurs. For example, with every contraction the skeletal muscle sarcolemma acts as an electrical conduit passing a charge directly in to the skeletal myofiber which releases Ca^{2+} into the cytosol at potentially toxic levels. The cytosolic influx of Ca^{2+} allows for cross-bridge cycling which produces high levels of shear stress to structural proteins within the myofiber[265]. In addition, the energy required for this process can be produced through oxidative metabolism which results in potentially damaging ROS production[216,265]. Given that muscle is exposed to repeated stressors, muscle requires processes to assist in recovery to ensure stressors do not accumulate. In support of our data, and the role of autophagy in recovery processes Lira et al. 2013 demonstrated that autophagy is required for skeletal muscle to adapt to exercise[124]. In addition, inhibition of autophagy in the absence of perturbations leads to the development of myopathic features and impaired contractile function[1]. Finally, in conditions where constant damage and regeneration are occurring such as in muscular dystrophies, the forced induction of autophagy can improve mitochondrial integrity, cell viability, and mitigate apoptotic signaling[179].

Although autophagy protected the myofiber from apoptotic cell death processes, we were surprised that there was no difference in myotube size between autophagy compromised and autophagy capable cells after 48 hr of recovery. Previous reports have shown that inhibition of autophagy increases myotube diameter in response to unloading and apoptotic stress[106,192]. It is important to note that skeletal muscle size does not always directly correlate with function and health[266]. Although, we found that cells lacking autophagy during recovery had similar size compared to autophagy competent cells in the absence of autophagy, we observed elevated

CASP activity and compromised mitochondrial viability during recovery. Under these conditions, skeletal muscle metabolic and contractile function could be compromised even though size is not altered. Further work to understand the metabolic contribution of autophagy during recovery will provide important insight into how to best treat skeletal muscle damage.

In response to myotrauma and stress, processes such as autophagy are required to improve cell viability. However, autophagy is also involved in regeneration events[1,214]. For example, autophagic processes can remove damaged mitochondria and promote mitochondrial biogenesis[176,259]. Furthermore, the upregulation of autophagy promotes the export of macronutrients, including amino acids from the lysosome which can initiate protein synthesis[267]. In addition to these anabolic processes, skeletal muscle is rebuilt after injury through the incorporation of new nuclei from a pool of adult stem-like cells called satellite cells[16]. The formation of skeletal muscle during myogenesis, satellite cell differentiation and fusion as well as the *de novo* synthesis of new muscle fibers share several biochemical and morphological similarities that can be examined in C2C12 cell cultures[26]. The ability of damaged myotubes to recover in our experiments may have been partially mediated through the increased differentiation and fusion of reserve cells. These reserve cells in differentiated C2C12 cultures have been shown to re-enter cell cycle, terminally differentiate, and contribute to myotube regeneration[268]. In cells allowed to recover, 3MA inhibited autophagy as well as impaired the differentiation and fusion indexes. This likely contributed to the inability to increase myotube size during recovery. Together, these effects may have contributed to the poor viability in these cells by 48 hr but this inability to regenerate could have dramatic consequences *in vivo* where muscle regeneration may take several days[16]. Therefore, future experiments aimed at investigating the role of autophagy in *in vivo* muscle regeneration will be of importance.

Autophagy is required for myoblast differentiation

Myoblast differentiation is an essential process in both myogenesis and muscle regeneration[16]. Myoblast differentiation is morphologically characterized by the fusion of differentiated myoblasts. Once a nascent myotube is formed, additional myoblasts fuse which increases the myonuclear number and size of the developing myotube[15]. Underlying the hallmark morphological features of myoblast differentiation and myotube formation is a highly regulated and hierarchical signaling cascade involving several myogenic regulatory factors (MRF)[15]. For example, the expression and transcriptional activity of MYOD and MYF-5, two primary bHLH transcription factors, by upstream PAX3/7 co-transcription factors results in the muscle specification of the committed myoblast cells. Binding of the E-Box (CANNTG) motif by these primary MRFs promotes the expression of myogenin and MRF4, two secondary MRFs responsible for the activation of the terminal differentiation, and fusion programs [17,19,22,23,269]. Although the basic signaling networks regulating the withdrawal from cell cycle, terminal differentiation and fusion of muscle cells has been well characterized, processes which regulate these signaling events, dramatic morphological changes, and organelle remodeling are not as well known. Since autophagy can quickly degrade proteins and organelles, autophagy has been speculated to contribute to the rapid morphological, biochemical, genetic, and organelle remodeling of complex, differentiating cell types[131]. In support of this, research has shown that autophagy is required for osteogenic, mesenchymal, erythrocyte, neuroblastoma, glioma-initiating, and monocyte differentiation[188-190]. Our data now demonstrates that autophagy is also required for myoblast differentiation and myotube formation.

To begin elucidating the role of autophagy in myoblast differentiation we first aimed to identify how this process was regulated. Several signaling events can promote the induction of

autophagy, and depending on the signaling pathways responsible; information on the role of autophagy is possible. For example, the induction of autophagy through AKT/FOXO3A signaling is commonly associated with perturbations to growth hormones, whereas AMPK-mediated autophagy occurs during intracellular nutrient stress[8,12]. Our data demonstrates that JNK, a cell stress kinase which governs several stress signaling pathways and responses[37,54] is partially responsible for the induction of autophagy during myoblast differentiation, suggesting the induction of autophagy may be due to cell stress. Interestingly, JNK-mediated autophagy is critical for the survival of monocytes as they differentiate into mature macrophages[200]. Similarly, in skeletal muscle the induction of JNK during differentiation was shown to be required for myoblast survival[57]. Based on these findings we hypothesized that JNK promotes the induction of autophagy for the purpose of cell survival. Furthermore, JNK can promote the induction of autophagy through the regulation of the BECN1:BCL2 complex[125]. Phosphorylation of BCL2 by JNK reduces the sensitivity of BCL2 for BECN1 resulting in their separation and the promotion of autophagy[126]. Accordingly, we found that myoblast differentiation was associated with an attenuation of BECN1:BCL2 complex formation, an effect which was inhibited by JNK inhibition. Furthermore, SP600125 also reduced autophagosomal markers suggesting that JNK mediates the induction of autophagy. The discovery that JNK mediates autophagy during myoblast differentiation via the BECN1:BCL2 complex, in addition to previous reports demonstrating that JNK protects myoblasts from cell death during differentiation, strongly suggests that autophagy is required to protect myoblasts from cell stress during differentiation.

Myoblast differentiation and myotube formation are associated with and require the induction of ER-stress, oxidative stress, metabolic stress, mitogen stress as well as the induction of CASP3 activity[30,31,34,37,211]. Our results demonstrate that autophagy plays a vital role in

attenuating the level of cell stress involved in myoblast differentiation. For example, we found that in the absence of autophagy HSP70 as well as CAPN activity are elevated. These are two features commonly observed during ER-stress. Furthermore, we also demonstrated attenuated mitochondrial membrane potential, increased permeability transition pore formation, and elevated mitochondrial 4-HNE content during early differentiation in shAtg7 cells. This suggested that a cellular environment without autophagy promotes mitochondrial damage and stress. One way in which autophagy can protect the cell from accumulation of damaged mitochondria and declined mitochondrial function is through mitophagy[238]. Mitophagy is a selective form of macroautophagy whereby damaged mitochondria are recognized by autophagic machinery and specifically degraded via the lysosome[238]. During erythrocyte and lens cell differentiation, the clearance of mitochondria requires mitophagy[131]. Similarly, we found that myoblast differentiation is also associated with mitophagy, a process which is dependent upon ATG7. This lack of mitophagy during differentiation may have promoted ROS generation through impaired mitochondria which induced mitochondrial-mediated apoptotic signaling. Previous reports have shown that inhibition of mitophagy allows pro-apoptotic factors to be released from the damaged mitochondria into the cytosol where they participate in apoptotic signaling[12]. As such we found an increase in cytosolic CYTO C and an increase in CASP9 during myoblast differentiation in absence of autophagy/mitophagy. Together, these data suggest that the induction of autophagy/mitophagy is required to protect the differentiating myoblast from cell stress and more specifically mitochondrial dysfunction.

Apoptotic signaling mediated by CASP3 is essential for myoblast differentiation and the formation of mature skeletal muscle[210]. For example, CASP3 induces the cleavage-mediated activation of MST1 which is required for the induction of myoblast differentiation[2]. Furthermore,

CASP3 also inhibits Twist, a bHLH protein which can prevent the transcriptional activity of MYOD[2]. However, these cleavage events only occur during early periods of differentiation. If the quantity of CASP3 activity is too great or the transient level of activity prolonged, CASP3 promotes cell death[210]. Because of the potential lethality of CASP3 activity, research has focused on understanding how CASP3 is regulated during differentiation. Fernando et al. found that the induction of CASP3 requires p38 activity[2,210]. However, typical canonical apoptotic pathways involving CASP8, CASP9, and CASP12 have also been observed[210]. For example, pharmacological inhibition of CASP8 reduced MYOD and MHC levels. Furthermore, forced expression of a dominant negative FADD protein also attenuates MYOD and MHC expression[212]. The induction of CASP12 activity following ER/SR-stress is also associated with CASP3 activation and promotion of myotube development[30]. Interestingly, the forced reduction of CASP9 activity has been shown to prevent the transient activation of CASP3 and attenuate myoblast fusion events[211]. In support of the involvement of mitochondrial-mediated apoptotic signaling during myoblast differentiation, previous results have shown that overexpression of BCL_{XL} also impairs myoblast fusion and CASP3 activity[211]. Furthermore, the overexpression of ARC in cardiac myocytes impairs CASP3 activity and differentiation[270].

The involvement of canonical mitochondrial-mediated pathways of apoptotic signaling in skeletal muscle differentiation is inconclusive. For example, although forced inhibition of CASP9 attenuates CASP3 and fusion[211], Bloemberg and Quadrilatero demonstrate that CASP9 is not involved in CASP3 activation during C2C12 differentiation[42]. In the present study, we observed an increase in cytosolic CYTO C during differentiation which is similar to findings from Shaltouki et al.[271] however; this finding is in contrast to results by Bloemberg and Quadrilatero, as well as Murray et al. who did not observe a change to cytosolic CYTO C[42,211].

The reasons for the discrepancies between the current study and results by Murray et al. may be due to the cytosolic isolation procedure, whereas the discrepancies between the current study and results from Bloemberg et al may be due to the difference in cell type, collection procedure and passage number. Regardless, the current work also demonstrates an increase in mitochondrial 4-HNE and a reduction of mitochondrial membrane potential supporting the observed rise in cytosolic CYTO C.

Although the exact mechanisms regulating the induction of CASP3 during myoblast differentiation are still unknown, observations made in dead myoblasts during differentiation demonstrate elevated levels of CASP12, CASP9, and CASP3 compared to healthy differentiating cells[29,210]. This observation suggests that cells which survive are able to defend and harness the cell stress and CASP3 activity whereas those cells which cannot die via apoptosis. Therefore, to improve myoblast differentiation it is important to identify processes which protect the myoblast from apoptosis. In the current work we demonstrate that autophagy protects the myoblasts from apoptosis during differentiation. In support of this, attenuation of CASP3 via CASP3 and CASP9 inhibitors partially recovered myoblast differentiation in the absence of autophagy. More specifically, our results point to a role of autophagy in regulating the level and temporal kinetics of CASP3 activity through the regulation of mitochondrial-mediated apoptotic pathways. An increase in mitophagy during early stages of differentiation, although modest, may provide the appropriate tempering of CYTO C release required for physiological levels of CASP9 activity to promote CASP3 activity. Without autophagy, a loss of mitochondrial viability was associated with a greater increase in CASP9 which promoted a robust increase in CASP3 and cell death instead of differentiation. In support of these findings, knockdown of histone deacetylase 1 and 2 resulted in a large increase in myofiber death and attenuated autophagy in perinatal mice[175].

Interestingly, forced induction of autophagy during this period via nutrient restriction improves myofiber viability [175]. In addition, inducible knockdown of ATG5 in MYF5 expressing cells results in smaller skeletal muscle and lower myogenic gene expression[206]. Together our data provide strong support for the role of autophagy in promoting myoblast differentiation through the regulation of caspase activity and apoptotic events.

CONCLUSION

This thesis demonstrates that autophagy is involved in processes determining the development, survival, and recovery of skeletal muscle. Both physiological levels of cell stress and/or pathological levels of apoptotic stress induced autophagy. Although, autophagy was associated with cell stress and cell death, autophagy did not contribute to apoptosis. In fact, autophagic processes and increased autophagic flux functioned as pro-survival mechanisms. Autophagy was able to govern the magnitude and temporal kinetics of apoptotic signaling through the regulation of mitochondrial viability and stress signaling. In this way this thesis demonstrates for the first time that autophagy is required and critical in regulating skeletal muscle cell death and differentiation.

Limitations

C2C12 myoblast cell lines have been extensively used for several years and have been widely accepted as a strong model for myoblast differentiation and myotube formation. However, C2C12's are an immortalized cell line which may not fully recapitulate *in vivo* differentiation. In addition, cells were grown on a 2D culture system and therefore may also behave differently than in an *in vivo* or 3D model system. In addition, culturing of C2C12 myoblasts for differentiation experiments results in a heterogeneous the cell population. For

example, in differentiated cultures, myotubes, differentiating myoblasts, as well as non-differentiated myoblasts are present. Thus, when differentiated cell cultures were collected, samples contained this heterogeneous population. Thus conclusions cannot be made only on "differentiated myotubes" as other myogenic cells at different stages of differentiation are present. However, comparisons between treatment and genotype groups were made on the same day and in cells grown/differentiated for the same duration. Thus in our analyses comparisons were made in cultures exposed to the same conditions. Furthermore, *in vivo* collection of tissue will also possess cellular heterogeneity. Further work should be conducted to isolate these different subpopulation of cells within differentiating cultures to closely examine the role of autophagy on each specific cell subtype and isolated phase of differentiation for example during fusion.

The use of chemical inhibitors is commonly used in experiments similar to those conducted in this thesis. The chemical inhibitors used in this thesis are well documented to inhibit thier intended targets and our results are in support of this. For example, 3MA significantly inhibited the formation of LC3B-II. Importantly, the effects of 3MA were replicated with shAtg7-mediated inhibition of LC3B-II and autophagy. Furthermore, we observed a significant increase in BCL2:BECN1 formation in the presence of JNK inhibitor SP600125. Moreover, inhibition of CASP3 resulted in a loss of CASP3 activity and inhibition of CASP9 resulted in a loss of activity in its downstream target CASP3. However, these compounds can have non-specific effects. For example, caspase inhibitors have been shown to inhibit several proteases in addition to the targeted caspase[272]. Therefore, further work utilizing specific measures of inhibition such as shRNA-mediated gene knockdown or site mutinogenesis would be valuable to ensure the results observed are in fact solely due to the inhibition of the target.

Stable transfection of any cell type requires the incorporation of foreign DNA into the host cells genome. Although in most cases it inserts into a random locus which does not affect cell physiology, studies have shown that this knockdown method can have off target effects which influence cell death pathways[273]. Although the use of SCR cell lines, which have been stably transfected and passed similarly to the shAtg7 cells lines, were used to control for the effects of stable transfection and pass number the possibility of the DNA being inserted into the same region is unlikely. However, shAtg7 and 3MA experiments displayed similar responses suggesting that the off target effects are likely not a significant in effect. When the studies were being designed, ATG7 was chosen due to the lack of a direct role in apoptotic signaling. However, as this thesis was being edited a study was published demonstrating a direct role of ATG7 in CASP9 activity[274]. Therefore, it is possible that effects observed to CASP9 activity in the absence of ATG7 may be related to the knockdown of the protein and independent of autophagy. However, considering 3MA resulted in similar apoptotic and differentiation defects we are confident that our results are due to the inhibition of ATG7 and the lack of autophagy.

In the first two studies 3MA was used to inhibit autophagy. 3MA has been shown to have off target effects especially when used at high doses[275]. However, we were able to recapitulate and confirm the effects using shRNA-mediated knockdown of ATG7. In the third study inhibition of autophagy was required in terminally differentiated myotubes which poses significant limitations to the ability to transfect efficiently with little to no cell damage. Moreover, the inhibition needed to be done on a specific timeline thus making transfection a nonviable option. Therefore a limitation to this particular study was the lack of a genetic knockdown model. However, considering our previous work with both 3MA and shAtg7 showed similar results we are confident in our 3MA data.

In several experiments, analyses were conducted to examine the effect of differentiation or CisPT on individual markers of apoptosis/autophagy over several time points. In such cases, hypotheses were tested using a one-way ANOVA with post hoc analyses to examine differences between time points (effects of differentiation or exposure time). In experiments where either a CTRL vs. drug or a CTRL vs. shRNA group was examined, we were only interested in the difference between specific groups within a single time point/condition and not in all possible comparisons. Therefore, planned T-Tests were used at (but within) each time point. Although factorial ANOVA could have been used to test for these differences as well as several additional interactions across/between groups, these effects (and all the interactions) were not within the scope/interest of these studies. Furthermore, the use of factorial ANOVA's within the relevant cell culture literature[211,42,29,30,214] is seldom used, likely due to the risk of type II error. For example, the use of a two-way ANOVA may have not been able to detect differences in situations where temporal changes occurred, especially with low sample sizes. To further add to the difficulty is the fact that some of these temporal changes occurred in opposite directions during various points during the sampling timeline. Therefore, given the simplicity of our experimental conditions, and the specificity of our hypotheses, we feel the data is appropriately analyzed, discussed and highly relevant/accurate for the cell biology and muscle biology field.

Future Directions

The results of this thesis show that autophagy plays a vital role in regulating apoptotic events during differentiation as well as in response to cisplatin and during stress recovery. The use of primary cell lines with an inducible "on/off" knockdown model and by using different ATG targets would provide further insight into this critical phenomena. Furthermore, consideration should be given to repeating key experiments in 3D culture systems which

resembles the cell niche. Importantly, examining skeletal muscle differentiation without autophagy during myogenesis *in vivo* would be of great interest as well as confirm the *in vivo* relevance of this work. Recovery from skeletal muscle apoptosis is essential for the continuation of muscle function and health. Although we demonstrated that autophagy is required to promote muscle recovery *in vitro* these experiments should be conducted in animal models since the regeneration process in culture is much different than that *in vivo*.

In the first study we demonstrate that autophagy is induced during myoblast differentiation, is partially regulated by JNK, and is required to promote the survival of the myoblast. However, future research should further investigate the pathways which may regulate autophagy during differentiation. For example, JNK inhibition did not completely inhibit LC3II content during myoblast differentiation. JNK inhibition only returned LC3II levels to those observed in D0 myoblasts suggesting that other signaling pathways are still contributing to the formation of the autophagosome. One particular avenue for exploration would be to characterize mTOR signaling as it is essential for myoblast differentiation and is also a potent regulator of autophagy[8,12]. Considering JNK significantly influences autophagy during myoblast differentiation it would be important to understand the mechanisms which promote the induction of JNK during myoblast differentiation. This again would provide information regarding potential autophagic targets during myoblast differentiation.

In the second study we demonstrated that mitophagy is increase during myoblast differentiation. Mitophagy is a highly controlled event and future work should be directed at better understanding the mechanisms underlying our observation[238]. Furthermore, other specific forms of selective autophagy should be investigated during differentiation. For example, ER/SR remodeling occurs during myoblast differentiation and the elimination of old/superfluous ER

components may require autophagy. In addition, significant remodeling of the cells structure and structural proteins occurs during myoblast fusion and myotube formation, again these events may require autophagy to degrade structural proteins. It would be interesting to identify whether or not autophagy, like the UPS, can degrade specific MRFs which would have major implications for the genetic reprogramming of the differentiating cell.

We also found that inhibition of autophagy increases in CASP3 and CASP9 activity, which resulted in impaired differentiation. Future work should examine the role and importance of autophagy or other potential pathways of caspase activation (death receptor, ER-stress and DNA damage) on apoptotic cells death.

In the third study we identified a role for autophagy in protecting differentiated myotubes from cisplatin induced apoptosis. It will be important to see how the inhibition of autophagy would affect skeletal muscle in response to cisplatin *in vivo*. Cisplatin causes significant muscle loss in cancer patients[245]. Therefore future research aimed at altering autophagy *in vivo* via dietary/nutritional manipulations may improve muscle viability in patients treated with cisplatin. Further, other stressors should be examined to determine if this is a common stress-related process.

References

1. Masiero E, Agatea L, Mammucari C, et al. Autophagy is required to maintain muscle mass. *Cell Metab*. 2009;10(6):507-515.

2. Fernando P, Kelly JF, Balazsi K, Slack RS, Megeney LA. Caspase 3 activity is required for skeletal muscle differentiation. *Proc Natl Acad Sci U S A*. 2002;99(17):11025-11030.

3. Castets P, Lin S, Rion N, et al. Sustained activation of mTORC1 in skeletal muscle inhibits constitutive and starvation-induced autophagy and causes a severe, late-onset myopathy. *Cell Metab*. 2013;17(5):731-744.

4. Lüthi AU, Martin SJ. The CASBAH: A searchable database of caspase substrates. *Cell Death Differ*. 2007;14(4):641-650.

5. Salucci S, Burattini S, Baldassarri V, et al. The peculiar apoptotic behavior of skeletal muscle cells. *Histol Histopathol*. 2013;28(8):1073-1087.

6. Plant PJ, Bain JR, Correa JE, Woo M, Batt J. Absence of caspase-3 protects against denervation-induced skeletal muscle atrophy. *J Appl Physiol*. 2009;107(1):224-234.

7. Ricci J-, Gottlieb RA, Green DR. Caspase-mediated loss of mitochondrial function and generation of reactive oxygen species during apoptosis. *J Cell Biol*. 2003;160(1):65-75.

8. He C, Klionsky DJ. Regulation mechanisms and signaling pathways of autophagy. *Annu Rev Genet*. 2009;43:67-93.

9. Klionsky DJ. Autophagy: From phenomenology to molecular understanding in less than a decade. *Nat Rev Mol Cell Biol*. 2007;8(11):931-937.

10. Galluzzi L, Vitale I, Abrams JM, et al. Molecular definitions of cell death subroutines: Recommendations of the nomenclature committee on cell death 2012. *Cell Death Differ*. 2012;19(1):107-120.

11. Kroemer G, Galluzzi L, Vandenabeele P, et al. Classification of cell death: Recommendations of the nomenclature committee on cell death 2009. *Cell Death Differ*. 2009;16(1):3-11.

12. Kroemer G, Marino G, Levine B. Autophagy and the integrated stress response. *Mol Cell*. 2010;40(2):280-293.

13. McClung JM, Judge AR, Powers SK, Yan Z. p38 MAPK links oxidative stress to autophagy-related gene expression in cachectic muscle wasting. *Am J Physiol Cell Physiol*. 2010;298(3):C542-9.

14. Grumati P, Coletto L, Sabatelli P, et al. Autophagy is defective in collagen VI muscular dystrophies, and its reactivation rescues myofiber degeneration. *Nat Med*. 2010;16(11):1313-1320.

15. Florian Bentzinger C, Wang YX, Rudnicki MA. Building muscle: Molecular regulation of myogenesis. *Cold Spring Harbor Perspect Biol*. 2012;4(2).

16. Wang YX, Rudnicki MA. Satellite cells, the engines of muscle repair. *Nat Rev Mol Cell Biol*. 2012;13(2):127-133.

17. Rudnicki MA, Braun T, Hinuma S, Jaenisch R. Inactivation of MyoD in mice leads to up-regulation of the myogenic HLH gene myf-5 and results in apparently normal muscle development. *Cell*. 1992;71(3):383-390.

18. Braun T, Rudnicki MA, Arnold H-, Jaenisch R. Targeted inactivation of the muscle regulatory gene myf-5 results in abnormal rib development and perinatal death. *Cell*. 1992;71(3):369-382.

19. Rudnicki MA, Schnegelsberg PNJ, Stead RH, Braun T, Arnold - HH, Jaenisch R. MyoD or myf-5 is required for the formation of skeletal muscle. *Cell*. 1993;75(7):1351-1359.

20. Megeney LA, Kablar B, Garrett K, Anderson JE, Rudnicki MA. MyoD is required for myogenic stem cell function in adult skeletal muscle. *Genes Dev*. 1996;10(10):1173-1183.

21. Sabourin LA, Rudnicki MA. The molecular regulation of myogenesis. *Clin Genet*. 2000;57(1):16-25.

22. Nabeshima Y, Hanaoka K, Hayasaka M, et al. Myogenin gene disruption results in perinatal lethality because of severe muscle defect. *Nature*. 1993;364(6437):532-535.

23. Rawls A, Valdez MR, Zhang W, Richardson J, Klein WH, Olson EN. Overlapping functions of the myogenic bHLH genes MRF4 and MyoD revealed in double mutant mice. *Development (Cambridge)*. 1998;125(13):2349-2358.

24. Kitzmann M, Fernandez A. Crosstalk between cell cycle regulators and the myogenic factor MyoD in skeletal myoblasts. *Cell Mol Life Sci*. 2001;58(4):571-579.

25. Wright WE, Sassoon DA, Lin VK. Myogenin, a factor regulating myogenesis, has a domain homologous to MyoD. *Cell*. 1989;56(4):607-617.

26. Lassar AB, Skapek SX, Novitch B. Regulatory mechanisms that coordinate skeletal muscle differentiation and cell cycle withdrawal. *Curr Opin Cell Biol*. 1994;6(6):788-794.

27. Yi M, Weaver D, Eisner V, et al. Switch from ER-mitochondrial to SR-mitochondrial calcium coupling during muscle differentiation. *Cell Calcium*. 2012;52(5):355-365.

28. Rutkowski DT, Kaufman RJ. A trip to the ER: Coping with stress. *Trends Cell Biol*. 2004;14(1):20-28.

29. Nakanishi K, Sudo T, Morishima N. Endoplasmic reticulum stress signaling transmitted by ATF6 mediates apoptosis during muscle development. *J Cell Biol*. 2005;169(4):555-560.

30. Nakanishi K, Dohmae N, Morishima N. Endoplasmic reticulum stress increases myofiber formation in vitro. *FASEB J*. 2007;21(11):2994-3003.

31. Jahnke VE, Sabido O, Freyssenet D. Control of mitochondrial biogenesis, ROS level, and cytosolic ca 2+ concentration during the cell cycle and the onset of differentiation in L6E9 myoblasts. *Am J Physiol Cell Physiol*. 2009;296(5):C1185-C1194.

32. Kim B, Kim J-, Yoon Y, Santiago MC, Brown MD, Park J-. Inhibition of Drp1-dependent mitochondrial division impairs myogenic differentiation. *Am J Physiol Regul Integr Comp Physiol*. 2013;305(8):R927-R938.

33. Chan DC. Mitochondria: Dynamic organelles in disease, aging, and development. *Cell*. 2006;125(7):1241-1252.

34. Lee S, Tak E, Lee J, et al. Mitochondrial H2 O2 generated from electron transport chain complex i stimulates muscle differentiation. *Cell Res*. 2011;21(5):817-834.

35. Van den Eijnde SM, Van den Hoff MJB, Reutelingsperger CPM, et al. Transient expression of phosphatidylserine at cell-cell contact areas is required for myotube formation. *J Cell Sci*. 2001;114(20):3631-3642.

36. Hengartner MO. The biochemistry of apoptosis. *Nature*. 2000;407(6805):770-776.

37. Keren A, Tamir Y, Bengal E. The p38 MAPK signaling pathway: A major regulator of skeletal muscle development. *Mol Cell Endocrinol*. 2006;252(1-2):224-230.

38. Xia Z, Dickens M, Raingeaud J, Davis RJ, Greenberg ME. Opposing effects of ERK and JNK-p38 MAP kinases on apoptosis. *Science*. 1995;270(5240):1326-1331.

39. Zetser A, Gredinger E, Bengal E. p38 mitogen-activated protein kinase pathway promotes skeletal muscle differentiation: Participation of the MEF2C transcription factor. *J Biol Chem*. 1999;274(8):5193-5200.

40. Borycki A-, Li J, Jin F, Emerson Jr. CP, Epstein JA. Pax3 functions in cell survival and in pax7 regulation. *Development*. 1999;126(8):1665-1674.

41. Margue CM, Bernasconi M, Barr FG, Schäfer BW. Transcriptional modulation of the anti-apoptotic protein BCL-XL by the paired box transcription factors PAX3 and PAX3/FKHR. *Oncogene*. 2000;19(25):2921-2929.

42. Bloemberg D, Quadrilatero J. Mitochondrial pro-apoptotic indices do not precede the transient caspase activation associated with myogenesis. *Biochimica et Biophysica Acta - Molecular Cell Research*. 2014;1843(12):2926-2936.

43. Erbay E, Chen J. The mammalian target of rapamycin regulates C2C12 myogenesis via a kinase-independent mechanism. *J Biol Chem*. 2001;276(39):36079-36082.

44. Erbay E, Park I-, Nuzzi PD, Schoenherr CJ, Chen J. IGF-II transcription in skeletal myogenesis is controlled by mTOR and nutrients. *J Cell Biol*. 2003;163(5):931-936.

45. Tureckova J, Wilson EM, Cappalonga JL, Rotwein P. Insulin-like growth factor-mediated muscle differentiation: Collaboration between phosphatidylinositol 3-kinase-akt-signaling pathways and myogenin. *J Biol Chem*. 2001;276(42):39264-39270.

46. Hribal ML, Nakae J, Kitamura T, Shutter JR, Accili D. Regulation of insulin-like growth factor-dependent myoblast differentiation by foxo forkhead transcription factors. *J Cell Biol*. 2003;162(4):535-541.

47. Datta SR, Dudek H, Xu T, et al. Akt phosphorylation of BAD couples survival signals to the cell- intrinsic death machinery. *CELL*. 1997;91(2):231-241.

48. Fujio Y, Mitsuuchi Y, Testa JR, Walsh K. Activation of Akt2 inhibits anoikis and apoptosis induced by myogenic differentiation. *Cell Death Differ*. 2001;8(12):1207-1212.

49. Blais A, Tsikitis M, Acosta-Alvear D, Sharan R, Kluger Y, Dynlacht BD. An initial blueprint for myogenic differentiation. *Genes and Development*. 2005;19(5):553-569.

50. Ryall JG. Metabolic reprogramming as a novel regulator of skeletal muscle development and regeneration. *FEBS Journal*. 2013;280(17):4004-4013.

51. Wagatsuma A, Sakuma K. Mitochondria as a potential regulator of myogenesis. *The Scientific World Journal*. 2013;2013.

52. Mihaylova MM, Shaw RJ. The AMPK signalling pathway coordinates cell growth, autophagy and metabolism. *Nature Cell Biol*. 2011;13(9):1016-1023.

53. Niesler CU, Myburgh KH, Moore F. The changing AMPK expression profile in differentiating mouse skeletal muscle myoblast cells helps confer increasing resistance to apoptosis. *Exp Physiol*. 2007;92(1):207-217.

54. Davis RJ. Signal transduction by the JNK group of MAP kinases. *Cell*. 2000;103(2):239-252.

55. Leppä S, Bohmann D. Diverse functions of JNK signaling and c-jun in stress response and apoptosis. *Oncogene*. 1999;18(45):6158-6162.

56. Wada T, Penninger JM. Mitogen-activated protein kinases in apoptosis regulation. *Oncogene*. 2004;23(16 REV. ISS. 2):2838-2849.

57. Khurana A, Dey CS. Involvement of c-jun N-terminal kinase activities in skeletal muscle differentiation. *J Muscle Res Cell Motil*. 2004;25(8):645-655.

58. Allen DL, Roy RR, Reggie Edgerton V. Myonuclear domains in muscle adaptation and disease. *Muscle Nerve*. 1999;22(10):1350-1360.

59. Quadrilatero J, Alway SE, Dupont-Versteegden E. Skeletal muscle apoptotic response to physical activity: Potential mechanisms for protection. *Appl Physiol Nutr Metab*. 2011;36(5):608-617.

60. Allen DL, Linderman JK, Roy RR, et al. Apoptosis: A mechanism contributing to remodeling of skeletal muscle in response to hindlimb unweighting. *AM J PHYSIOL CELL PHYSIOL*. 1997;273(2 42-2):C579-C587.

61. Bruusgaard JC, Egner IM, Larsen TK, Dupre-Aucouturier S, Desplanches D, Gundersen K. No change in myonuclear number during muscle unloading and reloading. *J Appl Physiol*. 2012;113(2):290-296.

62. Gundersen K, Bruusgaard JC. Nuclear domains during muscle atrophy: Nuclei lost or paradigm lost? *J Physiol*. 2008;586(11):2675-2681.

63. Thornberry NA, Lazebnik Y. Caspases: Enemies within. *Science*. 1998;281(5381):1312-1316.

64. Thorburn A. Death receptor-induced cell killing. *Cell Signal*. 2004;16(2):139-144.

65. Scaffidi G, Schmitz I, Zha J, Korsmeyer SJ, Krammer PH, Peter ME. Differential modulation of apoptosis sensitivity in CD95 type I and type II cells. *J Biol Chem*. 1999;274(32):22532-22538.

66. Adhihetty PJ, O'Leary MFN, Hood DA. Mitochondria in skeletal muscle: Adaptable rheostats of apoptotic susceptibility. *Exercise Sport Sci Rev*. 2008;36(3):116-121.

67. Wang C, Youle RJ, eds. *The role of mitochondria in apoptosis.* ; 2009; No. 43.

68. Chipuk JE, Moldoveanu T, Llambi F, Parsons MJ, Green DR. The BCL-2 family reunion. *Mol Cell*. 2010;37(3):299-310.

69. Antonsson B, Montessuit S, Lauper S, Eskes R, Martinou J-. Bax oligomerization is required for channel-forming activity in liposomes and to trigger cytochrome c release from mitochondria. *Biochem J*. 2000;345(2):271-278.

70. Dewson G, Kratina T, Czabotar P, Day CL, Adams JM, Kluck RM. Bak activation for apoptosis involves oligomerization of dimers via their a6 helices. *Mol Cell*. 2009;36(4):696-703.

71. Terrones O, Antonsson B, Yamaguchi H, et al. Lipidic pore formation by the concerted action of proapoptotic BAX and tBID. *J Biol Chem*. 2004;279(29):30081-30091.

72. Ichas F, Mazat J-. From calcium signaling to cell death: Two conformations for the mitochondrial permeability transition pore. switching from low- to high-conductance state. *Biochim Biophys Acta Bioenerg*. 1998;1366(1-2):33-50.

73. Baines CP. The molecular composition of the mitochondrial permeability transition pore. *J Mol Cell Cardiol*. 2009;46(6):850-857.

74. Fontaine E, Eriksson O, Ichas F, Bernardi P. Regulation of the permeability transition pore in skeletal muscle mitochondria modulation by electron flow through the respiratory chain complex I. *J Biol Chem*. 1998;273(20):12662-12668.

75. Marzo I, Brenner C, Zamzami N, et al. Bax and adenine nucleotide translocator cooperate in the mitochondrial control of apoptosis. *Science*. 1998;281(5385):2027-2031.

76. Scarlett JL, Murphy MP. Release of apoptogenic proteins from the mitochondrial intermembrane space during the mitochondrial permeability transition. *FEBS Lett*. 1997;418(3):282-286.

77. Puthalakath H, O'Reilly LA, Gunn P, et al. ER stress triggers apoptosis by activating BH3-only protein bim. *Cell*. 2007;129(7):1337-1349.

78. Dupont J, Fernandez AM, Glackin CA, Helman L, LeRoith D. Insulin-like growth factor 1 (IGF-1)-induced twist expression is involved in the anti-apoptotic effects of the IGF-1 receptor. *J Biol Chem*. 2001;276(28):26699-26707.

79. Kennedy SG, Kandel ES, Cross TK, Hay N. Akt/protein kinase B inhibits cell death by preventing the release of cytochrome c from mitochondria. *Mol Cell Biol*. 1999;19(8):5800-5810.

80. Segard HB, Moulin S, Boumard S, De Crémiers CA, Kelly PA, Finidori J. Autocrine growth hormone production prevents apoptosis and inhibits differentiation in C2C12 myoblasts. *Cell Signal*. 2003;15(6):615-623.

81. Li H, Zhu H, Xu C-, Yuan J. Cleavage of BID by caspase 8 mediates the mitochondrial damage in the fas pathway of apoptosis. *Cell*. 1998;94(4):491-501.

82. Siu PM, Pistilli EE, Alway SE. Apoptotic responses to hindlimb suspension in gastrocnemius muscles from young adult and aged rats. *Am J Physiol Regul Integr Comp Physiol*. 2005;289(4 58-4):R1015-R1026.

83. Gustafsson ÅB, Tsai JG, Logue SE, Crow MT, Gottlieb RA. Apoptosis repressor with caspase recruitment domain protects against cell death by interfering with bax activation. *J Biol Chem*. 2004;279(20):21233-21238.

84. Beere HM, Wolf BB, Cain K, et al. Heat-shock protein 70 inhibits apoptosis by preventing recruitment of procaspase-9 to the apaf-1 apoptosome. *Nature Cell Biol*. 2000;2(8):469-475.

85. Jäättelä M, Wissing D, Kokholm K, Kallunki T, Egeblad M. Hsp7O exerts its anti-apoptotic function downstream of caspase-3-like proteases. *EMBO J*. 1998;17(21):6124-6134.

86. Mosser DD, Caron AW, Bourget L, Denis-Larose C, Massie B. Role of the human heat shock protein hsp70 in protection against stress- induced apoptosis. *Mol Cell Biol*. 1997;17(9):5317-5327.

87. Polla BS, Kantengwa S, François D, et al. Mitochondria are selective targets for the protective effects of heat shock against oxidative injury. *Proc Natl Acad Sci U S A*. 1996;93(13):6458-6463.

88. Ravagnan L, Gurbuxani S, Susin SA, et al. Heat-shock protein 70 antagonizes apoptosis-inducing factor. *Nature Cell Biol*. 2001;3(9):839-843.

89. Green DR, Amarante-Mendes GP. The point of no return: Mitochondria, caspases, and the commitment to cell death. *Results Probl Cell Differ*. 1998;24:45-61.

90. Muñoz-Pinedo C, Guío-Carrión A, Goldstein JC, Fitzgerald P, Newmeyer DD, Green DR. Different mitochondrial intermembrane space proteins are released during apoptosis in a manner that is coordinately initiated but can vary in duration. *Proc Natl Acad Sci U S A*. 2006;103(31):11573-11578.

91. Joza N, Susin SA, Daugas E, et al. Essential role of the mitochondrial apoptosis-inducing factor in programmed cell death. *Nature*. 2001;410(6828):549-554.

92. Li LY, Luo X, Wang X. Endonuclease G is an apoptotic DNase when released from mitochondria. *Nature*. 2001;412(6842):95-99.

93. Dam AD, Mitchell AS, Quadrilatero J. Induction of mitochondrial biogenesis protects against caspase-dependent and caspase-independent apoptosis in L6 myoblasts. *Biochim Biophys Acta Mol Cell Res*. 2013.

94. Garrido C, Kroemer G. Life's smile, death's grin: Vital functions of apoptosis-executing proteins. *Curr Opin Cell Biol*. 2004;16(6):639-646.

95. Acehan D, Jiang X, Morgan DG, Heuser JE, Wang X, Akey CW. Three-dimensional structure of the apoptosome: Implications for assembly, procaspase-9 binding, and activation. *Mol Cell*. 2002;9(2):423-432.

96. Zou H, Li Y, Liu X, Wang X. An APAf-1 · cytochrome C multimeric complex is a functional apoptosome that activates procaspase-9. *J Biol Chem*. 1999;274(17):11549-11556.

97. Jiang X, Wang X. Cytochrome c promotes caspase-9 activation by inducing nucleotide binding to apaf-1. *J Biol Chem*. 2000;275(40):31199-31203.

98. Li P, Nijhawan D, Budihardjo I, et al. Cytochrome c and dATP-dependent formation of apaf-1/caspase-9 complex initiates an apoptotic protease cascade. *CELL*. 1997;91(4):479-489.

99. Riedl SJ, Salvesen GS. The apoptosome: Signalling platform of cell death. *Nat Rev Mol Cell Biol*. 2007;8(5):405-413.

100. Srinivasula SM, Hegde R, Saleh A, et al. A conserved XIAP-interaction motif in caspase-9 and smac/DIABLO regulates caspase activity and apoptosis. *Nature*. 2001;410(6824):112-116.

101. Scott FL, Denault J-, Riedl SJ, Shin H, Renatus M, Salvesen GS. XIAP inhibits caspase-3 and -7 using two binding sites: Evolutionary conserved mechanism of IAPs. *EMBO J*. 2005;24(3):645-655.

102. Komatsu M, Waguri S, Ueno T, et al. Impairment of starvation-induced and constitutive autophagy in Atg7-deficient mice. *J Cell Biol*. 2005;169(3):425-434.

103. He C, Bassik MC, Moresi V, et al. Exercise-induced BCL2-regulated autophagy is required for muscle glucose homeostasis. *Nature*. 2012;481(7382):511-515.

104. Mammucari C, Milan G, Romanello V, et al. FoxO3 controls autophagy in skeletal muscle in vivo. *Cell Metab*. 2007;6(6):458-471.

105. Ogata T, Oishi Y, Higuchi M, Muraoka I. Fasting-related autophagic response in slow- and fast-twitch skeletal muscle. *Biochem Biophys Res Commun*. 2010;394(1):136-140.

106. Bhatnagar S, Mittal A, Gupta SK, Kumar A. TWEAK causes myotube atrophy through coordinated activation of ubiquitin-proteasome system, autophagy, and caspases. *J Cell Physiol*. 2012;227(3):1042-1051.

107. Polson HE, de Lartigue J, Rigden DJ, et al. Mammalian Atg18 (WIPI2) localizes to omegasome-anchored phagophores and positively regulates LC3 lipidation. *Autophagy*. 2010;6(4):506-522.

108. Axe EL, Walker SA, Manifava M, et al. Autophagosome formation from membrane compartments enriched in phosphatidylinositol 3-phosphate and dynamically connected to the endoplasmic reticulum. *J Cell Biol*. 2008;182(4):685-701.

109. Tosch V, Rohde HM, Tronchere H, et al. A novel PtdIns3P and PtdIns(3,5)P2 phosphatase with an inactivating variant in centronuclear myopathy. *Hum Mol Genet*. 2006;15(21):3098-3106.

110. Vergne I, Roberts E, Elmaoued RA, et al. Control of autophagy initiation by phosphoinositide 3-phosphatase jumpy. *EMBO J*. 2009;28(15):2244-2258.

111. Klionsky DJ, Abeliovich H, Agostinis P, et al. Guidelines for the use and interpretation of assays for monitoring autophagy in higher eukaryotes. *Autophagy*. 2008;4(2):151-175.

112. Klionsky DJ, Abdalla FC, Abeliovich H, et al. Guidelines for the use and interpretation of assays for monitoring autophagy. *Autophagy*. 2012;8(4):445-544.

113. Pattingre S, Tassa A, Qu X, et al. Bcl-2 antiapoptotic proteins inhibit beclin 1-dependent autophagy. *Cell*. 2005;122(6):927-939.

114. Oberstein A, Jeffrey PD, Shi Y. Crystal structure of the bcl-XL-beclin 1 peptide complex: Beclin 1 is a novel BH3-only protein. *J Biol Chem*. 2007;282(17):13123-13132.

115. Noble CG, Dong JM, Manser E, Song H. Bcl-xL and UVRAG cause a monomer-dimer switch in Beclin1. *J Biol Chem*. 2008;283(38):26274-26282.

116. Maiuri MC, Criollo A, Tasdemir E, et al. BH3-only proteins and BH3 mimetics induce autophagy by competitively disrupting the interaction between beclin 1 and bcl-2/bcl-X(L). *Autophagy*. 2007;3(4):374-376.

117. Maiuri MC, Le Toumelin G, Criollo A, et al. Functional and physical interaction between bcl-X(L) and a BH3-like domain in beclin-1. *EMBO J*. 2007;26(10):2527-2539.

118. Akar U, Chaves-Reyez A, Barria M, et al. Silencing of bcl-2 expression by small interfering RNA induces autophagic cell death in MCF-7 breast cancer cells. *Autophagy*. 2008;4(5):669-679.

119. Fry CS, Drummond MJ, Lujan HL, DiCarlo SE, Rasmussen BB. Paraplegia increases skeletal muscle autophagy. *Muscle Nerve*. 2012;46(5):793-798.

120. Girolamo F, Lia A, Amati A, et al. Overexpression of autophagic proteins in the skeletal muscle of sporadic inclusion body myositis. *Neuropathol Appl Neurobiol*. 2013.

121. Kim CH, Kim KH, Yoo YM. Melatonin-induced autophagy is associated with degradation of MyoD protein in C2C12 myoblast cells. *J Pineal Res*. 2012;53(3):289-297.

122. Kim KH, Jeong YT, Oh H, et al. Autophagy deficiency leads to protection from obesity and insulin resistance by inducing Fgf21 as a mitokine. *Nat Med*. 2013;19(1):83-92.

123. Smuder AJ, Kavazis AN, Min K, Powers SK. Exercise protects against doxorubicin-induced markers of autophagy signaling in skeletal muscle. *J Appl Physiol*. 2011;111(4):1190-1198.

124. Lira VA, Okutsu M, Zhang M, et al. Autophagy is required for exercise training-induced skeletal muscle adaptation and improvement of physical performance. *FASEB J*. 2013;27(10):4184-4193.

125. He C, Levine B. The beclin 1 interactome. *Curr Opin Cell Biol*. 2010;22(2):140-149.

126. Wei Y, Sinha S, Levine B. Dual role of JNK1-mediated phosphorylation of bcl-2 in autophagy and apoptosis regulation. *Autophagy*. 2008;4(7):949-951.

127. Zalckvar E, Berissi H, Mizrachy L, et al. DAP-kinase-mediated phosphorylation on the BH3 domain of beclin 1 promotes dissociation of beclin 1 from bcl-XL and induction of autophagy. *EMBO Rep*. 2009;10(3):285-292.

128. Zalckvar E, Berissi H, Eisenstein M, Kimchi A. Phosphorylation of beclin 1 by DAP-kinase promotes autophagy by weakening its interactions with bcl-2 and bcl-XL. *Autophagy*. 2009;5(5):720-722.

129. Paul PK, Kumar A. TRAF6 coordinates the activation of autophagy and ubiquitin-proteasome systems in atrophying skeletal muscle. *Autophagy*. 2011;7(5):555-556.

130. Shi CS, Kehrl JH. TRAF6 and A20 regulate lysine 63-linked ubiquitination of beclin-1 to control TLR4-induced autophagy. *Sci Signal*. 2010;3(123):ra42.

131. Mizushima N, Levine B. Autophagy in mammalian development and differentiation. *Nat Cell Biol*. 2010;12(9):823-830.

132. Chan EY. mTORC1 phosphorylates the ULK1-mAtg13-FIP200 autophagy regulatory complex. *Sci Signal*. 2009;2(84):pe51.

133. Jung CH, Jun CB, Ro SH, et al. ULK-Atg13-FIP200 complexes mediate mTOR signaling to the autophagy machinery. *Mol Biol Cell*. 2009;20(7):1992-2003.

134. Hara T, Takamura A, Kishi C, et al. FIP200, a ULK-interacting protein, is required for autophagosome formation in mammalian cells. *J Cell Biol*. 2008;181(3):497-510.

135. Di Bartolomeo S, Corazzari M, Nazio F, et al. The dynamic interaction of AMBRA1 with the dynein motor complex regulates mammalian autophagy. *J Cell Biol*. 2010;191(1):155-168.

136. Hanada T, Noda NN, Satomi Y, et al. The Atg12-Atg5 conjugate has a novel E3-like activity for protein lipidation in autophagy. *J Biol Chem*. 2007;282(52):37298-37302.

137. Mizushima N, Kuma A, Kobayashi Y, et al. Mouse Apg16L, a novel WD-repeat protein, targets to the autophagic isolation membrane with the Apg12-Apg5 conjugate. *J Cell Sci*. 2003;116(Pt 9):1679-1688.

138. Tanida I, Tanida-Miyake E, Ueno T, Kominami E. The human homolog of saccharomyces cerevisiae Apg7p is a protein-activating enzyme for multiple substrates including human Apg12p, GATE-16, GABARAP, and MAP-LC3. *J Biol Chem*. 2001;276(3):1701-1706.

139. Shintani T, Mizushima N, Ogawa Y, Matsuura A, Noda T, Ohsumi Y. Apg10p, a novel protein-conjugating enzyme essential for autophagy in yeast. *EMBO J*. 1999;18(19):5234-5241.

140. Kirisako T, Ichimura Y, Okada H, et al. The reversible modification regulates the membrane-binding state of Apg8/Aut7 essential for autophagy and the cytoplasm to vacuole targeting pathway. *J Cell Biol*. 2000;151(2):263-276.

141. Kabeya Y, Mizushima N, Yamamoto A, Oshitani-Okamoto S, Ohsumi Y, Yoshimori T. LC3, GABARAP and GATE16 localize to autophagosomal membrane depending on form-II formation. *J Cell Sci*. 2004;117(Pt 13):2805-2812.

142. Raben N, Hill V, Shea L, et al. Suppression of autophagy in skeletal muscle uncovers the accumulation of ubiquitinated proteins and their potential role in muscle damage in pompe disease. *Hum Mol Genet*. 2008;17(24):3897-3908.

143. Johansen T, Lamark T. Selective autophagy mediated by autophagic adapter proteins. *Autophagy*. 2011;7(3):279-296.

144. Geisler S, Holmström KM, Skujat D, et al. PINK1/parkin-mediated mitophagy is dependent on VDAC1 and p62/SQSTM1. *Nat Cell Biol*. 2010;12(2):119-131.

145. Long J, Gallagher TRA, Cavey JR, et al. Ubiquitin recognition by the ubiquitin-associated domain of p62 involves a novel conformational switch. *J Biol Chem*. 2008;283(9):5427-5440.

146. Narendra D, Tanaka A, Suen D-, Youle RJ. Parkin is recruited selectively to impaired mitochondria and promotes their autophagy. *J Cell Biol*. 2008;183(5):795-803.

147. Pankiv S, Clausen TH, Lamark T, et al. p62/SQSTM1 binds directly to Atg8/LC3 to facilitate degradation of ubiquitinated protein aggregates by autophagy*[S]. *J Biol Chem*. 2007;282(33):24131-24145.

148. Park YE, Hayashi YK, Bonne G, et al. Autophagic degradation of nuclear components in mammalian cells. *Autophagy*. 2009;5(6):795-804.

149. Kirkin V, Lamark T, Sou Y-, et al. A role for NBR1 in autophagosomal degradation of ubiquitinated substrates. *Mol Cell*. 2009;33(4):505-516.

150. Bjørkøy G, Lamark T, Brech A, et al. p62/SQSTM1 forms protein aggregates degraded by autophagy and has a protective effect on huntingtin-induced cell death. *J Cell Biol*. 2005;171(4):603-614.

151. Noda T, Fujita N, Yoshimori T. The late stages of autophagy: How does the end begin? *Cell Death Differ*. 2009;16(7):984-990.

152. Kimura S, Noda T, Yoshimori T. Dynein-dependent movement of autophagosomes mediates efficient encounters with lysosomes. *Cell Struct Funct*. 2008;33(1):109-122.

153. Ravikumar B, Acevedo-Arozena A, Imarisio S, et al. Dynein mutations impair autophagic clearance of aggregate-prone proteins. *Nat Genet*. 2005;37(7):771-776.

154. Repnik U, Cesen MH, Turk B. The endolysosomal system in cell death and survival. *Cold Spring Harb Perspect Biol*. 2013;5(1):a008755.

155. Yu L, McPhee CK, Zheng L, et al. Termination of autophagy and reformation of lysosomes regulated by mTOR. *Nature*. 2010;465(7300):942-946.

156. Madaro L, Marrocco V, Carnio S, Sandri M, Bouche M. Intracellular signaling in ER stress-induced autophagy in skeletal muscle cells. *FASEB J*. 2013;27(5):1990-2000.

157. O'Leary MF, Hood DA. Denervation-induced oxidative stress and autophagy signaling in muscle. *Autophagy*. 2009;5(2):230-231.

158. Ciavarra G, Zacksenhaus E. Rescue of myogenic defects in rb-deficient cells by inhibition of autophagy or by hypoxia-induced glycolytic shift. *J Cell Biol*. 2010;191(2):291-301.

159. Chen Y, McMillan-Ward E, Kong J, Israels SJ, Gibson SB. Mitochondrial electron-transport-chain inhibitors of complexes I and II induce autophagic cell death mediated by reactive oxygen species. *J Cell Sci*. 2007;120(23):4155-4166.

160. Yu L, Wan F, Dutta S, et al. Autophagic programmed cell death by selective catalase degradation. *Proc Natl Acad Sci U S A*. 2006;103(13):4952-4957.

161. Scott RC, Juhász G, Neufeld TP. Direct induction of autophagy by Atg1 inhibits cell growth and induces apoptotic cell death. *Current Biology*. 2007;17(1):1-11.

162. Shimizu S, Kanaseki T, Mizushima N, et al. Role of bcl-2 family proteins in a non-apoptopic programmed cell death dependent on autophagy genes. *Nat Cell Biol*. 2004;6(12):1221-1228.

163. Lum JJ, Bauer DE, Kong M, et al. Growth factor regulation of autophagy and cell survival in the absence of apoptosis. *Cell*. 2005;120(2):237-248.

164. Ding Y, Kim JK, Kim SI, et al. TGF-ß1 protects against mesangial cell apoptosis via induction of autophagy. *J Biol Chem*. 2010;285(48):37909-37919.

165. Katayama M, Kawaguchi T, Berger MS, Pieper RO. DNA damaging agent-induced autophagy produces a cytoprotective adenosine triphosphate surge in malignant glioma cells. *Cell Death Differ*. 2007;14(3):548-558.

166. Martinet W, De Meyer GRY, Herman AG, Kockx MM. Amino acid deprivation induces both apoptosis and autophagy in murine C2C12 muscle cells. *Biotechnol Lett*. 2005;27(16):1157-1163.

167. Song J, Guo X, Xie X, et al. Autophagy in hypoxia protects cancer cells against apoptosis induced by nutrient deprivation through a beclin1-dependent way in hepatocellular carcinoma. *J Cell Biochem*. 2011;112(11):3406-3420.

168. Li H, Wang P, Sun Q, et al. Following cytochrome c release, autophagy is inhibited during chemotherapy-induced apoptosis by caspase 8-mediated cleavage of beclin 1. *Cancer Res*. 2011;71(10):3625-3634.

169. Luo S, Rubinsztein DC. Apoptosis blocks beclin 1-dependent autophagosome synthesis: An effect rescued by bcl-xL. *Cell Death Differ*. 2010;17(2):268-277.

170. Wirawan E, Vande Walle L, Kersse K, et al. Caspase-mediated cleavage of beclin-1 inactivates beclin-1-induced autophagy and enhances apoptosis by promoting the release of proapoptotic factors from mitochondria. *Cell Death and Disease*. 2010;1(1).

171. Djavaheri-Mergny M, Maiuri MC, Kroemer G. Cross talk between apoptosis and autophagy by caspase-mediated cleavage of beclin 1. *Oncogene*. 2010;29(12):1717-1719.

172. Betin VMS, Lane JD. Caspase cleavage of Atg4D stimulates GABARAP-L1 processing and triggers mitochondrial targeting and apoptosis. *J Cell Sci*. 2009;122(14):2554-2566.

173. Pyo J-, Jang M-, Kwon Y-, et al. Essential roles of Atg5 and FADD in autophagic cell death: Dissection of autophagic cell death into vacuole formation and cell death. *J Biol Chem*. 2005;280(21):20722-20729.

174. Yousefi S, Perozzo R, Schmid I, et al. Calpain-mediated cleavage of Atg5 switches autophagy to apoptosis. *Nat Cell Biol*. 2006;8(10):1124-1132.

175. Moresi V, Carrer M, Grueter CE, et al. Histone deacetylases 1 and 2 regulate autophagy flux and skeletal muscle homeostasis in mice. *Proc Natl Acad Sci U S A*. 2012;109(5):1649-1654.

176. De Palma C, Morisi F, Cheli S, et al. Autophagy as a new therapeutic target in duchenne muscular dystrophy. *Cell Death Dis*. 2012;3:e418.

177. Wohlgemuth SE, Seo AY, Marzetti E, Lees HA, Leeuwenburgh C. Skeletal muscle autophagy and apoptosis during aging: Effects of calorie restriction and life-long exercise. *Exp Gerontol*. 2010;45(2):138-148.

178. Grumati P, Coletto L, Schiavinato A, et al. Physical exercise stimulates autophagy in normal skeletal muscles but is detrimental for collagen VI-deficient muscles. *Autophagy*. 2011;7(12):1415-1423.

179. Grumati P, Coletto L, Sandri M, Bonaldo P. Autophagy induction rescues muscular dystrophy. *Autophagy*. 2011;7(4):426-428.

180. Sandri M. Autophagy in skeletal muscle. *FEBS Lett*. 2010;584(7):1411-1416.

181. Sandri M. Autophagy in health and disease. 3. involvement of autophagy in muscle atrophy. *American Journal of Physiology - Cell Physiology*. 2010;298(6):C1291-C1297.

182. Wenz T, Rossi SG, Rotundo RL, Spiegelman BM, Moraes CT. Increased muscle PGC-1alpha expression protects from sarcopenia and metabolic disease during aging. *Proc Natl Acad Sci U S A*. 2009;106(48):20405-20410.

183. Masiero E, Sandri M. Autophagy inhibition induces atrophy and myopathy in adult skeletal muscles. *Autophagy*. 2010;6(2):307-309.

184. Raben N, Schreiner C, Baum R, et al. Suppression of autophagy permits successful enzyme replacement therapy in a lysosomal storage disorder--murine pompe disease. *Autophagy*. 2010;6(8):1078-1089.

185. Nakashima K, Ishida A, Katsumata M. Changes in expression of proteolytic-related genes in chick myoblasts during myogenesis. *Journal of Poultry Science*. 2011;48(1):51-56.

186. Ebisui C, Tsujinaka T, Morimoto T, et al. Changes of proteasomes and cathepsins activities and their expression during differentiation of C2C12 myoblasts. *J Biochem*. 1995;117(5):1088-1094.

187. Ciechanover A, Breitschopf K, Abu Hatoum O, Bengal E. Degradation of MyoD by the ubiquitin pathway: Regulation by specific DNA-binding and identification of a novel site for ubiquitination. *Mol Biol Rep*. 1999;26(1-2):59-64.

188. Pantovic A, Krstic A, Janjetovic K, et al. Coordinated time-dependent modulation of AMPK/akt/mTOR signaling and autophagy controls osteogenic differentiation of human mesenchymal stem cells. *Bone*. 2013;52(1):524-531.

189. Zeng M, Zhou J-. Roles of autophagy and mTOR signaling in neuronal differentiation of mouse neuroblastoma cells. *Cell Signal*. 2008;20(4):659-665.

190. Zhuang W, Li B, Long L, Chen L, Huang Q, Liang Z. Induction of autophagy promotes differentiation of glioma-initiating cells and their radiosensitivity. *International Journal of Cancer*. 2011;129(11):2720-2731.

191. Sandoval H, Thiagarajan P, Dasgupta SK, et al. Essential role for nix in autophagic maturation of erythroid cells. *Nature*. 2008;454(7201):232-235.

192. Mammucari C, Schiaffino S, Sandri M. Downstream of akt: FoxO3 and mTOR in the regulation of autophagy in skeletal muscle. *Autophagy*. 2008;4(4):524-526.

193. Sanchez AM, Csibi A, Raibon A, et al. AMPK promotes skeletal muscle autophagy through activation of forkhead FoxO3a and interaction with Ulk1. *J Cell Biochem*. 2012;113(2):695-710.

194. Sandri M, Carraro U. Apoptosis of skeletal muscles during development and disease. *International Journal of Biochemistry and Cell Biology*. 1999;31(12):1373-1390.

195. Long L, Yang X, Southwood M, et al. Chloroquine prevents progression of experimental pulmonary hypertension via inhibition of autophagy and lysosomal bone morphogenetic protein type II receptor degradation. *Circ Res*. 2013;112(8):1159-1170.

196. Shacka JJ, Klocke BJ, Shibata M, et al. Bafilomycin A1 inhibits chloroquine-induced death of cerebellar granule neurons. *Mol Pharmacol*. 2006;69(4):1125-1136.

197. Dam AD, Mitchell AS, Quadrilatero J. Induction of mitochondrial biogenesis protects against caspase-dependent and caspase-independent apoptosis in L6 myoblasts. *Biochimica et Biophysica Acta - Molecular Cell Research*. 2013;1833(12):3426-3435.

198. Bloemberg D, Mcdonald E, Dulay D, Quadrilatero J. Autophagy is altered in skeletal and cardiac muscle of spontaneously hypertensive rats. *Acta Physiologica*. 2014;210(2):381-391.

199. Nagendran J, Waller TJ, Dyck JRB. AMPK signalling and the control of substrate use in the heart. *Mol Cell Endocrinol*. 2013;366(2):180-193.

200. Zhang Y, Morgan MJ, Chen K, Choksi S, Liu Z-. Induction of autophagy is essential for monocyte-macrophage differentiation. *Blood*. 2012;119(12):2895-2905.

201. Remels AHV, Langen RCJ, Schrauwen P, Schaart G, Schols AMWJ, Gosker HR. Regulation of mitochondrial biogenesis during myogenesis. *Mol Cell Endocrinol*. 2010;315(1-2):113-120.

202. Coux O, Tanaka K, Goldberg AL, eds. *Structure and functions of the 20S and 26S proteasomes.* ; 1996Annual Review of Biochemistry; No. 65.

203. Jacquel A, Obba S, Boyer L, et al. Autophagy is required for CSF-1-induced macrophagic differentiation and acquisition of phagocytic functions. *Blood*. 2012;119(19):4527-4531.

204. Zhang S, Li X, Li L, Yan X. Autophagy up-regulation by early weaning in the liver, spleen and skeletal muscle of piglets. *Br J Nutr*. 2011;106(2):213-217.

205. Hasty P, Bradley A, Morris JH, et al. Muscle deficiency and neonatal death in mice with a targeted mutation in the myogenin gene. *Nature*. 1993;364(6437):501-506.

206. Martinez-Lopez N, Athonvarangkul D, Sahu S, et al. Autophagy in Myf5+ progenitors regulates energy and glucose homeostasis through control of brown fat and skeletal muscle development. *EMBO Rep*. 2013.

207. Iovino S, Oriente F, Botta G, et al. PED/PEA-15 induces autophagy and mediates TGF-beta1 effect on muscle cell differentiation. *Cell Death Differ*. 2012;19(7):1127-1138.

208. Xu Q, Wu Z. The insulin-like growth factor-phosphatidylinositol 3-kinase-akt signaling pathway regulates myogenin expression in normal myogenic cells but not in rhabdomyosarcoma-derived RD cells. *J Biol Chem*. 2000;275(47):36750-36757.

209. Ramos FJ, Kaeberlein M, Kennedy BK. Elevated MTORC1 signaling and impaired autophagy. *Autophagy*. 2013;9(1):108-109.

210. Fernando P, Megeney LA. Is caspase-dependent apoptosis only cell differentiation taken to the extreme? *FASEB Journal*. 2007;21(1):8-17.

211. Murray TVA, McMahon JM, Howley BA, et al. A non-apoptotic role for caspase-9 in muscle differentiation. *J Cell Sci*. 2008;121(22):3786-3793.

212. Freer-Prokop M, O'Flaherty J, Ross JA, Weyman CM. Non-canonical role for the TRAIL receptor DR5/FADD/caspase pathway in the regulation of MyoD expression and skeletal myoblast differentiation. *Differentiation*. 2009;78(4):205-212.

213. Weber GF, Menko AS. The canonical intrinsic mitochondrial death pathway has a non-apoptotic role in signaling lens cell differentiation. *J Biol Chem*. 2005;280(23):22135-22145.

214. McMillan EM, Quadrilatero J. Autophagy is required and protects against apoptosis during myoblast differentiation. *Biochem J*. 2014.

215. Youle RJ, Narendra DP. Mechanisms of mitophagy. *Nature Reviews Molecular Cell Biology*. 2011;12(1):9-14.

216. Lee J, Giordano S, Zhang J. Autophagy, mitochondria and oxidative stress: Cross-talk and redox signalling. *Biochem J*. 2012;441(2):523-540.

217. McMillan EM, Graham DA, Rush JW, Quadrilatero J. Decreased DNA fragmentation and apoptotic signaling in soleus muscle of hypertensive rats following 6 weeks of treadmill training. *J Appl Physiol (1985)*. 2012;113(7):1048-1057.

218. Blais A, Tsikitis M, Acosta-Alvear D, Sharan R, Kluger Y, Dynlacht BD. An initial blueprint for myogenic differentiation. *Genes and Development*. 2005;19(5):553-569.

219. Franco AA, Odom RS, Rando TA. Regulation of antioxidant enzyme gene expression in response to oxidative stress and during differentiation of mouse skeletal muscle. *Free Radical Biology and Medicine*. 1999;27(9-10):1122-1132.

220. Zhou LZ-, Johnson AP, Rando TA. NFκB and AP-1 mediate transcriptional responses to oxidative stress in skeletal muscle cells. *Free Radical Biology and Medicine*. 2001;31(11):1405-1416.

221. Zlatkovic J, Filipovic D. Stress-induced alternations in CuZnSOD and MnSOD activity in cellular compartments of rat liver. *Mol Cell Biochem*. 2011;357(1-2):143-150.

222. Petersen DR, Doorn JA. Reactions of 4-hydroxynonenal with proteins and cellular targets. *Free Radical Biology and Medicine*. 2004;37(7):937-945.

223. Arya R, Mallik M, Lakhotia SC. Heat shock genes - integrating cell survival and death. *Journal of Biosciences*. 2007;32(3):595-610.

224. Stankiewicz AR, Lachapelle G, Foo CPZ, Radicioni SM, Mosser DD. Hsp70 inhibits heat-induced apoptosis upstream of mitochondria by preventing bax translocation. *J Biol Chem*. 2005;280(46):38729-38739.

225. Davenport EL, Moore HE, Dunlop AS, et al. Heat shock protein inhibition is associated with activation of the unfolded protein response pathway in myeloma plasma cells. *Blood*. 2007;110(7):2641-2649.

226. Huang J, Forsberg NE. Role of calpain in skeletal-muscle protein degradation. *Proc Natl Acad Sci U S A*. 1998;95(21):12100-12105.

227. Smith IJ, Dodd SL. Calpain activation causes a proteasome-dependent increase in protein degradation and inhibits the akt signalling pathway in rat diaphragm muscle. *Exp Physiol*. 2007;92(3):561-573.

228. Polster BM, Basanez G, Etxebarria A, Hardwick JM, Nicholls DG. Calpain I induces cleavage and release of apoptosis-inducing factor from isolated mitochondria. *J Biol Chem*. 2005;280(8):6447-6454.

229. Nakagawa T, Yuan J. Cross-talk between two cysteine protease families: Activation of caspase-12 by calpain in apoptosis. *J Cell Biol*. 2000;150(4):887-894.

230. Youle RJ, Strasser A. The BCL-2 protein family: Opposing activities that mediate cell death. *Nature Reviews Molecular Cell Biology*. 2008;9(1):47-59.

231. Orrenius S, Gogvadze V, Zhivotovsky B, eds. *Mitochondrial oxidative stress: Implications for cell death.* ; 2007; No. 47.

232. Ekhterae D, Lin Z, Lundberg MS, Crow MT, Brosius 3rd. FC, Núñez G. ARC inhibits cytochrome c release from mitochondria and protects against hypoxia-induced apoptosis in heart-derived H9c2 cells. *Circ Res*. 1999;85(12):e70-77.

233. Boya P, González-Polo R-, Casares N, et al. Inhibition of macroautophagy triggers apoptosis. *Mol Cell Biol*. 2005;25(3):1025-1040.

234. Hill BG, Haberzettl P, Ahmed Y, Srivastava S, Bhatnagar A. Unsaturated lipid peroxidation-derived aldehydes activate autophagy in vascular smooth-muscle cells. *Biochem J*. 2008;410(3):525-534.

235. Kubli DA, Gustafsson AB. Mitochondria and mitophagy: The yin and yang of cell death control. *Circ Res*. 2012;111(9):1208-1221.

236. Wang H-, Zhang D, Tan Y-, Li T. Autophagy in endothelial progenitor cells is cytoprotective in hypoxic conditions. *American Journal of Physiology - Cell Physiology*. 2013;304(7):C617-C626.

237. Doyle A, Zhang G, Abdel Fattah EA, Eissa NT, Li Y-. Toll-like receptor 4 mediates lipopolysaccharide-induced muscle catabolism via coordinate activation of ubiquitin-proteasome and autophagy-lysosome pathways. *FASEB Journal*. 2011;25(1):99-110.

238. Gottlieb RA, Carreira RS. Autophagy in health and disease. 5. mitophagy as a way of life. *American Journal of Physiology - Cell Physiology*. 2010;299(2):C203-C210.

239. Twig G, Elorza A, Molina AJA, et al. Fission and selective fusion govern mitochondrial segregation and elimination by autophagy. *EMBO Journal*. 2008;27(2):433-446.

240. Lamark T, Johansen T. Aggrephagy: Selective disposal of protein aggregates by macroautophagy. *International Journal of Cell Biology*. 2012.

241. Argilés JM, López-Soriano FJ, Busquets S. Apoptosis signalling is essential and precedes protein degradation in wasting skeletal muscle during catabolic conditions. *International Journal of Biochemistry and Cell Biology*. 2008;40(9):1674-1678.

242. Du J, Wang X, Miereles C, et al. Activation of caspase-3 is an initial step triggering accelerated muscle proteolysis in catabolic conditions. *J Clin Invest*. 2004;113(1):115-123.

243. Andrianjafiniony T, Dupré-Aucouturier S, Letexier D, Couchoux H, Desplanches D. Oxidative stress, apoptosis, and proteolysis in skeletal muscle repair after unloading. *American Journal of Physiology - Cell Physiology*. 2010;299(2):C307-C315.

244. Teng BT, Pei XM, Tam EW, Benzie IF, Siu PM. Opposing responses of apoptosis and autophagy to moderate compression in skeletal muscle. *Acta Physiol (Oxf)*. 2011;201(2):239-254.

245. Cepeda V, Fuertes MA, Castilla J, Alonso C, Quevedo C, Pérez JM. Biochemical mechanisms of cisplatin cytotoxicity. *Anti-Cancer Agents in Medicinal Chemistry*. 2007;7(1):3-18.

246. Dodson S, Baracos VE, Jatoi A, et al, eds. *Muscle wasting in cancer cachexia: Clinical implications, diagnosis, and emerging treatment strategies.* ; 2011; No. 62.

247. Salucci S, Battistelli M, Burattini S, et al. C2C12 myoblast sensitivity to different apoptotic chemical triggers. *Micron*. 2010;41(8):966-973.

248. Stacchiotti A, Rovetta F, Ferroni M, et al. Taurine rescues cisplatin-induced muscle atrophy in vitro: A morphological study. *Oxidative Medicine and Cellular Longevity*. 2014;2014.

249. Fanzani A, Zanola A, Rovetta F, Rossi S, Aleo MF. Cisplatin triggers atrophy of skeletal C2C12 myotubes via impairment of akt signalling pathway and subsequent increment activity of proteasome and autophagy systems. *Toxicol Appl Pharmacol*. 2011;250(3):312-321.

250. Reed SA, Sandesara PB, Senf SM, Judge AR. Inhibition of FoxO transcriptional activity prevents muscle fiber atrophy during cachexia and induces hypertrophy. *FASEB Journal*. 2012;26(3):987-1000.

251. Bloemberg D, Mcdonald E, Dulay D, Quadrilatero J. Autophagy is altered in skeletal and cardiac muscle of spontaneously hypertensive rats. *Acta Physiologica*. 2014;210(2):381-391.

252. Thorburn A. Apoptosis and autophagy: Regulatory connections between two supposedly different processes. *Apoptosis*. 2008;13(1):1-9.

253. Twig G, Elorza A, Molina AJA, et al. Fission and selective fusion govern mitochondrial segregation and elimination by autophagy. *EMBO J*. 2008;27(2):433-446.

254. Xiao R, Ferry AL, Dupont-Versteegden EE. Cell death-resistance of differentiated myotubes is associated with enhanced anti-apoptotic mechanisms compared to myoblasts. *Apoptosis*. 2011;16(3):221-234.

255. Cantini M, Massimino ML, Bruson A, Catani C, Dalla Libera L, Carraro U. Macrophages regulate proliferation and differentiation of satellite cells. *Biochem Biophys Res Commun*. 1994;202(3):1688-1696.

256. Wu JJ, Quijano C, Chen E, et al. Mitochondrial dysfunction and oxidative stress mediate the physiological impairment induced by the disruption of autophagy. *Aging (Albany NY)*. 2009;1(4):425-437.

257. Vanhorebeek I, Gunst J, Derde S, et al. Insufficient activation of autophagy allows cellular damage to accumulate in critically ill patients. *J Clin Endocrinol Metab*. 2011;96(4):E633-E645.

258. Melser S, Chatelain EH, Lavie J, et al. Rheb regulates mitophagy induced by mitochondrial energetic status. *Cell Metabolism*. 2013;17(5):719-730.

259. Loos B, Engelbrecht A-, Lockshin RA, Klionsky DJ, Zakeri Z. The variability of autophagy and cell death susceptibility: Unanswered questions. *Autophagy*. 2013;9(9):1270-1285.

260. Han J, Hou W, Goldstein LA, Stolz DB, Watkins SC, Rabinowich H. A complex between Atg7 and caspase-9: A novel mechanism of cross-regulation between autophagy and apoptosis. *J Biol Chem*. 2014;289(10):6485-6497.

261. Betin VMS, Lane JD. Caspase cleavage of Atg4D stimulates GABARAP-L1 processing and triggers mitochondrial targeting and apoptosis. *J Cell Sci*. 2009;122(14):2554-2566.

262. Zhu Y, Zhao L, Liu L, et al. Beclin 1 cleavage by caspase-3 inactivates autophagy and promotes apoptosis. *Protein and Cell*. 2010;1(5):468-477.

263. Skidmore R, Gutierrez JA, Guerriero Jr. V, Kregel KC. HSP70 induction during exercise and heat stress in rats: Role of internal temperature. *American Journal of Physiology - Regulatory Integrative and Comparative Physiology*. 1995;268(1 37-1):R92-R97.

264. Du J, Wang X, Miereles C, et al. Activation of caspase-3 is an initial step triggering accelerated muscle proteolysis in catabolic conditions. *J Clin Invest*. 2004;113(1):115-123.

265. Brookes PS, Yoon Y, Robotham JL, Anders MW, Sheu S-. Calcium, ATP, and ROS: A mitochondrial love-hate triangle. *American Journal of Physiology - Cell Physiology*. 2004;287(4 56-4):C817-C833.

266. Newman AB, Kupelian V, Visser M, et al. Strength, but not muscle mass, is associated with mortality in the health, aging and body composition study cohort. *Journals of Gerontology - Series A Biological Sciences and Medical Sciences*. 2006;61(1):72-77.

267. Mackenzie MG, Hamilton DL, Murray JT, Taylor PM, Baar K. mVps34 is activated following high-resistance contractions. *J Physiol (Lond)*. 2009;587(1):253-260.

268. Stuelsatz P, Pouzoulet F, Lamarre Y, et al. Down-regulation of MyoD by calpain 3 promotes generation of reserve cells in C2C12 myoblasts. *J Biol Chem*. 2010;285(17):12670-12683.

269. Lassar AB, Skapek SX, Novitch B. Regulatory mechanisms that coordinate skeletal muscle differentiation and cell cycle withdrawal. *Curr Opin Cell Biol*. 1994;6(6):788-794.

270. Hunter AL, Zhang J, Chen SC, et al. Apoptosis repressor with caspase recruitment domain (ARC) inhibits myogenic differentiation. *FEBS Lett*. 2007;581(5):879-884.

271. Shaltouki A, Freer M, Mei Y, Weyman CM. Increased expression of the pro-apoptotic Bcl2 family member PUMA is required for mitochondrial release of cytochrome C and the apoptosis associated with skeletal myoblast differentiation. *Apoptosis*. 2007;12(12):2143-2154.

272. Pereira NA, Song Z. Some commonly used caspase substrates and inhibitors lack the specificity required to monitor individual caspase activity. *Biochem Biophys Res Commun*. 2008;377(3):873-877.

273. Castanotto D, Rossi JJ. The promises and pitfalls of RNA-interference-based therapeutics. *Nature*. 2009;457(7228):426-433.

274. Han J, Hou W, Goldstein LA, Stolz DB, Watkins SC, Rabinowich H. A complex between Atg7 and caspase-9: A NOVEL MECHANISM OF CROSS-REGULATION BETWEEN AUTOPHAGY AND APOPTOSIS. *J Biol Chem*. 2014;289(10):6485-6497.

275. Hou H, Zhang Y, Huang Y, et al. Inhibitors of phosphatidylinositol 3'-kinases promote mitotic cell death in HeLa cells. *PLoS One*. 2012;7(4):e35665.

APPENDIX A

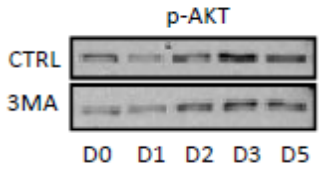

Supplemental Figure 1. Qualitative analysis of the effect of 5mM 3MA on AKT phosphorylation status during D0, D1, D2, D3, and D5 of C2C12 myoblast differentiation.